

ANALYSIS OF CONTINUOUS ARCHES ON ELASTIC PIERS

by

DICK CHAO WONG

B.Sc., National Yunnan University, China, 1947

A THESIS SUBMITTED IN PARTIAL FULFILMENT OF THE  
REQUIREMENTS FOR THE DEGREE OF

M.A.Sc.

in the Department

of

Civil Engineering

We accept this thesis as conforming to the  
required standard

THE UNIVERSITY OF BRITISH COLUMBIA

September, 1959

## ABSTRACT

This thesis presents the investigation of the behaviour of continuous arches on elastic piers about which little is currently known. A series of studies were made to indicate the effects of pier dimensions on extreme fiber stresses at a number of critical sections of arches. Such results are of particular interest to the bridge designer.

Six numerical examples of symmetrical arch systems have been solved, using an interesting variation of the force distribution method of the late Prof. Hardy Cross.<sup>(1)</sup> The relative proportions of the system were based primarily upon aesthetic considerations. In the six structures which were investigated two systems of arches and piers, called I and II, were considered. Each system has five spans. The variable span lengths are the same in each system. The arches in each were selected from Whitney's paper<sup>(2)</sup> and are linear arches for dead load only. In System I the arch ribs are lighter and flatter than in System II, and the piers are more flexible. In each system the variation of span lengths and arch rises are such so that there is no unbalanced dead load horizontal thrust on the piers. In both systems all piers are of single equal batter. Three different heights of pier 40', 60', and 80' were investigated in each system. Figs. 1,

2 and 3 clarify the foregoing while Tables 1 and 2 give the properties of the elements making up each system. In System I twenty influence lines for upper, lower, right, and left kern moments at springings, crowns, and pier tops were constructed. In System II "portions" of sixteen influence lines for upper and lower kern moment at springings and crowns sufficient to establish the trend of alteration of proportions were constructed.

The large number of variables involved in the design of such indeterminate structures as continuous arch systems makes it inadvisable to draw too definite conclusions, but some results of studies obviously indicate that: (1) All controlling L.L. fiber stresses are greater than those in fixed ended arches and increase as the height of piers increases, but the maximum D.L. + L.L. fiber stresses do not exhibit this characteristic as might be expected but depend, of course, upon the ratio of dead load to live load as well as upon the proportions of the structure. (2) It would appear that the analysis may be confined to three spans for arches and two spans for piers, save in the case of a long centre span combined with very flexible piers. In such a case the complete structure must be involved in the analysis. (3) The effect of rotation of the pier tops on L.L. stresses at crowns is small and almost independent of pier height, whereas the effect on L.L. stresses at springings is somewhat greater

and increases slowly as the height of piers increases. The effect of translation of the pier tops on L.L. stresses at springings and crowns is usually the greatest and increases rapidly as the height of piers increases. The results presented herein are, of course, true only for this particular type of system, but the author feels that the system chosen is more representative of a structure which might be constructed than are the typical three or four equal span systems of the text book variety with which some writers, more concerned with simplicity than reality, have dealt.

In presenting this thesis in partial fulfilment of the requirements for an advanced degree at the University of British Columbia, I agree that the Library shall make it freely available for reference and study. I further agree that permission for extensive copying of this thesis for scholarly purposes may be granted by the Head of my Department or by his representatives. It is understood that copying or publication of this thesis for financial gain shall not be allowed without my written permission.

Department of Civil Engineering

The University of British Columbia,  
Vancouver 8, Canada.

Date Sept. 30th. 1959

## Contents

	Page
Chapter I Introduction . . . . .	1
Chapter II Numerical Examples . . . . .	5
Chapter III Conclusions . . . . .	6
APPENDIX I Dead Load horizontal thrusts on Arches for numerical Examples . . . . .	65
II Formulae for Analysis . . . . .	71
BIBLIOGRAPHY . . . . .	87

---

#### ACKNOWLEDGMENT

The author wishes to acknowledge his indebtedness to his supervisor, Professor A.H. Finlay, who spent many hours and took much patience in discussions on this thesis and gave valuable suggestions and unforgettable encouragement.

September, 1959

Vancouver, B. C., Canada

## CHAPTER I

### Introduction

More than two thousand years ago arches were widely used for the first time by the Romans. In the form of masonry, concrete, steel and timber arches, they have been in wide use ever since. The terminal forces essential for arch action tend to counteract simple beam moments and yield economy while the usually graceful curvature of the arch axis yields a pleasing appearance. These form two essential advantages of arches. In the last thirty years, a series of arches of reinforced concrete resting on slender piers have received a great deal of attention and have occupied an increasingly important position in bridges in this continent. The continuous arches on elastic piers have some of the same advantages as does the single arch. But this type of structure like all arches is suitable only if the ratio of live load to dead load is rather small, otherwise the large live load produces large bending moments in arches and in piers resulting in a loss of economy.

This thesis restricts itself to the analysis of two carefully selected systems (I and II) of arches on elastic piers. As has been stated in the Abstract these systems were "designed" for dead load, using results of

C.S. Whitney<sup>(2)</sup> after relative span lengths rises and pier heights had been selected on the basis of aesthetics combined with keeping the structure free of bending moments (save those due to rib-shortening) under dead load. They present in every way structures which could be built and it is hoped that the conclusions reached may assist designers.

This thesis will not deal, save in a general way, with the analytical procedure, which has been proposed by many people.<sup>(1,3,4,5,6,7,8,9,10)</sup> For analysing the problem a variation of the "Moment Distribution Method" will be used in this thesis. The mentioned method, which might be termed "Force Distribution", was developed by the late Prof. Hardy Cross. He distributed force functions successively by pure translation and pure rotation of the neutral point of the joint with the neutral points of the adjacent joints kept fixed temporarily. The neutral point is so chosen that it translates only under the action of a suitably directed force acting upon it and rotates only under the action of a moment acting upon it. The pier top is "replaced" by the neutral point of the joint in order to diminish the disadvantage of slow convergence. The method has been popularized and improved in a proper form of calculations by Prof. A.H. Finlay.<sup>(11)</sup> Besides that, Prof. Finlay has extended the central idea of the method to construct influence lines for arches on elastic piers by applying a unit load on each span in only one position. Having found, for this one position, the stress function desired the

remaining ordinates to its influence line follow at once from the fact that the shape of the desired influence line is similar to the more familiar influence line if the arch had been fixed-ended. This will be clear upon referring to Fig. 5. This extension has made the original method more brilliant and powerful, which becomes the most ingenious and perfect method in continuous arch analysis.

Usually the design is governed by the combined effect of normal thrust and axial bending moment, and since the former is a maximum under full span loadings, while the latter is not, it is evident that the independent influence lines do not directly give the loading producing the maximum combined stress at any section. For designing purposes it is necessary to construct influence lines for maximum total fiber stress rather than for maximum axial moment and thrust. At any section the extreme fiber stress may be obtained by dividing the kern moment by the appropriate section modulus (see Appendix II). Such use of the concept of kern moment yields the combination of normal thrust and axial bending moment effects and gives directly the loading conditions for maximum total fiber stress, therefore the concept of kern moment will be used in this thesis.

In continuous arch system, its dimensions are based on the topographic conditions and the transportation requirements. The author has not collected any data of such structures. But design is an engineering problem and also an architectural

problem too. Economy requires that dead load thrusts shall be balanced at the pier tops and aesthetic considerations usually indicates an unequal number of arches with span lengths decreasing towards the abutments. From these two basic ideas the author has roughly designed six different five span continuous symmetrical arch systems. They are made up of reasonable dimensions and pleasing appearance and were used to investigate the effects of pier dimensions upon extreme dead plus live load fiber stresses at a number of critical sections of arches.

## CHAPTER II

### Numerical Examples

In order to make the investigation as stated in Chapter I, six examples will be solved and the resulting influence lines compared with the influence lines for fixed ended arches and the components of influence lines caused by pier top translation and rotation separately will be shown (see Abstract).

The characteristics of the examples have been stated in the Abstract. The bases of the piers are fixed rigidly, as are the outer ends of the ribs at the abutments. The effects of rib-shortening and pier-shortening are not considered, as they are negligible in all cases.

The properties of arch ribs and piers are listed in Tables 1 and 2.

The constants for analysis are shown in Table 3.

The thrusts produced on arches by applying a unit force (horizontal directed force or couple) at the neutral point of Joint, B or C, are shown in Tables 4 to 7. The thrusts on arches due to a unit force at the neutral point of Joint, D or E, may be obtained by symmetry.

The influence lines for kern moments at springings, crowns and pier tops of System I are shown in Figs 5 to 24, inclusive.

To study the relative importance of rotation and translation of the pier tops, the two effects are plotted separately as shown in Figs. 5 to 20, inclusive, for System I, and their results on fiber stresses in arches are shown in Figs. 43 and 44.

Maximum total live load lower kern moments at the springings and crowns are shown in Tables 8 and 9 respectively.

Maximum total live load right kern moments at pier tops are shown in Table 10.

The ratio of dead load to live load is an important factor in the design, usually, the dead load stresses govern largely. To facilitate the analysis the relatively small live load was assumed uniformly distributed. A thousand pounds per linear foot per rib of live load is assumed in these examples. The maximum total kern moments at the springings and crowns due to the combination of dead load and live load are shown in Tables 11 and 12, and the changes in fiber stresses in arches from fixed ends are shown in Figs. 41 and 42.

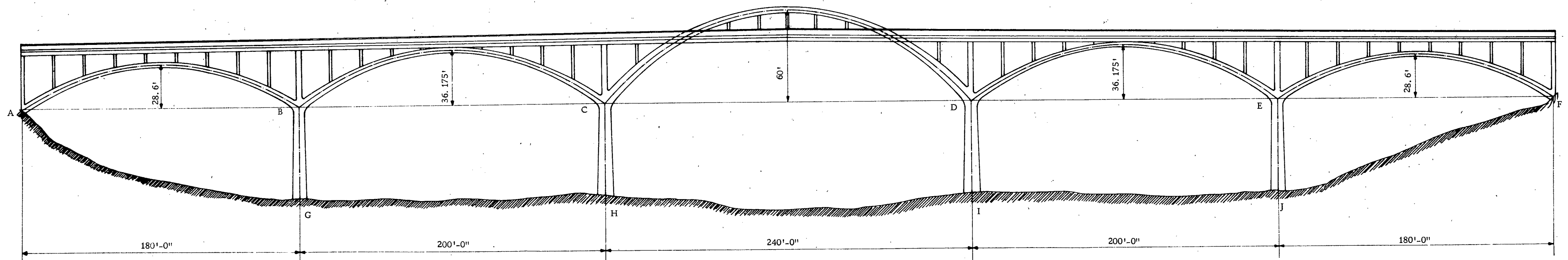
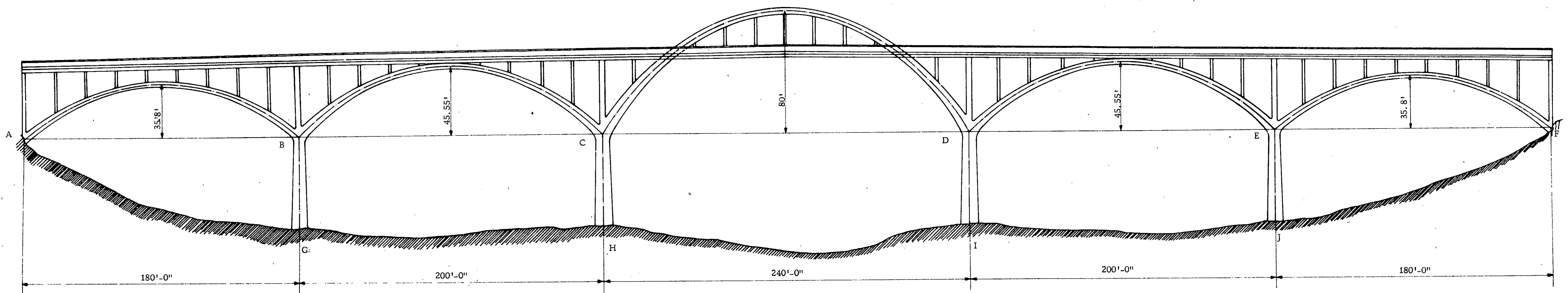
The controlling compressive upper extreme fiber stresses at the springings and crowns, and the compressive left extreme fiber stresses at the pier tops due to the combination of dead load and live load are shown in Tables 13 and 14, respectively.

The sign convention is the same as usual in arch analysis. Moments are considered as positive if they produce

tension on the inside fiber of an arch or on the right fiber of pier, and normal forces as positive if they produce compression in the member.

Computations for the most part were made with the "Friden" desk calculator, and the areas under influence line diagrams were carefully measured by means of a planimeter.

Scale in ft.  
0 20 40 60 80 100



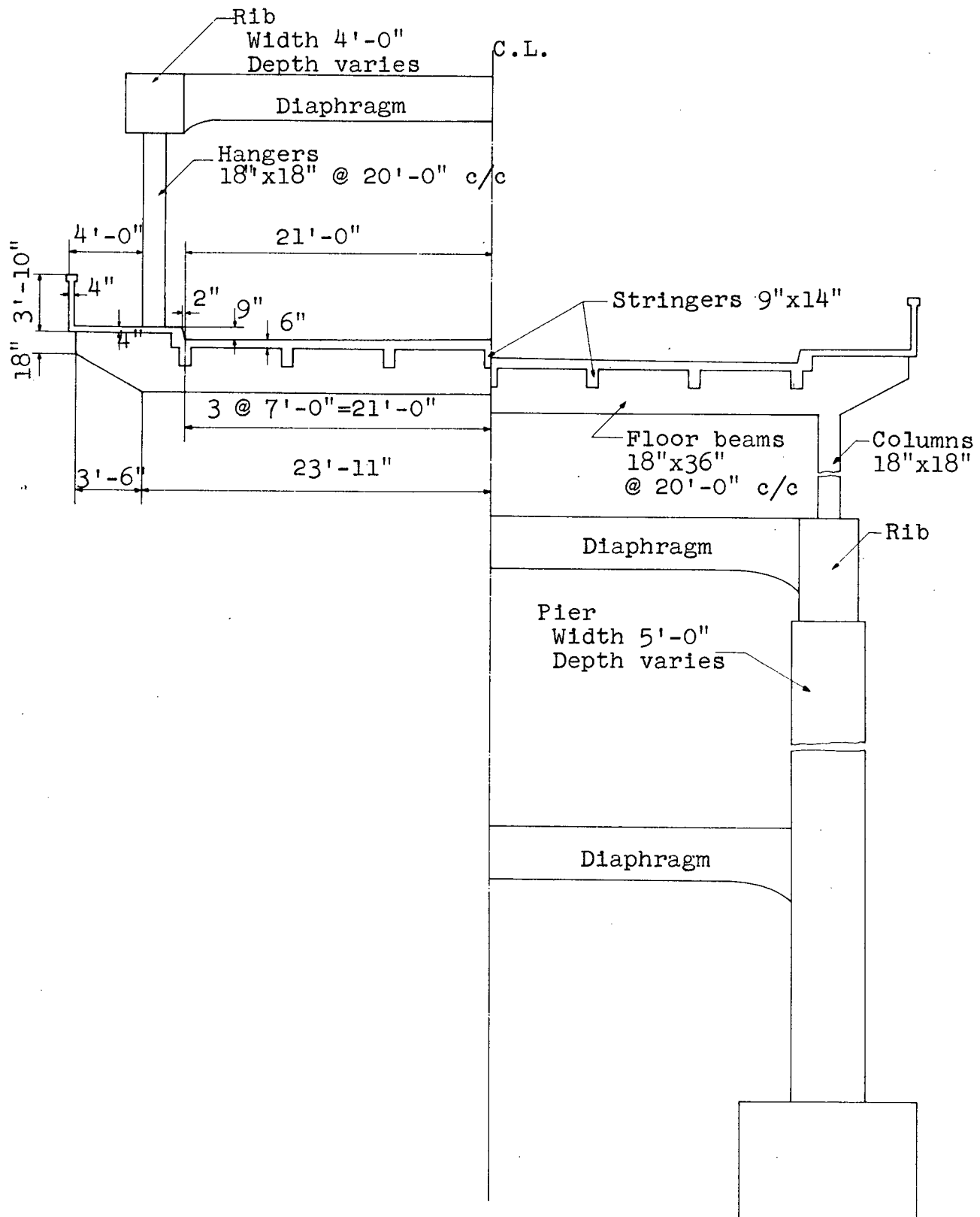


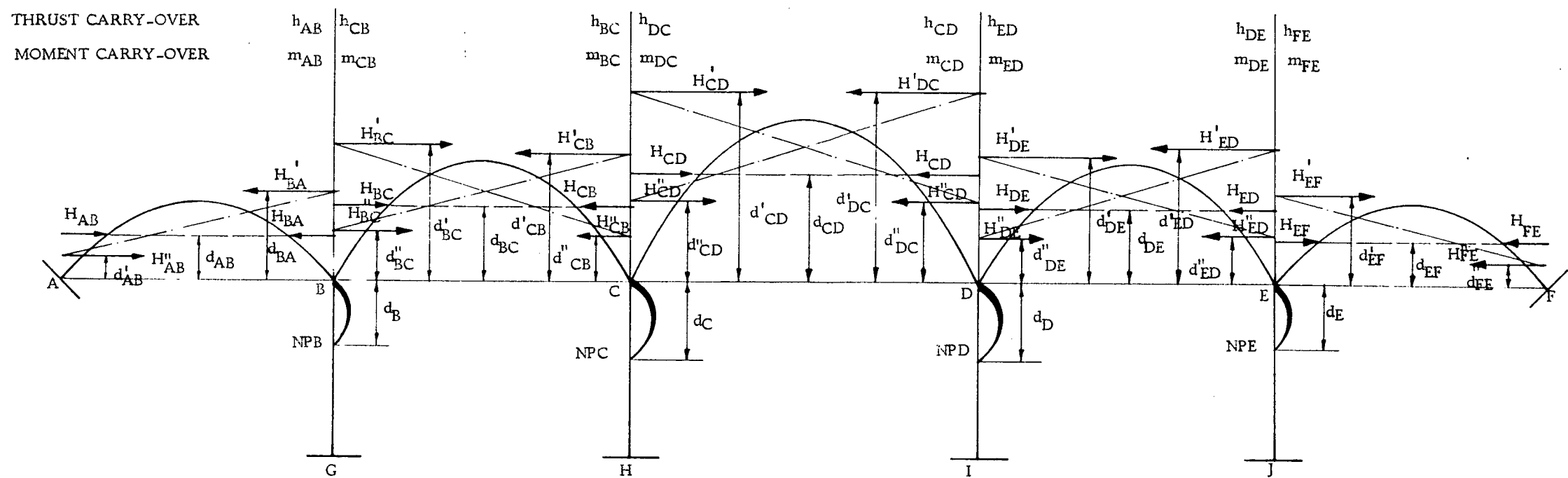
FIG. 3 CROSS SECTIONS OF SYSTEMS I &amp; II

Table 1 Properties of Arch Ribs

System	I			II		
	AB & EF	BC & DE	CD	AB & EF	BC & DE	CD
L in ft.	180	200	240	180	200	240
r in ft.	28.6	36.175	60	35.8	45.55	80
g	1.455	1.543	1.756	1.543	1.756	2.24
m	0.325	0.300	0.275	0.375	0.275	0.200
y <sub>c</sub> in ft.	6.89	8.47	13.45	8.87	10.21	16.31
w in ft.	4	4	4	4	4	4
d <sub>c</sub> in ft.	3	3.25	4	3.25	3.5	4.25
d <sub>s</sub> in ft.	4.65	5.24	7.03	4.95	6.05	8.93
φ <sub>s</sub>	34°2'	37°17'	47°52'	40°44'	45°20'	57°20'

Table 2 Properties of Piers

System	$H_P$ in ft.	$W_P$ in ft.	$d_{T_1}$ in ft.	$d_{T_2}$ in ft.	$q$
I	40	5	6.5	8	1.2
	60	5	6.5	8	1.3
	80	5	6.5	8	1.4
II	40	5	7.5	9	1.2
	60	5	7.5	9	1.3
	80	5	7.5	9	1.4



THRUST LINE FOR TRANSLATION

Fig. 4\*

THRUST LINE FOR ROTATION

System	$H_p$ in ft.	$d_B$ $\&$ $d_E$	$d_C$ $\&$ $d_D$	$d_{AB}$ $\&$ $d_{EF}$	$d''_{AB}$ $\&$ $d''_{FE}$	$d'_{BA}$ $\&$ $d''_{EF}$	$d_{BC}$ $\&$ $d'_{ED}$	$d'_{BC}$ $\&$ $d''_{ED}$	$d''_{CB}$ $\&$ $d''_{DE}$	$d_C$	$d_{CD}$	$d'_{CD}$ $\&$ $d''_{DC}$	$d''_{CD}$ $\&$ $d''_{DC}$	$h_{AB}$ $\&$ $h_{FE}$	$h_{CB}$ $\&$ $h_{DE}$	$m_{AB}$ $\&$ $m_{FE}$	$m_{CB}$ $\&$ $m_{DE}$	$h_{BC}$ $\&$ $h_{ED}$	$h_{DC}$ $\&$ $h_{ED}$	$m_{BC}$ $\&$ $m_{ED}$	$m_{DC}$ $\&$ $m_{CD}$	
		in ft.	in ft.	in ft.	in ft.	in ft.	in ft.	in ft.	in ft.	in ft.	in ft.	in ft.	in ft.	in ft.	%	%	%	%	%	%	%	%
I	40	14.91	16.61	21.72	17.09	29.35	27.71	38.15	21.58	37.75	21.35	46.55	65.50	34.85	4.40	3.28	9.93	19.25	1.85	1.11	12.90	15.49
	60	16.11	21.04	21.72	17.26	29.13	27.71	37.87	22.16	36.84	21.53	46.55	64.30	35.65	11.34	8.46	10.44	22.27	5.19	3.10	15.68	19.26
	80	13.66	22.45	21.72	16.96	29.63	27.71	38.40	22.25	36.50	21.16	46.55	63.90	37.20	19.56	14.60	9.72	21.81	9.99	5.97	15.29	20.82
II	40	16.19	17.09	26.93	21.00	37.20	35.34	48.75	27.30	48.55	27.14	63.69	88.30	47.70	2.23	1.86	8.35	17.31	1.01	0.64	11.26	14.95
	60	19.69	22.50	26.93	21.33	36.40	35.34	47.90	28.00	47.35	27.67	63.69	86.86	48.70	6.18	5.09	9.49	21.69	3.15	1.83	14.72	18.95
	80	19.83	25.50	26.93	21.33	36.33	35.34	47.90	28.38	47.25	27.71	63.69	86.00	49.15	11.52	9.50	9.53	23.11	6.27	3.63	15.95	20.95

Table 3 Constants for Analysis

\* Only the horizontal components of the thrusts due to the distributed moments are shown in the figure, the vertical components may be obtained by proportion

Table 4 Thrusts on Arches Produced by Applying a Unit Force to the Right at the Neutral Point of Joint B.- (Minus sign means arch in tension)

II		I				System H <sub>P</sub>
80'	60'	40'	80'	60'	40'	
-.11859	-.06253	-.02236	-.20655	-.11615	-.04427	HAB
-.00660	-.00257	-.00050	-.01207	-.00577	-.00133	" HAB
-.11859	-.06253	-.02236	-.20655	-.11615	-.04427	H <sub>BA</sub>
-.00660	-.00257	-.00050	-.01207	-.00577	-.00133	H <sub>BA</sub> '
.09089	.04974	.01845	.13644	.08166	.03235	H <sub>BC</sub>
.00642	.00249	.00049	.01053	.00500	.00116	H <sub>BC</sub> '
-.02256	-.01008	-.00265	-.03824	-.01927	-.00549	H <sub>BC</sub> "
.09089	.04974	.01845	.13644	.08166	.03235	H <sub>CB</sub>
-.02256	-.01008	-.00265	-.03824	-.01927	-.00549	H <sub>CB</sub> '
.00642	.00249	.00049	.01053	.00500	.00116	H <sub>CB</sub> "
.00300	.00084	.00011	.00776	.00235	.00033	H <sub>CD</sub>
.01915	.00869	.00236	.03135	.01598	.00468	H <sub>CD</sub> '
-.00545	-.00197	-.00038	-.00998	-.00401	-.00083	H <sub>CD</sub> "
.00300	.00084	.00011	.00776	.00235	.00033	H <sub>DC</sub>
-.00545	-.00197	-.00038	-.00998	-.00401	-.00083	H <sub>DC</sub> '
.01915	.00869	.00236	.03135	.01598	.00468	H <sub>DC</sub> "
.00092	.00019	.00001	.00227	.00057	.00006	H <sub>DE</sub>
.00646	.00229	.00043	.01218	.00483	.00097	H <sub>DE</sub> '
-.00177	.00055	-.00007	-.00316	-.00118	-.00020	H <sub>DE</sub> "
.00092	.00019	.00001	.00227	.00057	.00006	H <sub>ED</sub>
-.00177	-.00055	-.00007	-.00316	-.00118	-.00020	H <sub>ED</sub> '
.00646	.00229	.00043	.01218	.00483	.00097	H <sub>ED</sub> "
.00093	.00016	.00001	.00331	.00067	.00005	H <sub>EF</sub>
.00432	.00056	.00007	.00362	.00139	.00023	H <sub>EF</sub> '
.00093	.00016	.00001	.00331	.00067	.00005	H <sub>FE</sub>
.00432	.00056	.00007	.00362	.00139	.00023	H <sub>FE</sub> "

Table 5 Thrusts on Arches Produced by Applying a Unit Force to the right at the Neutral Point of Joint, C. (Minus sign means arch in tension)

II		I			System			
		80'	60'	40'	80'	60'	40'	H <sub>P</sub>
- .00839	- .00216	- .00024	- .02376	- .00670	- .00087	HAB		
- .01712	- .00840	- .00216	- .02833	- .01545	- .00486	H'AB		
- .00839	- .00216	- .00024	- .02376	- .00670	- .00087	HBA		
- .01712	- .00840	- .00216	- .02833	- .01545	- .00486	H'B A		
- .05814	- .03021	- .00993	- .08889	- .04837	- .01799	HBC		
.01724	.00819	.00212	.02472	.01336	.00424	H'BC		
- .00782	- .00277	- .00049	- .01486	- .00569	- .00112	H"BC		
- .05814	- .03021	- .00093	- .08889	- .04837	- .01799	HCB		
- .00782	- .00277	- .00049	- .01486	- .00569	0.00112	H'C B		
.01724	.00819	.00212	.02472	.01336	.00424	H"CB		
.03637	.01817	.00638	.05856	.03067	.01104	HCD		
.00665	.00239	.00044	.01218	.00472	.00096	H'C D		
- .01165	- .00494	- .00128	- .01963	- .00876	- .00233	HCD		
.03637	.01817	.00638	.05856	.03067	.01104	HDC		
- .01165	- .00494	- .00128	- .01963	- .00876	- .00233	H'DC		
.00665	.00239	.00044	.01218	.00472	.00096	H"DC		
.00152	.00039	.00004	.00390	.00095	.00014	HDE		
.01370	.00573	.00144	.02395	.01057	.00273	H'DE		
- .00362	- .00135	- .00026	- .00609	- .00257	- .00056	H"DE		
.00152	.00039	.00004	.00390	.00095	.00014	HED		
- .00362	- .00135	- .00026	- .00609	- .00257	- .00056	H'E D		
.01370	.00573	.00144	.02395	.01057	.00273	HED		
.00193	.00011	.00003	.00638	.00143	.00013	HEF		
.00372	.00139	.00026	.00698	.00297	.00064	H'E F		
.00193	.00011	.00003	.00638	.00143	.00013	HFF		
.00372	.00139	.00026	.00698	.00297	.00064	H"FF		

Table 6 Thrusts on Arches Produced by Applying a Unit Couple in the clockwise direction at the Neutral Point of Joint B. (Minus sign means arch in tension )

II		I		System	
80'	60'	40'	80'	60'	40'
- .00014	-.00005	-.00001	-.00033	-.00014	-.00004
- .00479	-.00464	-.00406	-.00610	-.00637	-.00599
- .00014	-.00005	-.00001	-.00033	-.00014	-.00004
- .00474	-.00464	-.00406	-.00610	-.00637	-.00599
- .00019	-.00010	-.00003	-.00035	-.00019	-.00007
.00461	.00451	.00399	.00532	.00551	.00523
- .00089	-.00074	-.00047	-.00113	-.00104	-.00073
- .00019	-.00010	-.00003	-.00035	-.00019	-.00007
- .00089	-.00074	-.00047	-.00113	-.00104	-.00073
.00461	.00451	.00399	.00532	.00551	.00523
.00014	.00007	.00003	.00027	.00015	.00005
.00076	.00064	.00042	.00093	.00087	.00062
- .00021	- .00014	- .00006	- .00030	- .00022	- .00011
.00014	.00007	.00003	.00027	.00015	.00005
- .00021	- .00014	- .00006	- .00030	- .00022	- .00011
.00076	.00064	.00042	.00093	.00087	.00062
.00004	.00001	0	.00007	.00003	.00001
.00025	.00017	.00007	.00036	.00027	.00013
- .00007	- .00004	- .00001	- .00009	- .00007	- .00003
.00004	.00001	0	.00007	.00003	.00001
- .00007	- .00004	- .00001	- .00009	- .00007	- .00003
.00025	.00017	.00007	.00036	.00027	.00013
.00004	.00001	0	.00010	.00003	.00001
.00007	.00004	.00001	.00010	.00008	.00003
.00004	.00001	0	.00010	.00003	.00001
.00007	.00004	.00001	.00010	.00008	.00003
.00004	.00001	0	.00010	.00003	.00001
.00007	.00004	.00001	.00010	.00008	.00003
.00004	.00001	0	.00010	.00003	.00001
.00007	.00004	.00001	.00010	.00008	.00003
.00004	.00001	0	.00010	.00003	.00001
.00007	.00004	.00001	.00010	.00008	.00003

Table 7 Thrusts on Arches Produced by Applying a Unit Couple in the clockwise direction at the Neutral Point of Joint, C. (Minus sign means arch in tension)

II		I		System	
80'	60'	40'	80'	60'	40'
- .00045	- .00021	- .00006	- .00096	- .00053	- .00012
- .00084	- .00072	- .00046	- .00102	- .00108	- .00080
- .00045	- .00021	- .00006	- .00096	- .00053	- .00012
- .00084	- .00072	- .00046	- .00102	- .00108	- .00080
.00025	.00012	.00004	.00044	.00028	.00010
.00082	.00070	.00046	.00089	.00093	.00070
- .00375	- .00337	- .00268	- .00466	- .00455	- .00375
.00025	.00012	.00004	.00044	.00028	.00010
- .00375	- .00337	- .00268	- .00466	- .00455	- .00375
.00082	.00070	.00046	.00089	.00093	.00070
- .00006	- .00002	- .00001	- .00010	- .00006	- .00002
.00318	.00291	.00238	.00382	.00378	.00319
- .00073	- .00059	- .00036	- .00091	- .00079	- .00051
- .00006	- .00002	- .00001	- .00010	- .00006	- .00002
- .00073	- .00059	- .00036	- .00091	- .00079	- .00051
.00318	.00291	.00238	.00382	.00378	.00319
.00012	.00005	.00001	.00022	.00012	.00004
.00086	.00068	.00041	.00111	.00095	.00060
- .00023	- .00016	- .00007	- .00029	- .00024	- .00013
.00012	.00005	.00001	.00022	.00012	.00004
- .00023	- .00016	- .00007	- .00029	- .00024	- .00013
.00086	.00068	.00041	.00011	.00095	.00060
.00012	.00005	.00001	.00030	.00013	.00003
.00024	.00017	.00007	.00033	.00028	.00014
.00012	.00005	.00001	.00030	.00013	.00003
.00024	.00017	.00007	.00033	.00028	.00014

Table 8 Max. L.L. Kerns Moments at Springings

Max M <sub>KL</sub> at	H <sub>P</sub> in ft	Value of $\frac{M_{KL}}{P}$ when Live Load on Span					Considering 5-Spans		Considering 3-Spans only	
		A B in ft	B C in ft	C D in ft	D E in ft	E F in ft	Total $\frac{M_{KL}}{P}$ in ft	Cor- res. F.E. Val- ues	Total $(\frac{M_{KL}}{P})_{max}$ in ft	% Error
A of Arch	80	+ 317.00 - 1015.00	+ 666.00 - 26.50	+ 222.00 - 21.20	+ 42.30 - 10.60	+ 21.20 $\approx 0$	+1268.50 - 1073.30	158.00 178.00	+1205.00 - 1062.70	- 5.00 - 0.99
	60	+ 454.50 - 889.00	+ 549.50 - 31.80	+ 116.20 - 21.20	+ 21.20 - 7.40	$\approx 0$ $\approx 0$	+1141.40 - 949.40	142.20 157.20	+1120.20 - 942.00	- 1.85 - 0.78
	40	+ 602.50 - 762.00	+ 359.40 - 42.30	+ 63.40 - 21.20	$\approx 0$ $\approx 0$	$\approx 0$ $\approx 0$	+1025.30 - 825.50	127.80 136.70	+1025.30 - 825.50	$\approx 0$ $\approx 0$
	A B Fixed Ends	+ 803.00 - 603.00								
B of Arch	80	+ 74.00 - 952.00	+ 740.00 - 63.50	+ 208.00 - 34.90	+ 63.40 $\approx 0$	+ 21.20 $\approx 0$	+1106.60 - 1050.40	137.80 174.00	+1022.00 - 1050.40	- 7.65 $\approx 0$
	60	+ 158.50 - 793.00	+ 666.00 - 74.00	+ 179.80 - 40.20	+ 42.30 - 4.20	$\approx 0$ $\approx 0$	+1046.60 - 911.40	130.10 151.00	+1004.30 - 907.20	- 4.04 - 0.46
	40	+ 327.50 - 666.00	+ 518.00 - 84.60	+ 105.80 - 42.30	+ 10.60 - 6.20	$\approx 0$ $\approx 0$	+ 961.90 - 799.10	119.80 132.50	+ 951.30 - 792.90	- 1.10 - 0.78
	A B Fixed Ends	+ 803.00 - 603.00								
B of Arch	80	+ 856.00 - 21.20	+ 158.70 - 1174.00	+ 317.40 - 31.70	+ 84.60 - 2.00	+ 31.80 $\approx 0$	+1448.50 - 1228.90	150.40 173.20	+1332.10 - 1226.90	- 8.04 - 0.16
	60	+ 771.50 - 31.70	+ 232.50 - 1015.00	+ 264.40 - 39.10	+ 63.50 - 5.00	$\approx 0$ $\approx 0$	+1331.90 - 1090.80	138.20 153.80	+1268.40 - 1085.80	- 4.76 - 0.46
	40	+ 571.00 - 42.30	+ 402.00 - 867.50	+ 190.40 - 42.30	+ 21.20 - 9.00	$\approx 0$ $\approx 0$	+1184.60 - 961.10	123.20 135.60	+1163.40 - 952.10	- 1.79 - 0.94
	B C Fixed Ends	+ 962.50 - 709.00								
C of Arch	80	+ 508.00 - 3.20	+ 169.20 - 1185.00	+ 603.00 - 84.60	+ 201.00 - 10.60	+ 74.00 $\approx 0$	+1555.20 - 1283.40	161.60 181.00	+1280.20 - 1272.80	- 17.68 - 0.83
	60	+ 423.00 - 7.40	+ 296.20 - 1079.00	+ 539.50 - 87.80	+ 137.50 - 9.50	+ 42.30 $\approx 0$	+1438.50 - 1183.70	149.30 167.00	+1258.70 - 1174.20	- 12.50 - 0.80
	40	+ 327.90 - 10.60	+ 481.50 - 952.00	+ 402.00 - 90.00	+ 63.50 - 7.40	+ 10.60 $\approx 0$	+1285.50 - 1060.00	133.60 149.50	+1211.40 - 1052.60	- 5.76 - 0.70
	B C Fixed Ends	+ 962.50 - 709.00								
C of Arch	80	+ 402.00 - 8.50	+ 740.50 - 95.20	+ 412.50 - 1440.00	+ 370.50 - 21.20	+ 190.40 - 4.20	+2115.90 - 1569.10	144.90 142.60	+1523.50 - 1556.40	- 28.00 - 0.81
	60	+ 285.50 - 12.70	+ 666.00 - 105.80	+ 560.50 - 1312.00	+ 317.50 - 24.40	+ 137.50 - 5.30	+1967.00 - 1460.20	134.80 132.80	+1544.00 - 1442.20	- 21.50 - 1.23
	40	+ 137.50 - 21.20	+ 497.00 - 99.50	+ 835.50 - 1090.00	+ 222.20 - 31.80	+ 63.50 - 8.50	+1755.70 - 1251.00	120.20 113.90	+1554.70 - 1221.30	- 11.44 - 2.37
	C D Fixed Ends			+1460.00 - 1100.00						

Table 9 Max. L.L. Lower Kern Moments at Crowns

Max $M_{KL}$ at Crown of Arch	$H_P$ in ft	Value of $\frac{M_{KL}}{P}$ when Live Load on Span					Considering 5 spans		Considering 1-Span for + $M_{KL}$ & 3-Span for - $M_{KL}$	
		A B	B C	C D	D E	E F	Total $\frac{M_{KL}}{P}$	% of Cor- res. F.E. Val- ues	Total $\frac{M_{KL}}{P}$	% Error
		in ft	in ft	in ft	in ft	in ft	in ft	in ft	in ft	
A B	80	+370.50	+ 7.40	+ 3.70	≈0	≈0	+381.60	212.00	+370.50	- 2.91
		- 31.70	-179.90	- 63.50	≈0	≈0	-275.10	289.80	-275.10	≈0
	60	+317.50	+ 8.50	+ 4.20	≈0	≈0	+330.20	183.40	+317.50	- 3.85
		- 47.50	-158.80	- 52.90	≈0	≈0	-259.20	273.00	-259.20	≈0
	40	+254.00	+ 10.60	+ 5.30	≈0	≈0	+269.00	150.00	+254.00	- 5.90
		- 74.00	-105.80	- 21.20	≈0	≈0	-201.00	211.60	-201.00	≈0
B C	Fixed Ends	+179.90								
		- 95.00								
	80	+ 3.70	+487.00	+ 7.40	≈0	≈0	+498.10	209.20	+487.00	- 2.23
		-201.00	- 63.50	-127.00	- 52.90	≈0	-444.00	300.00	-391.10	-11.90
	60	+ 4.20	+412.50	+ 8.50	≈0	≈0	+425.20	178.60	+412.50	- 2.99
		-169.20	- 84.60	-105.80	- 31.70	0	-391.30	264.00	-359.60	- 8.10
C D	40	+ 5.30	+338.50	+ 10.60	≈0	≈0	+364.40	152.90	+338.50	- 7.10
		-105.80	-105.80	- 74.00	- 10.00	≈0	-295.60	199.50	-294.60	- 3.40
	Fixed Ends	+238.00								
		-148.00								
	80	+ 5.00	+ 10.00	+508.00	+ 10.00	+ 5.00	+538.00	181.70	+508.00	- 5.68
		- 52.90	-121.70	- 84.60	-121.70	-52.90	-433.80	256.00	-328.00	-24.40
C D	60	+ 5.30	+ 10.50	+455.00	+ 10.50	+ 5.30	+486.60	164.00	+455.00	- 6.50
		- 42.30	-105.80	-105.80	-105.80	-42.30	-402.00	238.00	-317.40	-21.00
	40	+ 5.50	+ 10.60	+391.50	+ 10.60	+ 5.50	+423.70	143.00	+391.50	- 7.60
		- 15.90	- 79.30	-148.00	- 79.30	-15.90	-338.40	202.00	-306.60	- 9.70
	Fixed Ends			+296.30						
				-169.00						

Table 10 Max. L.L. Right Kern Moments at Pier Tops

Pier	$H_p$ in ft	Value of $\frac{M_{KRPT}}{P}$ when Live Load on Span					Considering 5 Spans  Total Max $\frac{M_{KRPT}}{P}$ in ft	Considering 2-Span only	
		A B in ft	B C in ft	C D in ft	D E in ft	E F in ft		Total Max $\frac{M_{KRPT}}{P}$ in ft	% Error
BG	80	+1883.00	+ 0	+ 116.30	$\approx$ 0	$\approx$ 0	+1999.30	+1883.00	- 6.18
		- 0	-1713.00	- 8.50	$\approx$ 0	$\approx$ 0	-1721.50	-1713.00	- 0.50
	40	+1079.00	+ 52.90	+ 74.10	$\approx$ 0	$\approx$ 0	+1206.00	+1131.90	- 6.14
		- 10.60	- 973.00	- 31.70	$\approx$ 0	$\approx$ 0	-1015.30	- 983.60	- 3.12
CH	80	+ 0	+1958.00	+ 84.60	+201.00	+95.20	+2338.80	+2042.60	-12.65
		- 84.60	- 0	-1588.00	- 10.60	- 3.20	-1686.40	-1588.00	- 5.83
	40	+ 21.20	+1196.00	+ 476.00	+158.80	+42.30	+1894.30	+1672.00	-11.73
		- 158.80	- 84.60	-1080.00	- 21.20	-10.60	-1355.20	-1164.60	-14.05

Table 11 Max. D.L. + L.L. Lower Kern Moments at Springings

M <sub>KL</sub> at	H <sub>P</sub> in ft	Due to Dead Load of Arch						Due to Live Load k-ft	Total DL+LL k-ft	% of Corresponding F.E. Values
		A B k-ft	B C k-ft	C D k-ft	D E k-ft	E F k-ft	Total k-ft			
A of Arch A B	80	-4830	4635	1760	295	147	2007	1269	3276	149.75
	60	-3006	3750	833	100	0	1677	1141	2818	128.75
	40	-1103	2296	370	0	0	1563	1025	2588	118.25
	F.E.	1383								
B of Arch A B	80	-6075	4900	1518	460	147	950	1107	2057	94.00
	60	-4385	4285	1219	276	0	1395	1047	2442	111.50
	40	-2340	3140	557	32	0	1389	962	2351	107.30
	F.E.	1383					1383	803	2186	
B of Arch B C	80	5775	-7355	2540	599	220	1779	1449	3228	115.10
	60	5150	-5670	1975	424	0	1879	1332	3211	114.60
	40	3660	-3373	1299	88	0	1674	1185	2859	112.20
	F.E.	1838					1838	963	2801	
C of Arch B C	80	3490	-7360	4545	1378	512	2565	1555	4120	147.00
	60	2875	-5672	3952	928	293	2376	1439	3815	136.00
	40	2195	-3407	2735	406	73	2002	1286	3288	117.50
	F.E.	1838					1838	963	2801	
C of Arch C D	80	2722	4575	-9015	2530	1288	2100	2116	4216	91.30
	60	1888	4060	-6585	2124	915	2402	1967	4369	94.75
	40	805	2875	-2232	1378	381	3207	1756	4963	107.50
	F.E.			3144			3155	1460	4615	

Table 12 Max. D.L.+ L.L. Lower Kern Moments at Crowns

Span	H <sub>p</sub> in ft	Due to D.L. of Arch						Due to LL k-ft	Total DL+ LL k-ft	% of Corresponding F.E. Values
		A B k-ft	B C k-ft	C D k-ft	D E k-ft	E F k-ft	Total k-ft			
A B	80	2343	-1250	-525	≈ 0	≈ 0	567	382	949	123.90
	60	1867	-1087	-427	≈ 0	≈ 0	353	330	683	89.10
	40	1244	- 689	-139	≈ 0	≈ 0	416	270	686	89.35
	F.E.	587					587	180	767	
B C	80	-1364	3065	-1049	-383	≈ 0	269	498	767	86.25
	60	-1141	2375	- 853	-230	≈ 0	151	425	576	64.85
	40	- 695	1687	- 556	- 73	≈ 0	363	364	727	81.70
	F.E.		652				652	238	890	
C D	80	- 332	- 809	3715	-809	-332	1433	538	1971	139.50
	60	- 256	- 691	3060	-691	-256	1166	487	1653	116.90
	40	- 72	- 498	2135	-498	- 72	995	424	1419	100.20
	F.E.			1117			1117	296	1413	

Table 13 Max. D.L. + L.L. Compressive Upper Extreme Fiber Stresses  
in Arches

Span	Location	$H_p$ in ft	Total Max $M_{KL}$ k - ft	$f_{cu} = \frac{M_{KL}C_T}{I}$ * psi	% of allowable fiber stress 1,350 psi
A B & E F	Springings A & F	80	3276	1580	117.00
		60	2818	1360	100.70
		40	2588	1250	92.60
	Crowns	80	949	1100	81.50
		60	683	790	58.50
		40	686	794	58.80
B C & D E	Springings C & D	80	4120	1564	116.00
		60	3815	1446	107.00
		40	3288	1248	92.40
	Crowns	80	767	760	56.30
		60	576	572	42.40
		40	727	722	53.50
C D	Springing C & D	80	4216	890	66.00
		60	4369	922	68.30
		40	4963	1048	77.60
	Crowns	80	1971	1282	95.00
		60	1653	1076	79.70
		40	1419	922	68.30

\* I based on total depth of rib steel ignored.

Table 14 Max. D.L. + L.L. Compressive Left Extreme  
Fiber Stresses at Pier Tops

Pier	$H_p$ in ft	$M_{KRPT}$ Due to D.L. of Arch						$M_{KRPT}$ due to L.L. k-ft	Total Max. $M_{KRPT}$ k-ft	$f_c = \frac{MC}{I}$ p.s.i.
		A k-ft	B k-ft	C k-ft	D k-ft	E k-ft	F k-ft			
BG & EJ	80 40	13,020 7,385	-12,410 - 6,670	945 372	0 0	0 0	1555 1087	1999 1206	3554 2293	702 453
CH & DI	80 40	- 585 - 952	14,190 8,055	-13,180 - 5,300	1380 998	637 220	2442 3021	2339 1894	4781 4915	599 640

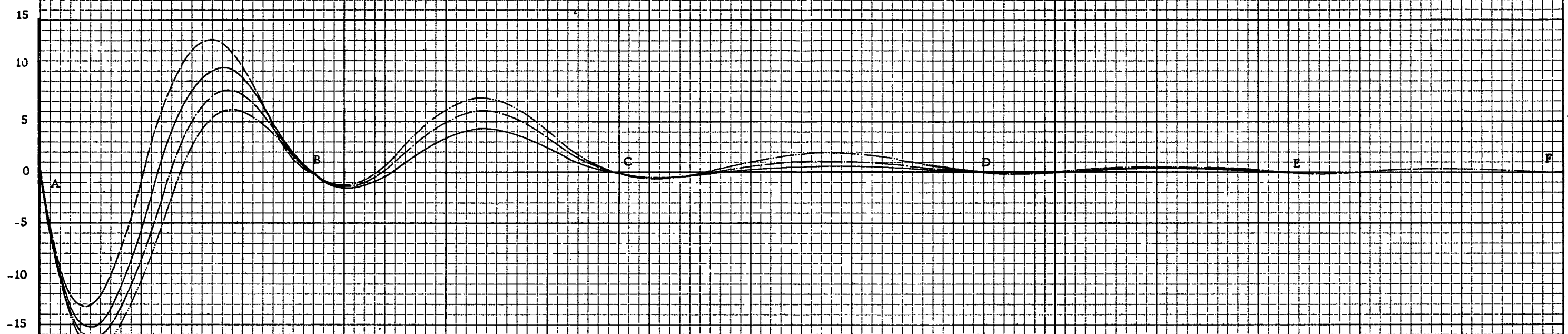
FIG. 5 INFLUENCE LINES FOR  $M_{KL}$  AT SPRINGING A,  
SYSTEM I

FOR FIXED ENDS

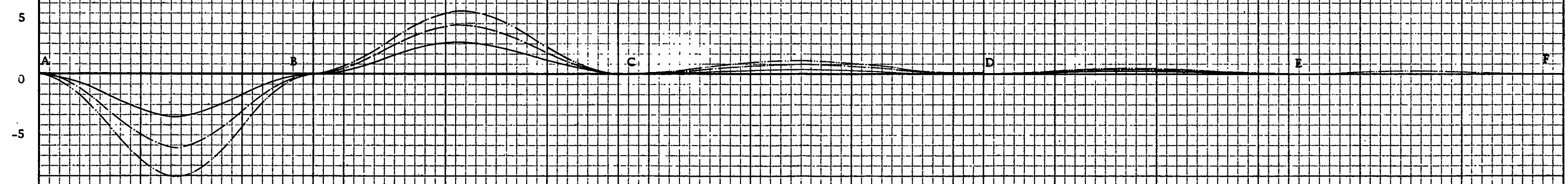
FOR  $H_p = 40$  FT.

FOR  $H_p = 60$  FT.

FOR  $H_p = 80$  FT.



COMPONENT OF  $M_{KL}$  CAUSED BY TRANSLATION OF PIER TOPS



COMPOSITION OF  $M_{KL}$  CAUSED BY ROTATION OF PIER TOPS

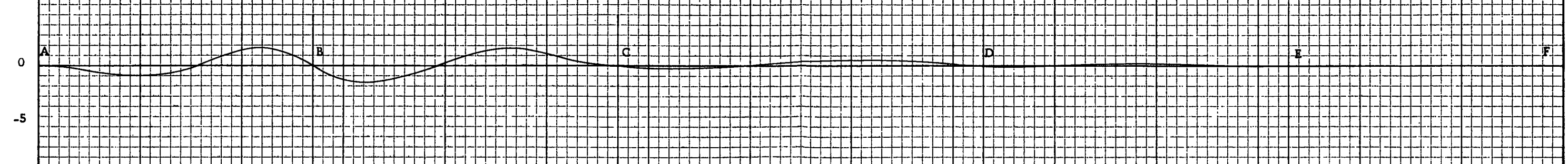


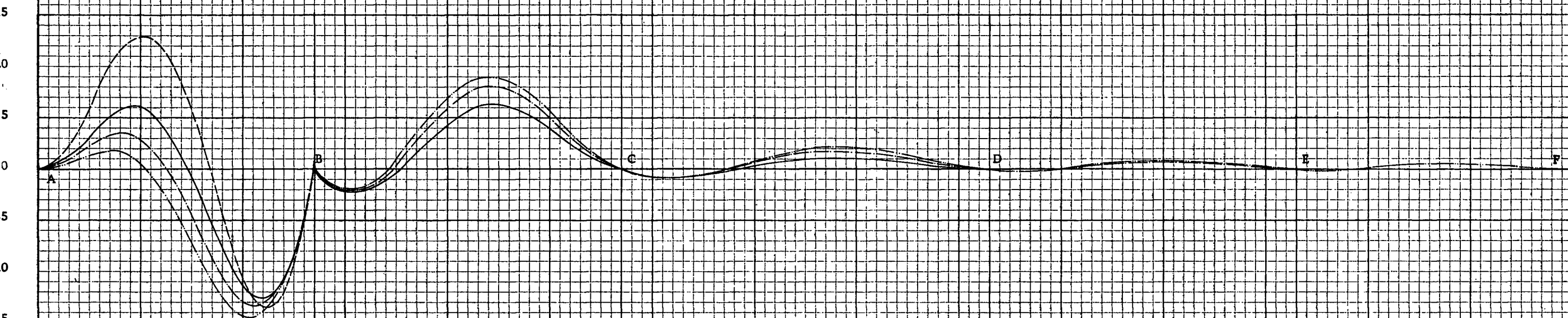
FIG. 6 INFLUENCE LINES FOR  $M_{KL}$  AT SPRINGING B OF ARCH AB, SYSTEM-I

FOR FIXED ENDS

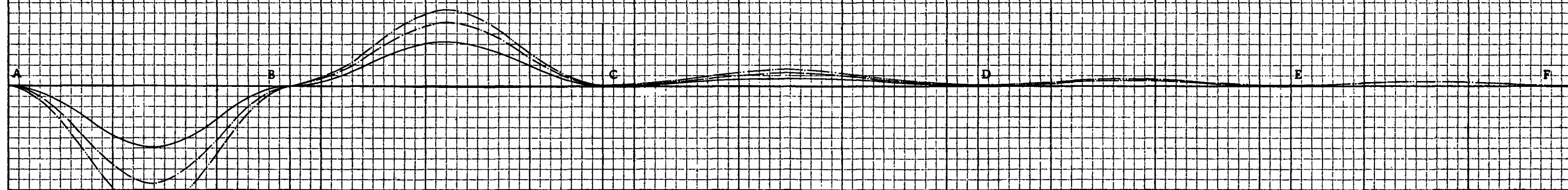
FOR  $H_p = 40$  FT.

FOR  $H_p = 60$  FT.

FOR  $H_p = 80$  FT.



COMPONENT OF  $M_{KL}$  CAUSED BY TRANSLATION OF PIER TOPS



COMPONENT OF  $M_{KL}$  CAUSED BY ROTATION OF PIER TOPS

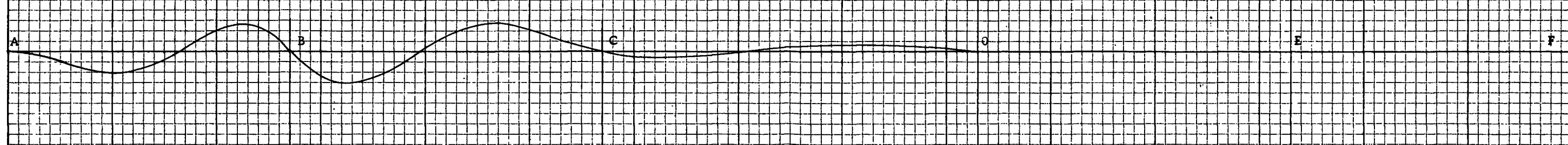


FIG. 7 INFLUENCE LINE FOR  $M_{KL}$  AT SPRINGING B OF ARCH BC, SYSTEM I

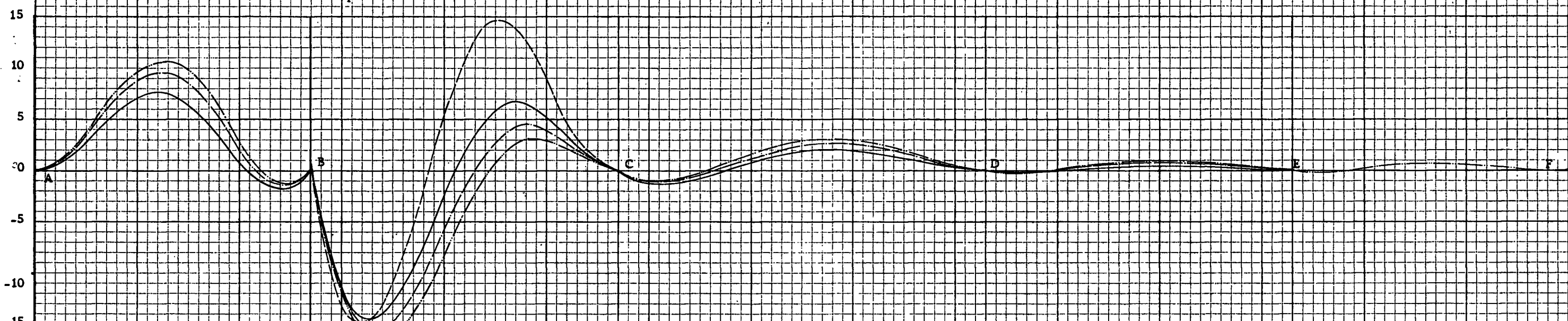
26

FOR FIXED ENDS

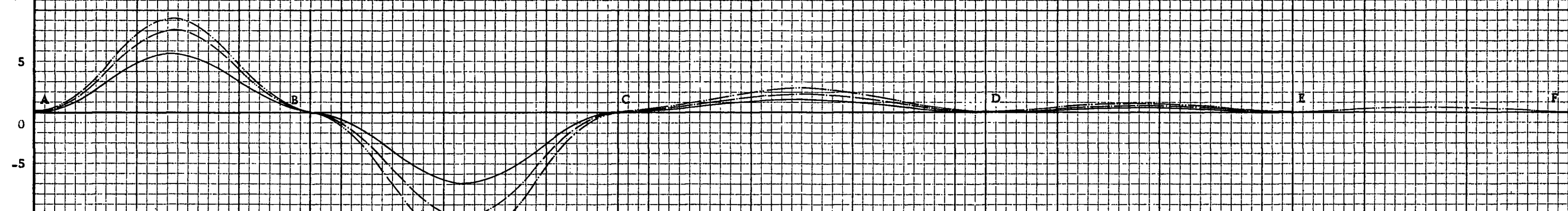
FOR  $H_p = 40$  FT.

FOR  $H_p = 60$  FT.

FOR  $H_p = 80$  FT.



COMPONENT OF  $M_{KL}$  CAUSED BY TRANSLATION OF PIER TOPS



COMPONENT OF  $M_{KL}$  CAUSED BY ROTATION OF PIER TOPS

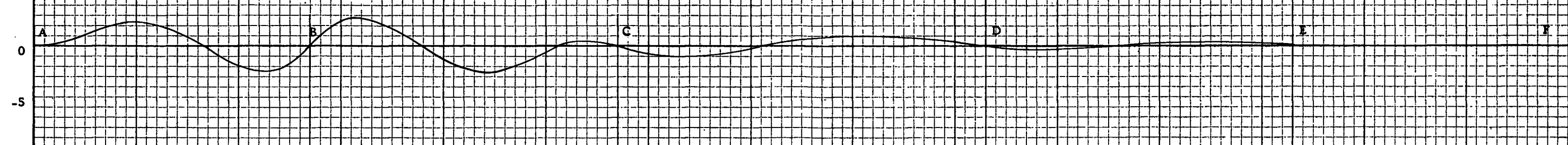


FIG. 8 INFLUENCE LINES FOR  $M_{KL}$  AT SPRINGING C OF ARCH BC, SYSTEM I

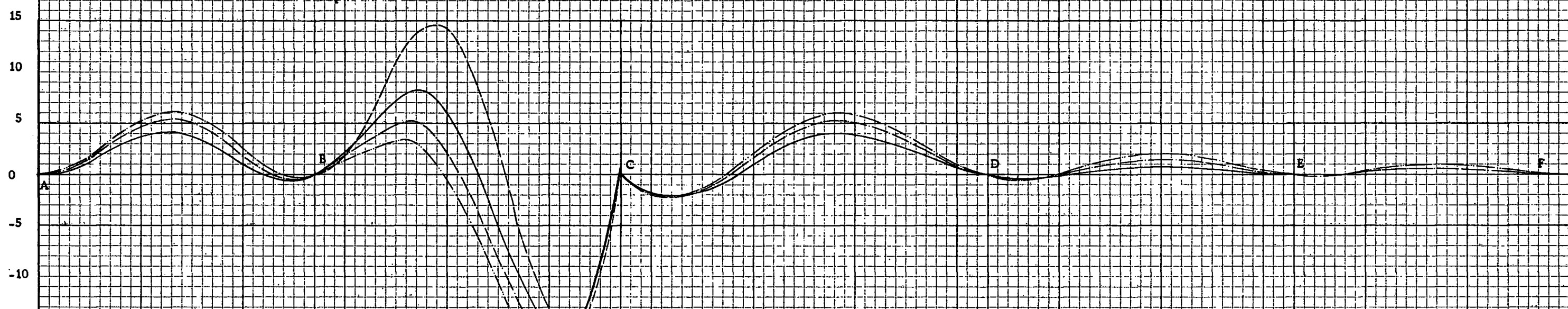
27

FOR FIXED ENDS

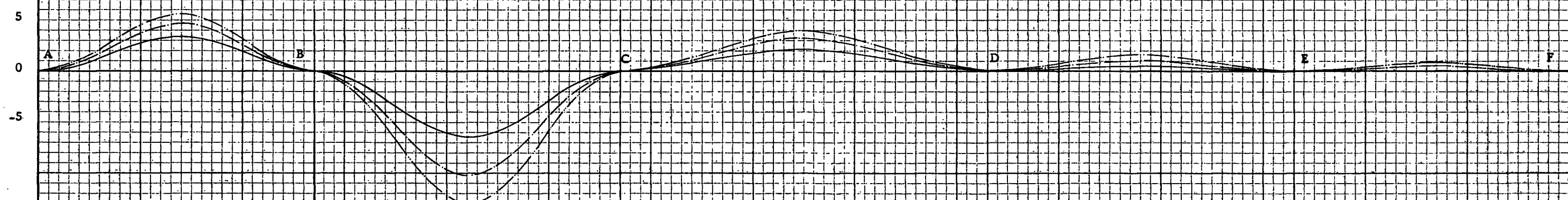
FOR  $H_p = 40$  FT.

FOR  $H_p = 60$  FT.

FOR  $H_p = 80$  FT.



COMPONENT OF  $M_{KL}$  CAUSED BY TRANSLATION OF PIER TOPS



COMPONENT OF  $M_{KL}$  CAUSED BY ROTATION OF PIER TOPS

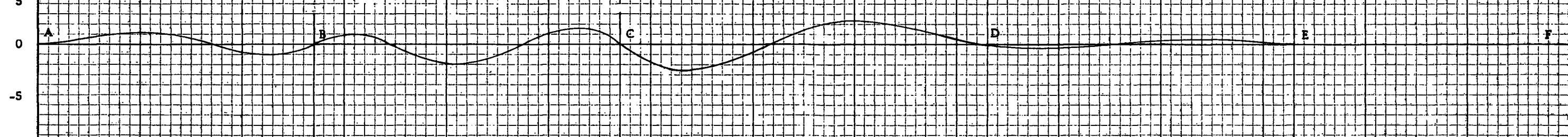


FIG. 9 INFLUENCE LINES FOR  $M_{KL}$  AT SPRINGING C OF ARCH CD, SYSTEM 1

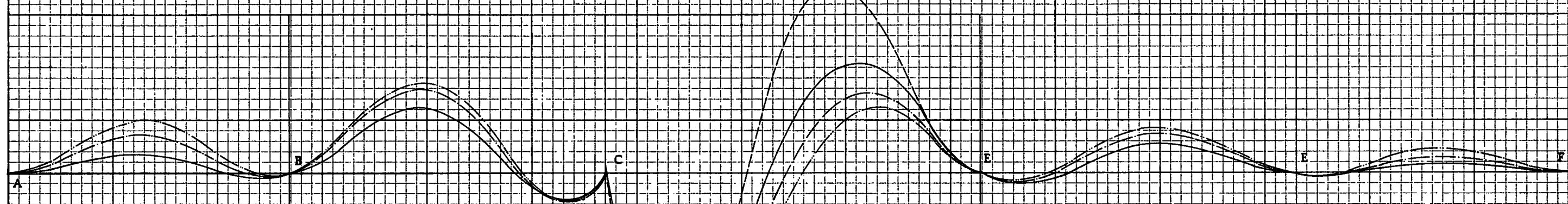
28

FOR FIXED ENDS

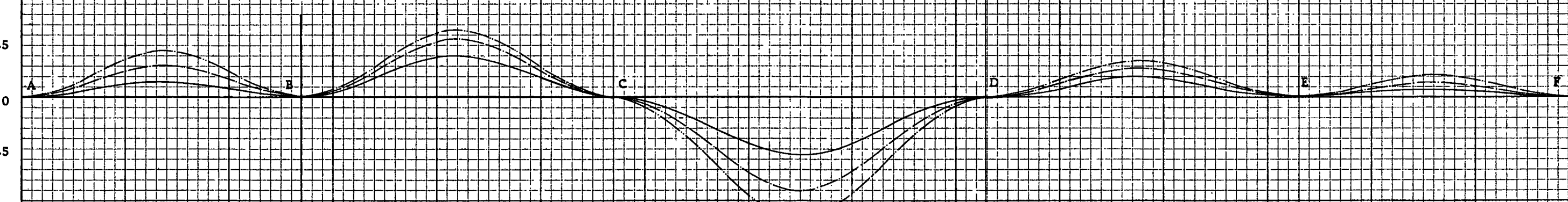
FOR  $H_p = 40$  FT.

FOR  $H_p = 60$  FT.

FOR  $H_p = 80$  FT.



COMPONENT OF  $M_{KL}$  CAUSED BY TRANSLATION OF PIER TOPS



COMPONENT OF  $M_{KL}$  CAUSED BY ROTATION OF PIER TOPS

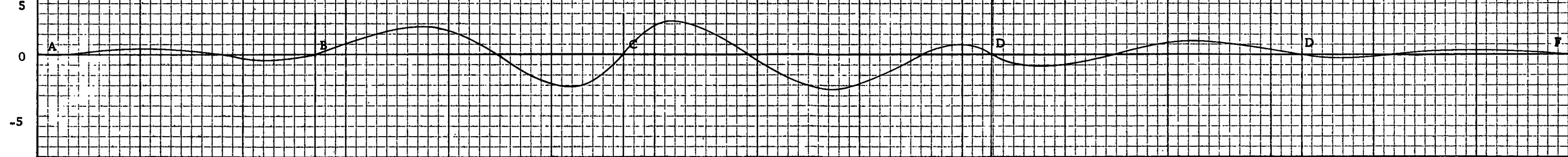


FIG. 10-INFLUENCE LINES FOR  $M_{KL}$  AT CROWN OF ARCH AB, SYSTEM I

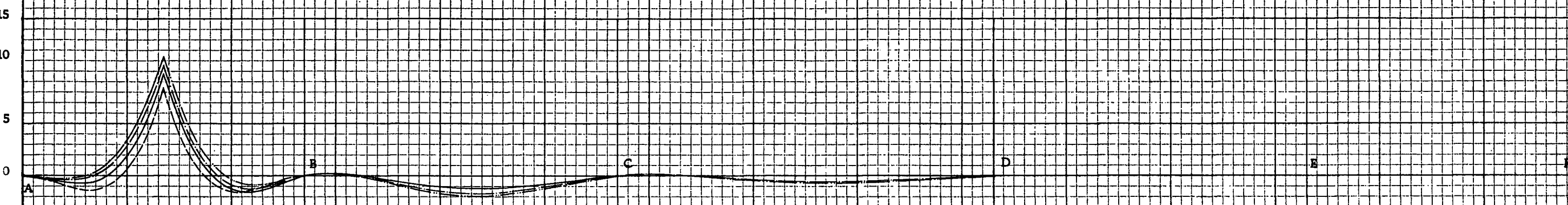
29

FOR FIXED ENDS

FOR  $H_B = 40$  FT.

FOR  $H_B = 60$  FT.

FOR  $H_B = 80$  FT.



COMPONENT OF  $M_{KL}$  CAUSED BY TRANSLATION OF PIER TOPS

COMPONENT OF  $M_{KL}$  CAUSED BY ROTATION OF PIER TOPS

FIG. 11 INFLUENCE LINES FOR  $M_{KL}$  AT CROWN OF ARCH BC, SYSTEM I

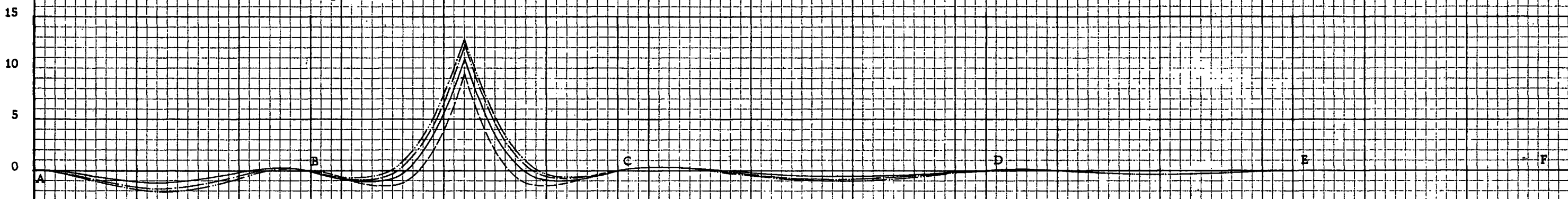
30

FOR FIXED ENDS

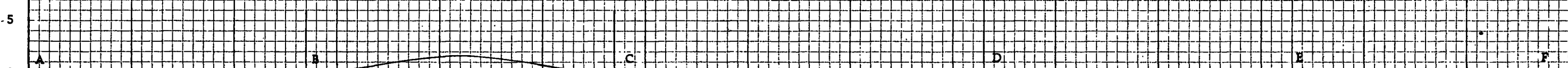
FOR  $H_2 = 40$  FT.

FOR  $H_p = 60$  FT.

FOR  $H_p = 80$  FT.



COMPONENT OF  $M_{KL}$  CAUSED BY TRANSLATION OF PIER TOPS



COMPONENT OF  $M_{KL}$  CAUSED BY ROTATION OF PIER TOPS

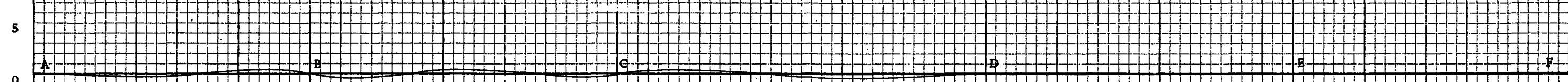


FIG. 12 INFLUENCE LINES FOR  $M_{KL}$  AT CROWN OF ARCH CD, SYSTEM I

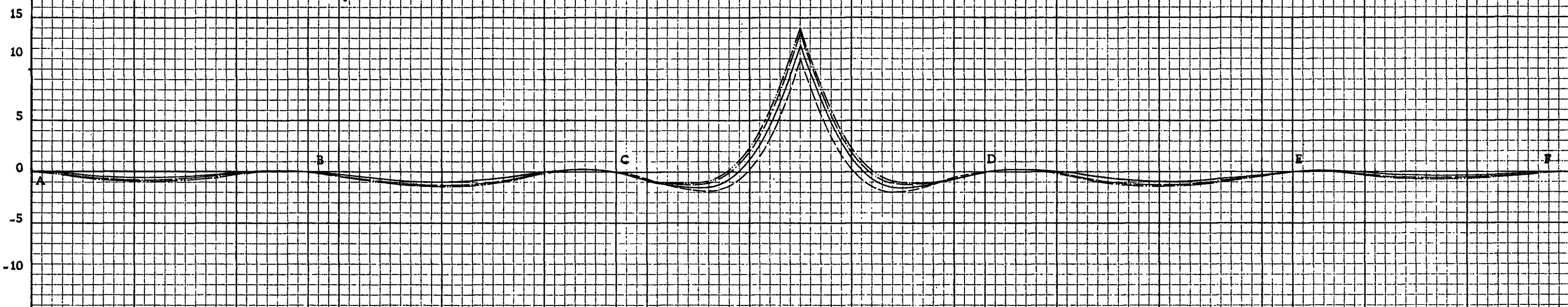
31

FOR FIXED ENDS

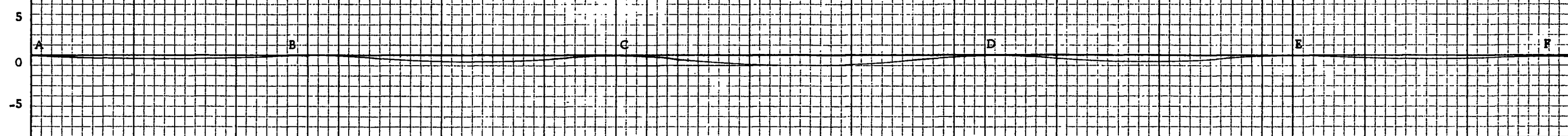
FOR  $H_p = 40$  FT.

FOR  $H_p = 60$  FT.

FOR  $H_p = 80$  FT.



COMPONENT OF  $M_{KL}$  CAUSED BY TRANSLATION OF PIER TOPS



COMPONENT OF  $M_{KL}$  CAUSED BY ROTATION OF PIER TOPS

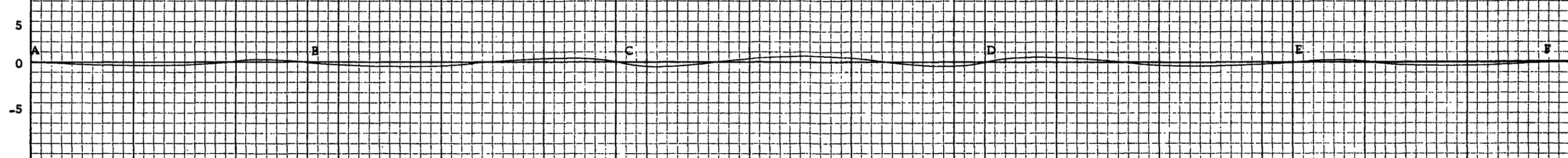
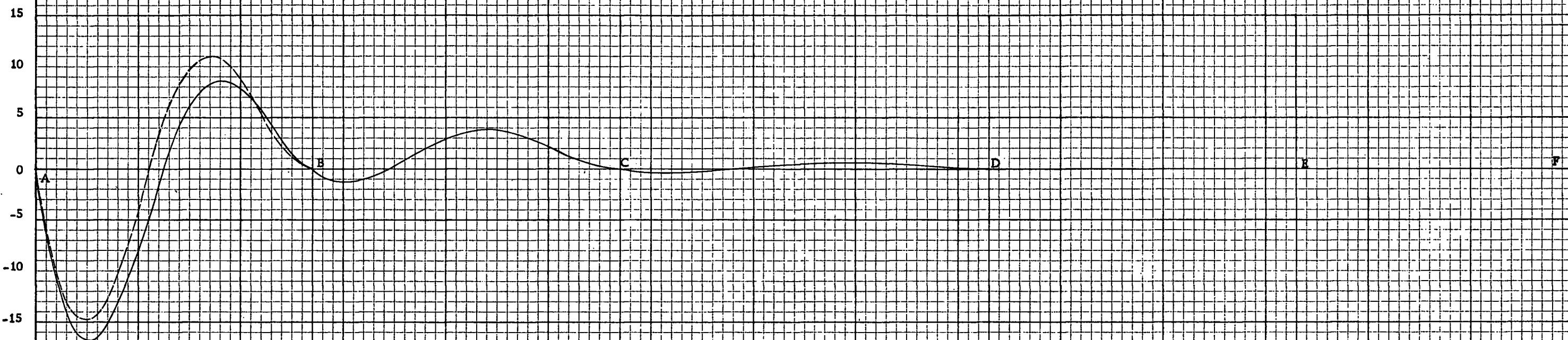


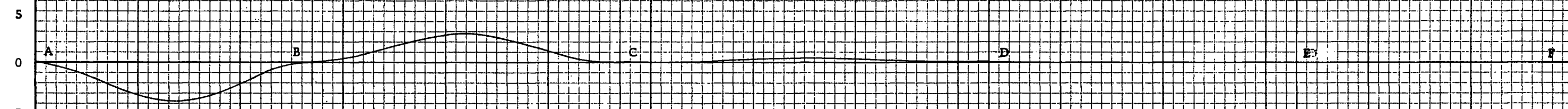
FIG. 13 INFLUENCE LINES FOR  $M_{KU}$  AT SPRINGING 'A'

SYSTEM I

FOR FIXED ENDS  
FOR  $H_F = 40$  FT.



COMPONENT OF  $M_{KU}$  CAUSED BY TRANSLATION OF PIER TOPS



COMPONENT OF  $M_{KU}$  CAUSED BY ROTATION OF PIER TOPS

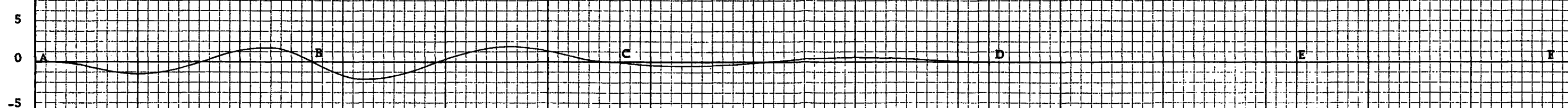
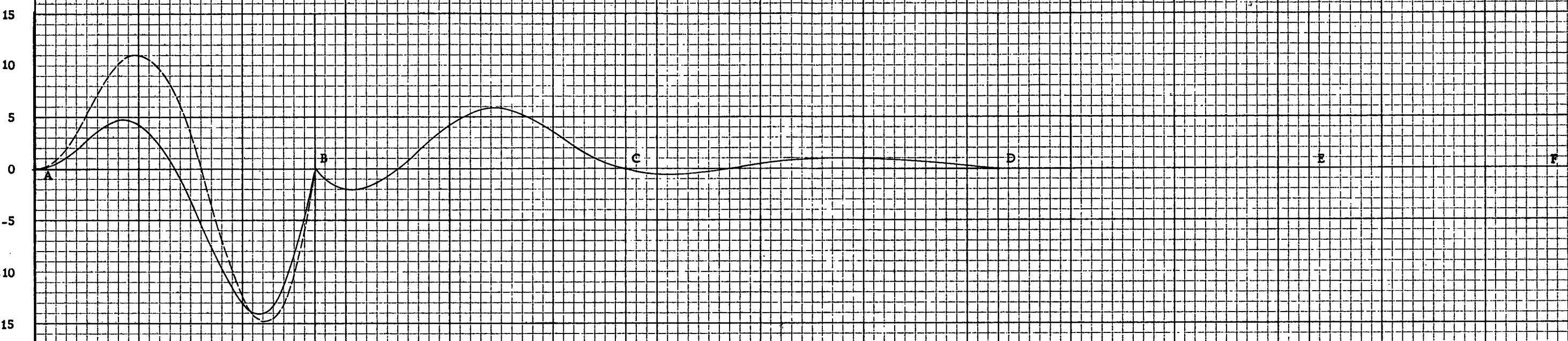


FIG. 14 INFLUENCE LINES FOR  $M_{KU}$  AT SPRINGING B OF ARCH AB<sub>1</sub> SYSTEM I

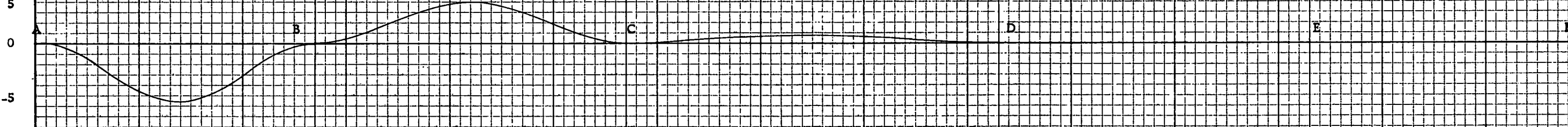
33

FOR FIXED ENDS

FOR  $H_p = 40$  FT.



COMPONENT OF  $M_{KU}$  CAUSED BY TRANSLATION OF PIER TOPS



COMPONENT OF  $M_{KU}$  CAUSED BY ROTATION OF PIER TOPS

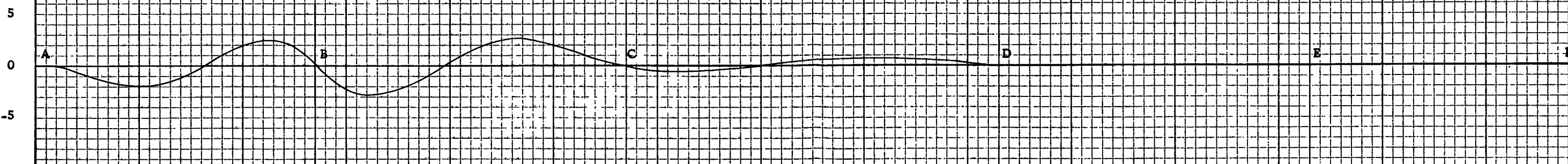


FIG. 15. INFLUENCE LINES FOR  $M_{KU}$  AT SPRINGING B OF ARCH BC, SYSTEM I

34

FOR FIXED ENDS  
FOR  $H_p = 40$  FT.

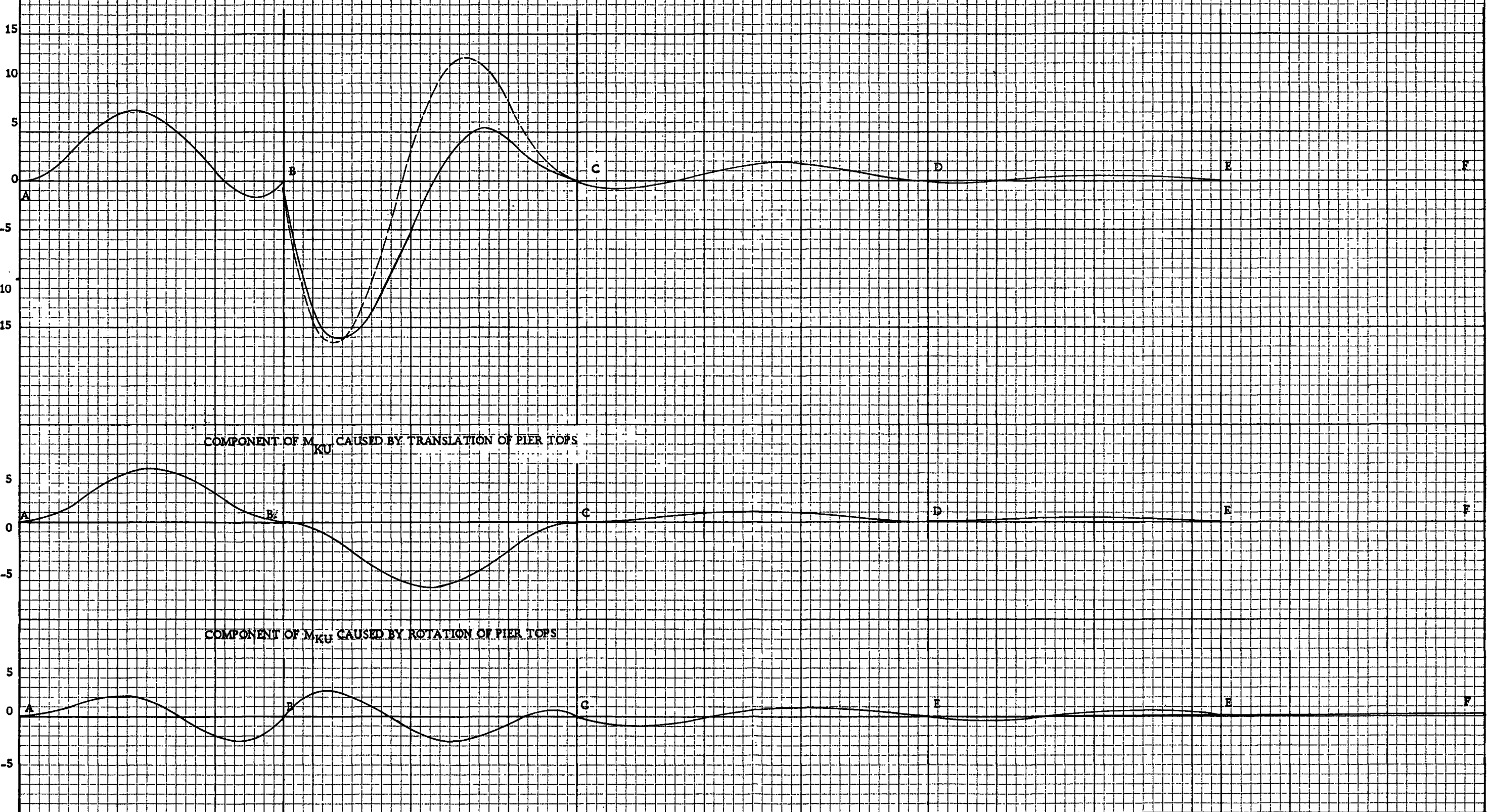
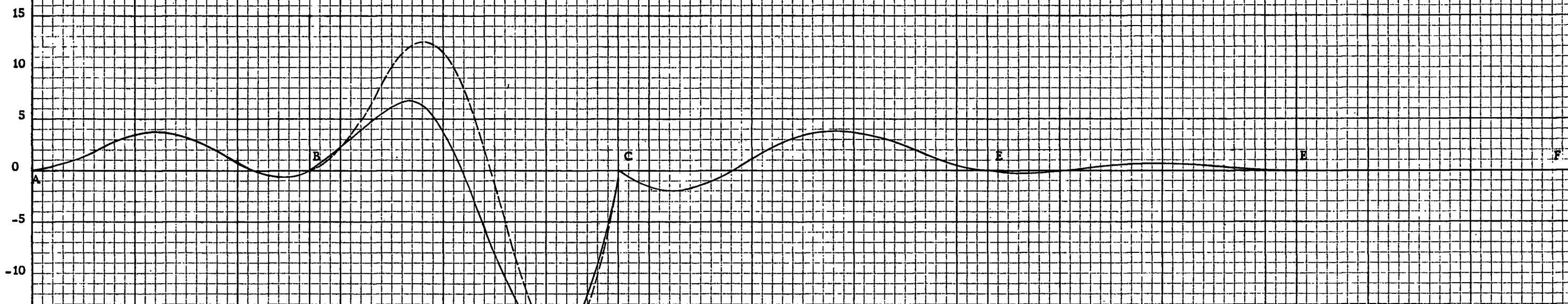


FIG. 16. INFLUENCE LINES FOR  $M_{KU}$  AT SPRINGING C OF ARCH BC, SYSTEM I

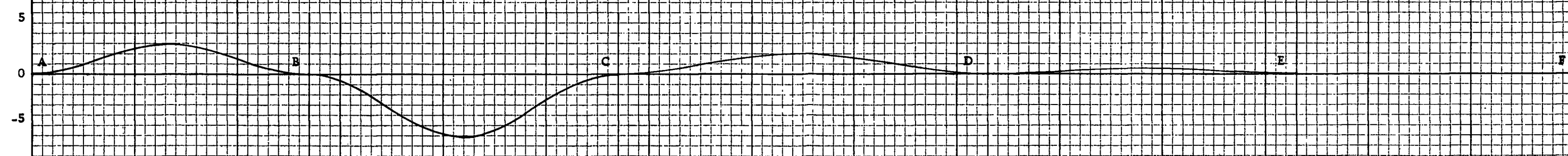
85

FOR FIXED ENDS

FOR  $H_p = 40$  FT



COMPONENT OF  $M_{KU}$  CAUSED BY TRANSLATION OF PIER TOPS



COMPONENT OF  $M_{KU}$  CAUSED BY ROTATION OF PIER TOPS

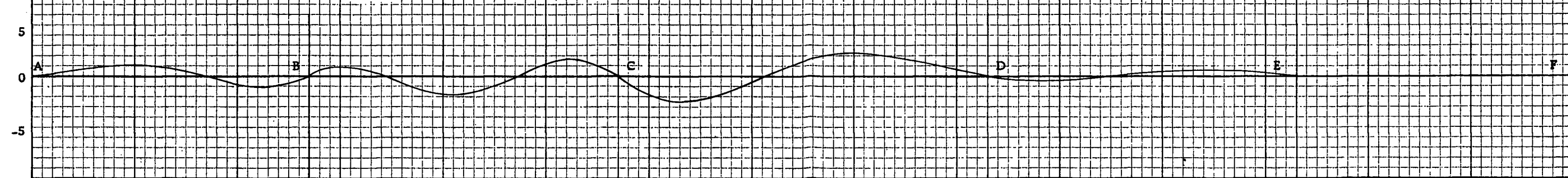


FIG. 17 INFLUENCE LINES FOR  $M_{KU}$  AT SPRINGING C OF ARCH CD, SYSTEM I

36

FOR FIXED ENDS

FOR  $H_P = 40$  FT.

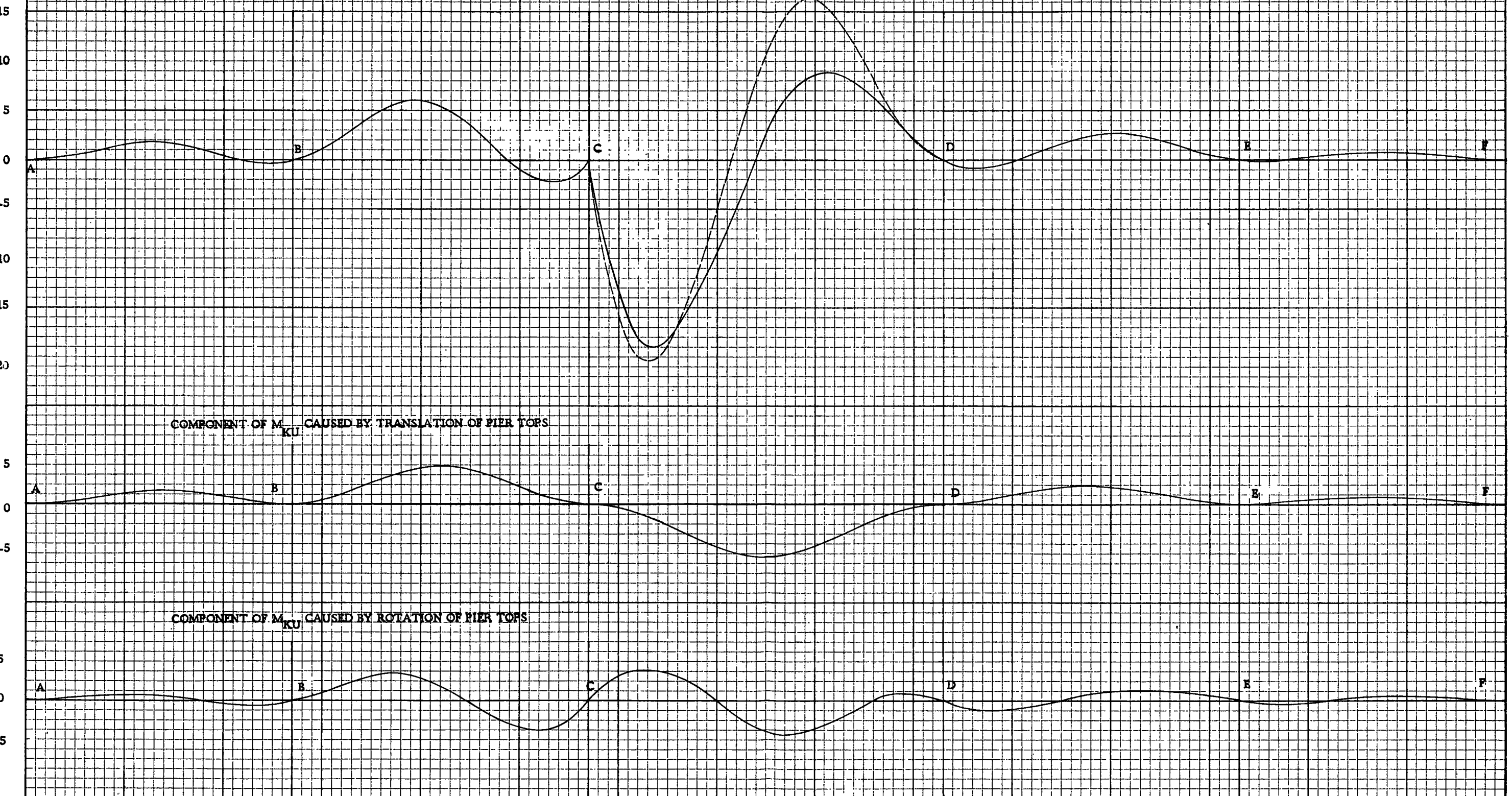
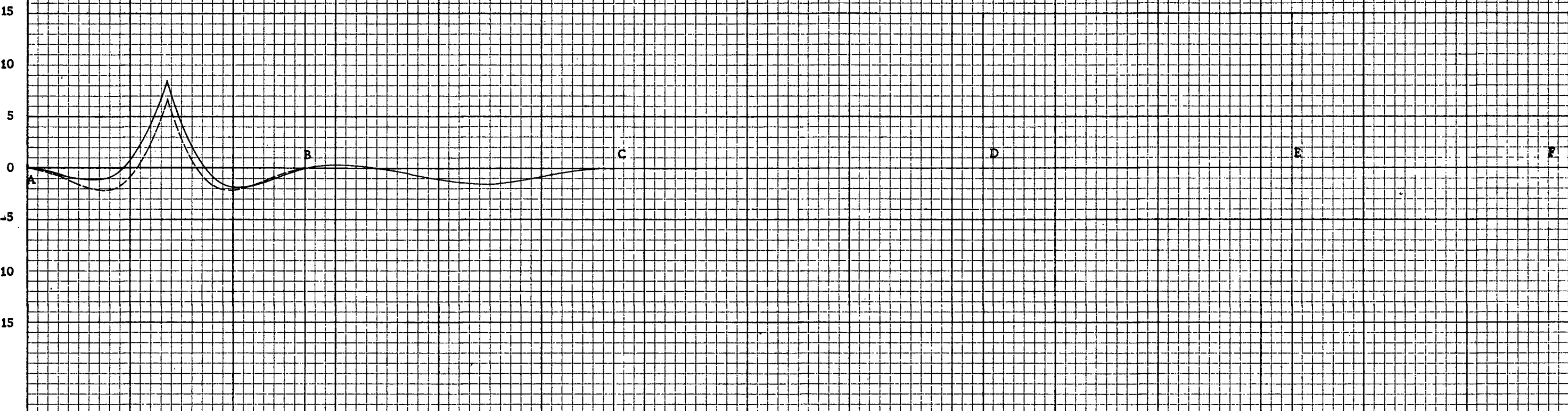


FIG. 18 INFLUENCE LINES FOR  $M_{KU}$  AT CROWN OF ARCH AB, SYSTEM I

FOR FIXED ENDS

FOR  $H_p = 40$  FT.



COMPONENT OF  $M_{KU}$  CAUSED BY TRANSLATION OF PIER TOPS

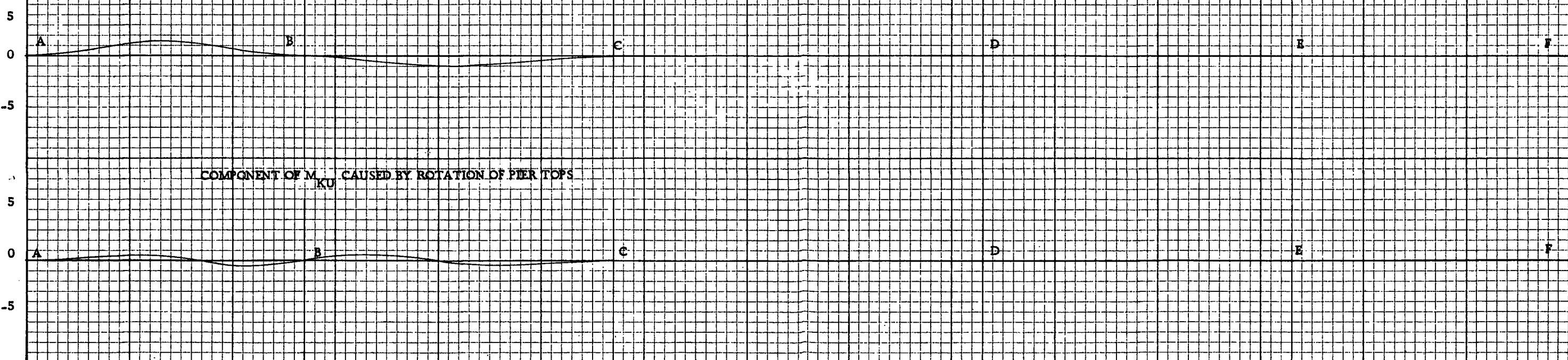
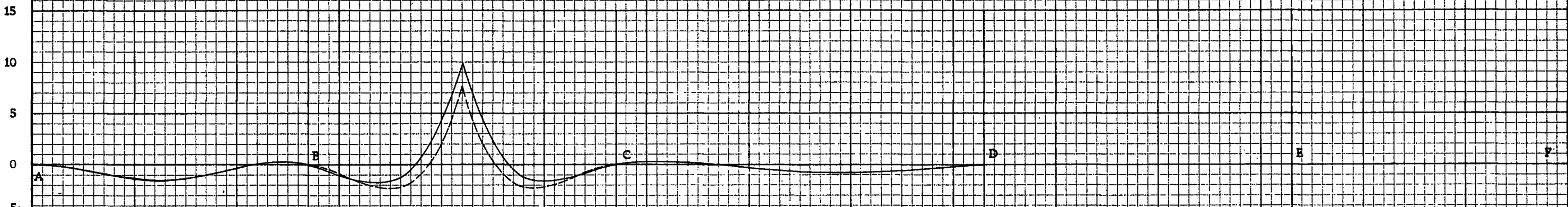


FIG. 19. INFLUENCE LINES FOR  $M_{KU}$  AT CROWN OF ARCH BC, SYSTEM I

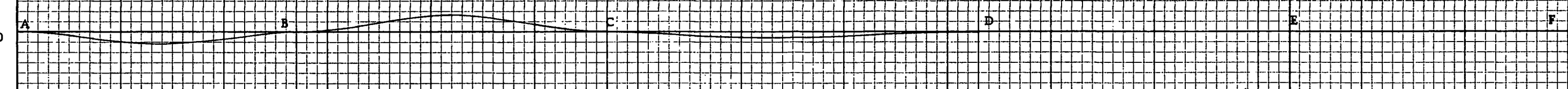
38

FOR FIXED ENDS

FOR  $H_p = 40$  FT.



COMPONENT OF  $M_{KU}$  CAUSED BY TRANSLATION OF PIER TOPS



COMPONENT OF  $M_{KU}$  CAUSED BY ROTATION OF PIER TOPS

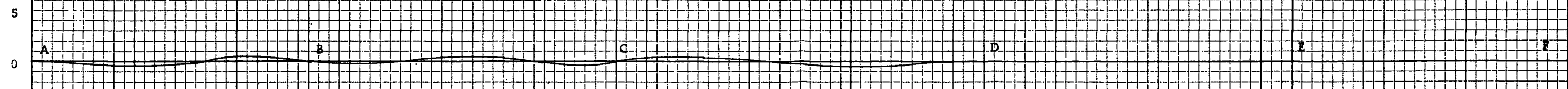
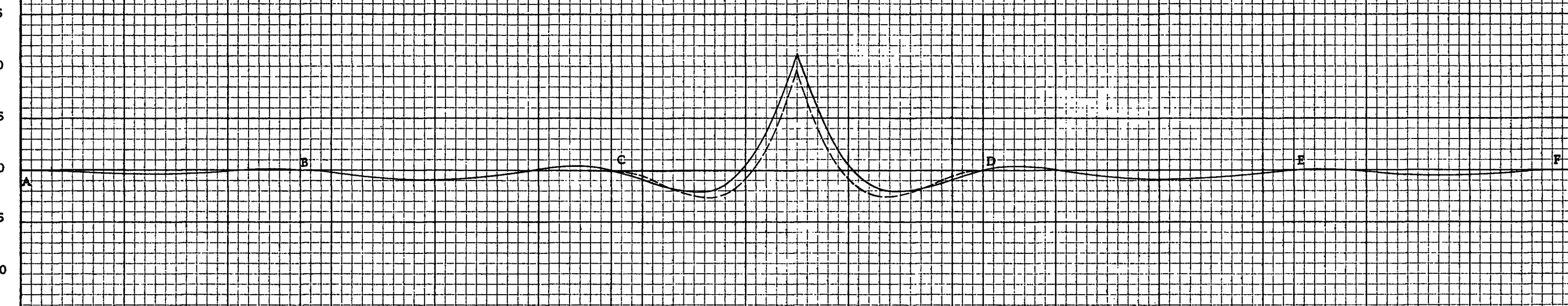


FIG. 20. INFLUENCE LINES FOR  $M_{KU}$  AT CROWN OF ARCH CD, SYSTEM I

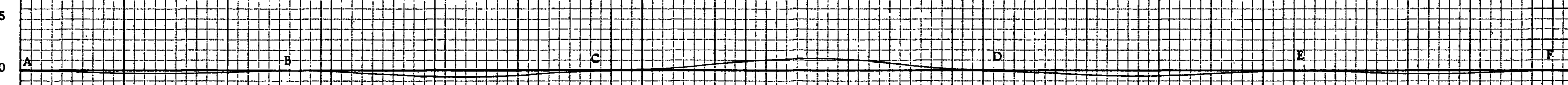
39

FOR FIXED ENDS

FOR  $H_p = 40$  FT.



COMPONENT OF  $M_{KU}$  CAUSED BY TRANSLATION OF PIER TOPS



COMPONENT OF  $M_{KU}$  CAUSED BY ROTATION OF PIER TOPS

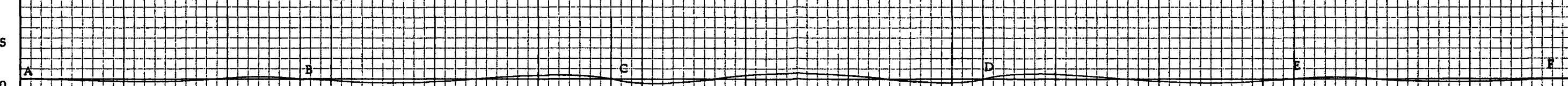


FIG. 21 INFLUENCE LINES FOR  $M_x$  AT TOP OF PIER BG, SYSTEM I  
KRPT

FOR  $H_p = 40$  FT.  
FOR  $H_p = 80$  FT.

40

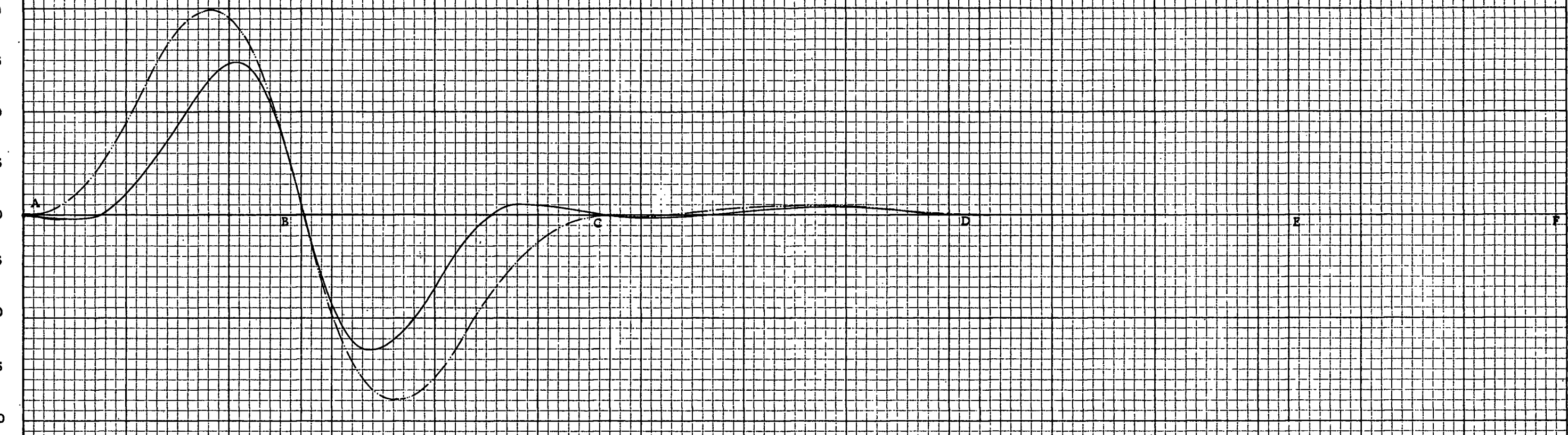


FIG. 22 INFLUENCE LINES FOR  $M_x$  AT TOP OF PIER CH, SYSTEM I  
KRPT

FOR  $H_p = 40$  FT.  
FOR  $H_p = 80$  FT.

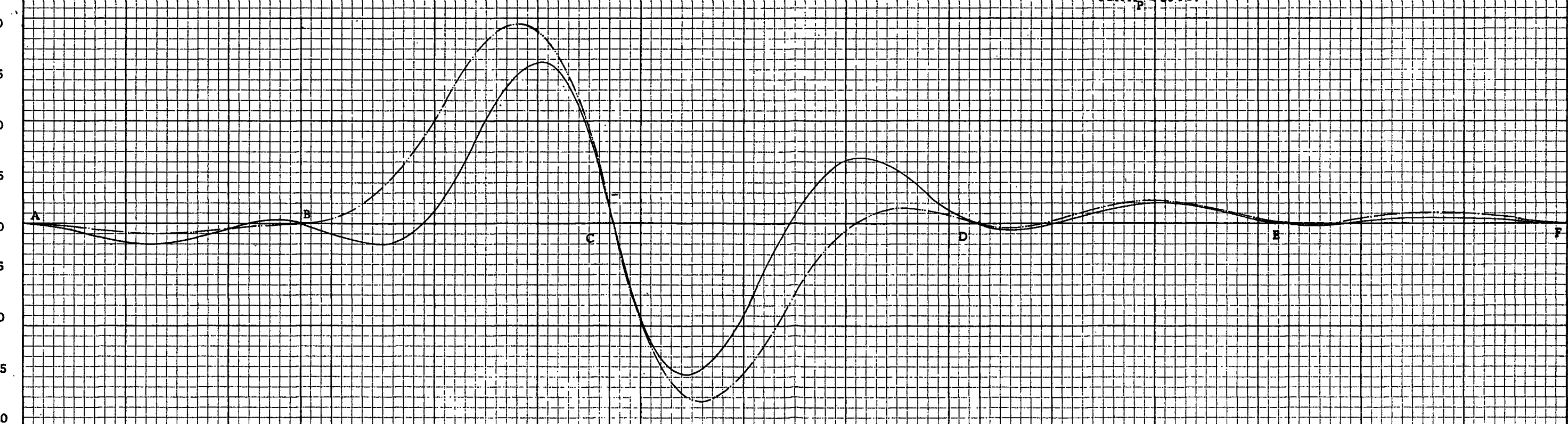


FIG. 23 INFLUENCE LINE FOR  $M_{KLPT}$  AT TOP OF PIER BG, SYSTEM I (FOR  $H_p = 40$  FT. ONLY)

41

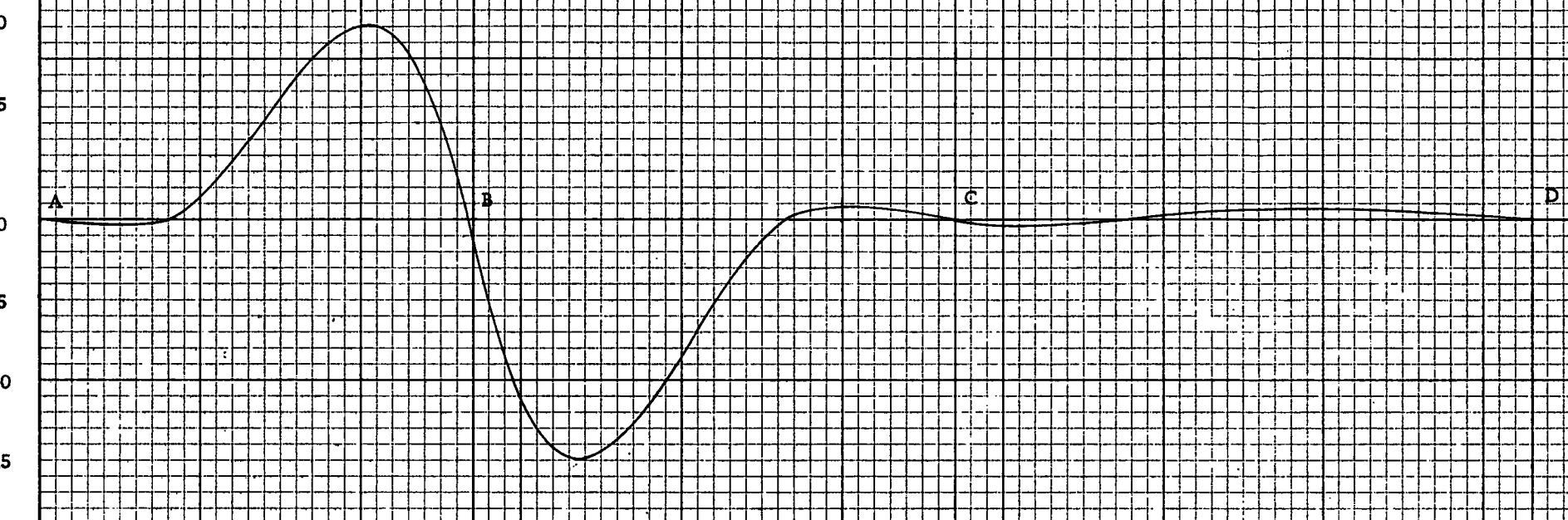


FIG. 24 INFLUENCE LINE FOR  $M_{KLPT}$  AT TOP OF PIER CH, SYSTEM I (FOR  $H_p = 40$  FT. ONLY)

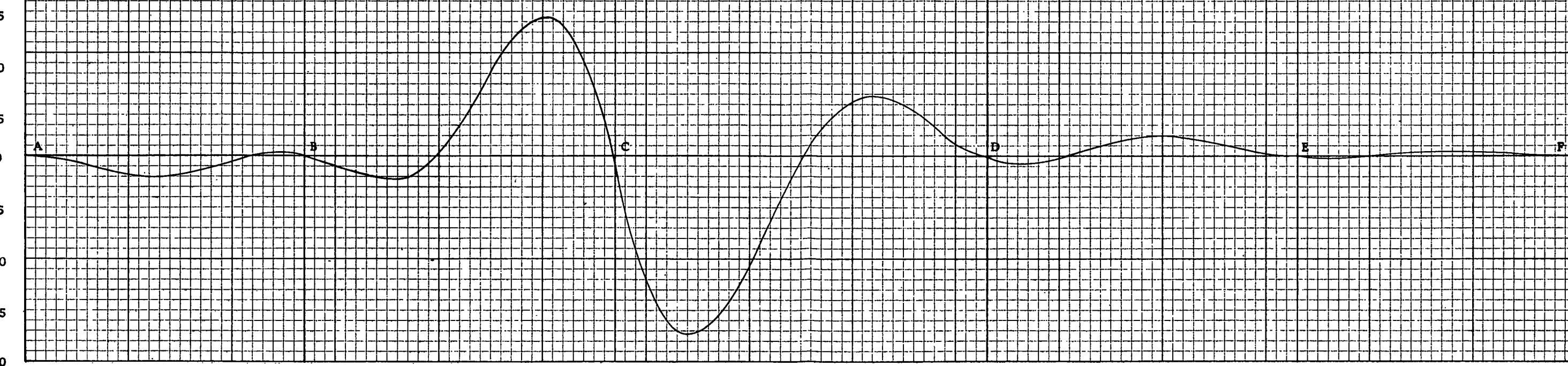


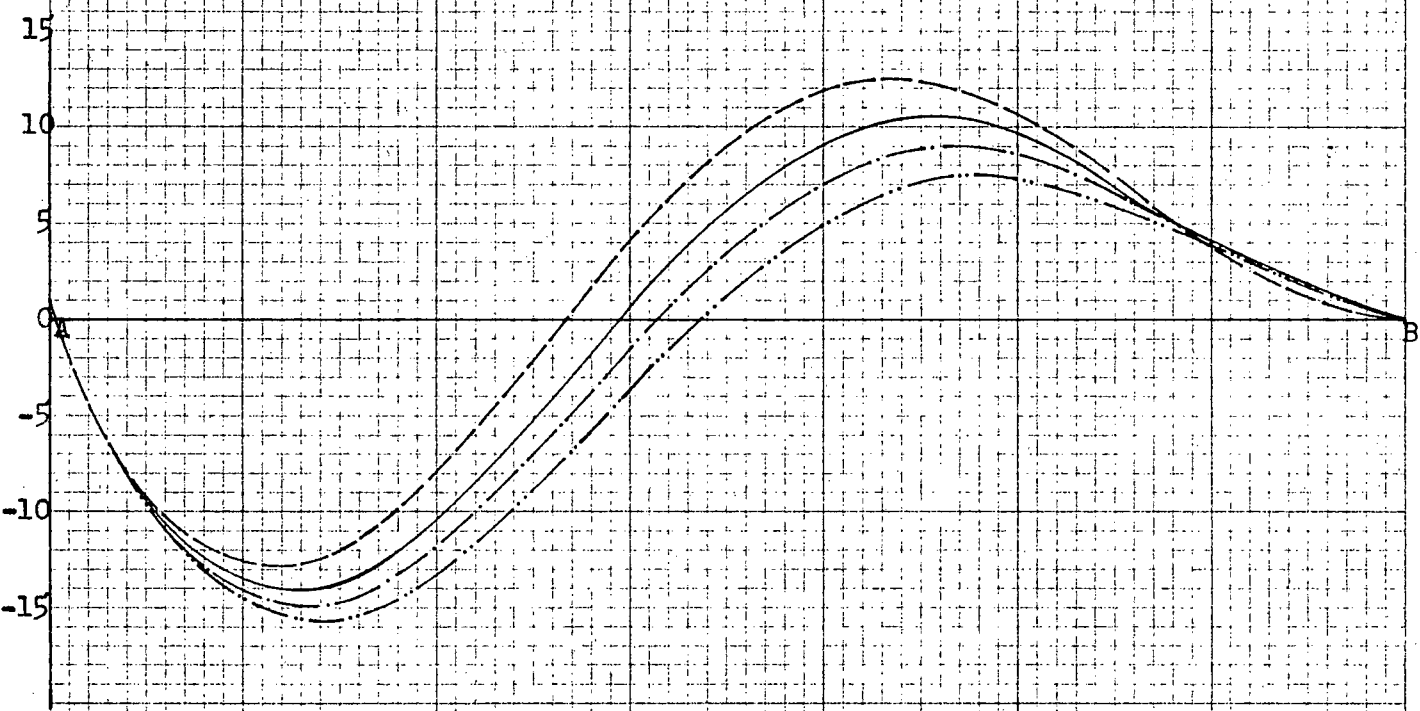
FIG. 25 INFLUENCE LINES (SPAN AB ONLY) FOR MKL AT A, SYSTEM II

FOR FIXED ENDS

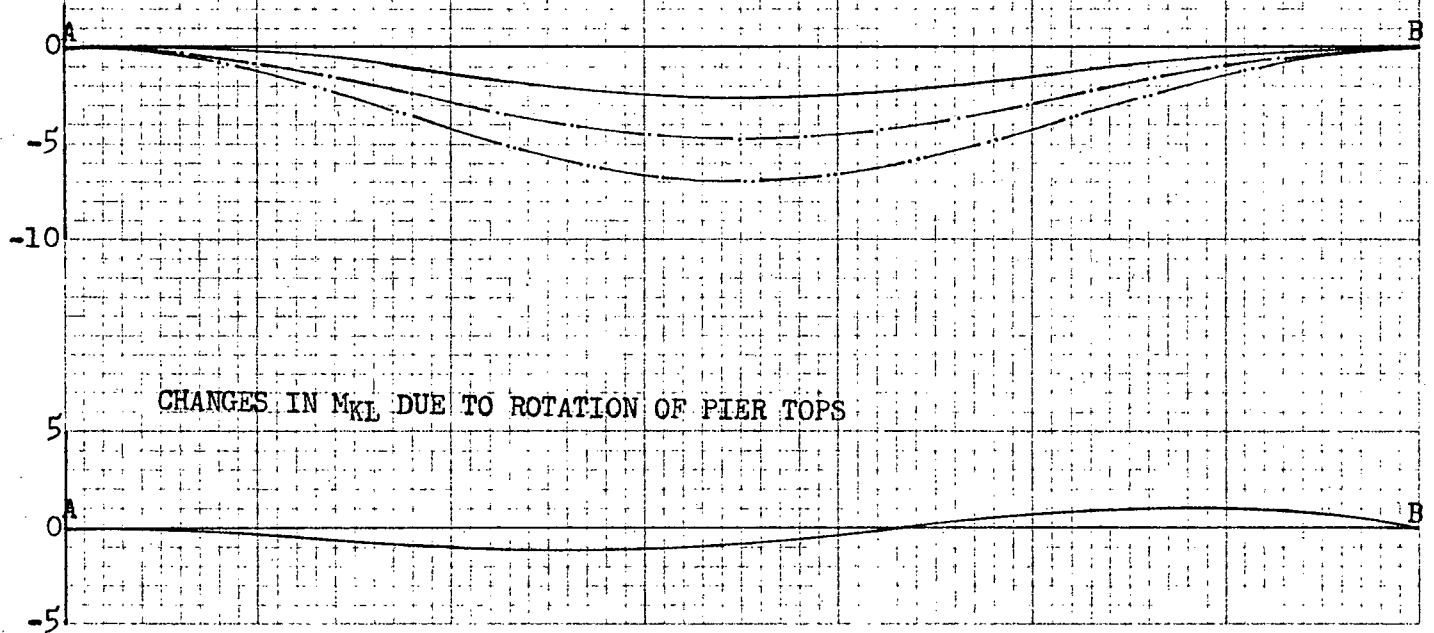
FOR  $H_p = 40$  ft.

FOR  $H_p = 60$  ft.

FOR  $H_p = 80$  ft.



CHANGES IN MKL DUE TO TRANSLATION OF PIER TOPS



CHANGES IN MKL DUE TO ROTATION OF PIER TOPS

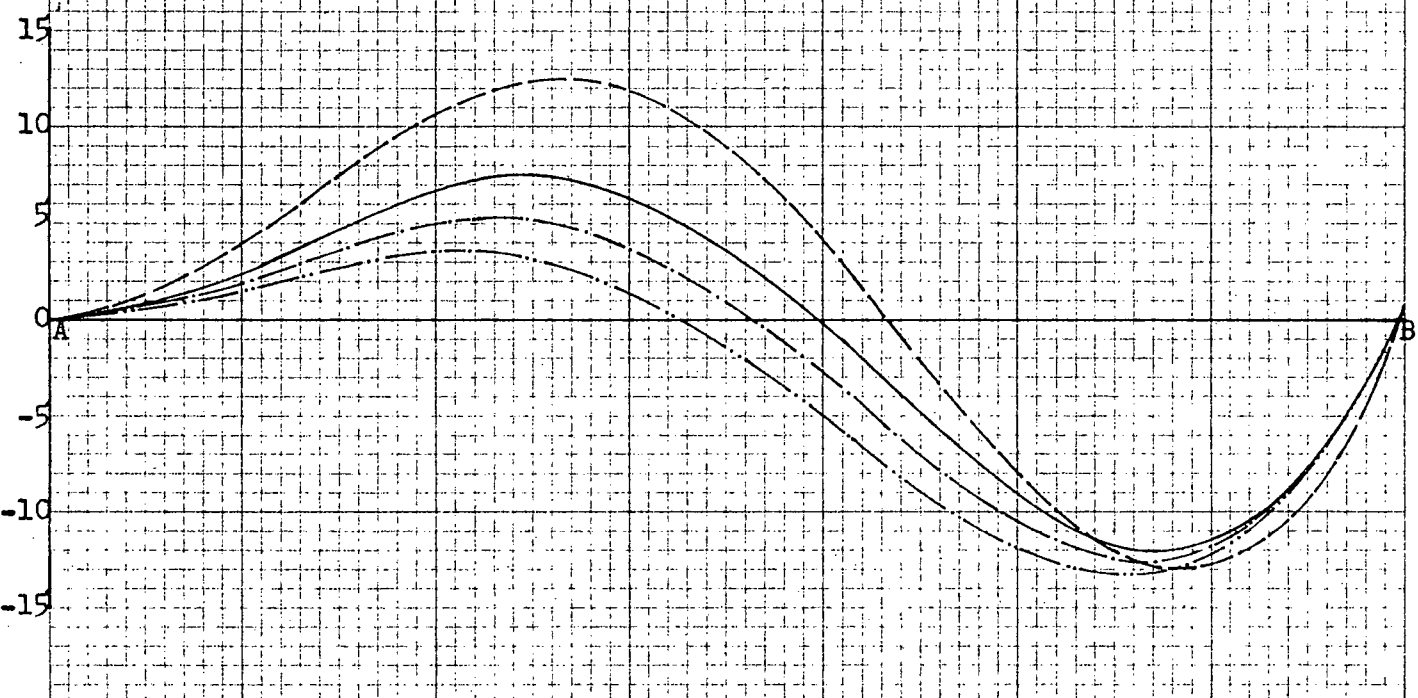
FIG. 26 INFLUENCE LINES (SPAN AB ONLY) FOR  $M_{KL}$  AT B OF ARCH AB, SYSTEM II

FOR FIXED ENDS

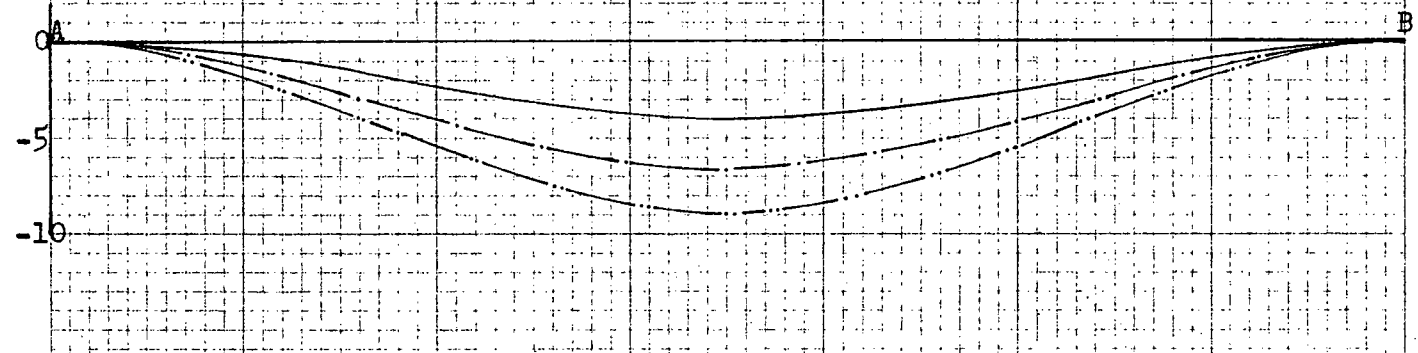
FOR  $H_p = 40$  ft.

FOR  $H_p = 60$  ft.

FOR  $H_p = 80$  ft.



CHANGES IN  $M_{KL}$  DUE TO TRANSLATION OF PIER TOPS



CHANGES IN  $M_{KL}$  DUE TO ROTATION OF PIER TOPS

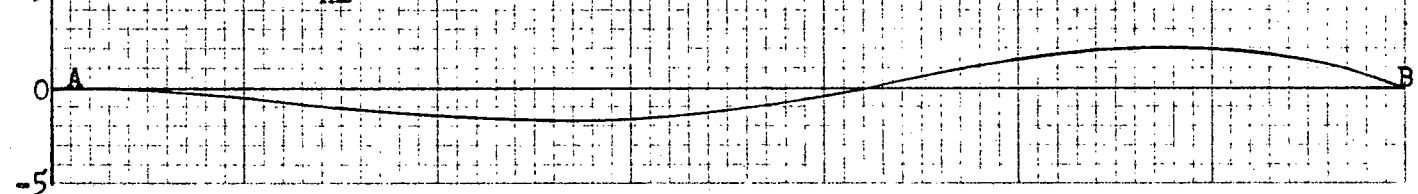


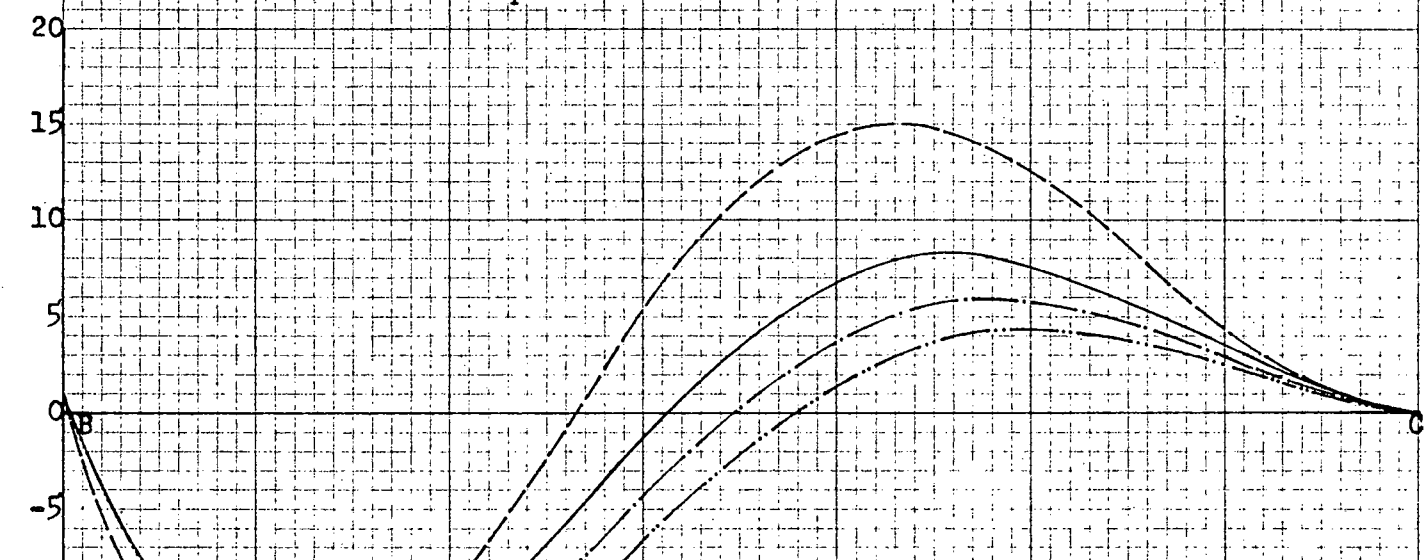
FIG. 27 INFLUENCE LINES (SPAN BC ONLY) FOR  $M_{KL}$  AT B OF ARCH BC, SYSTEM II

FOR FIXED ENDS

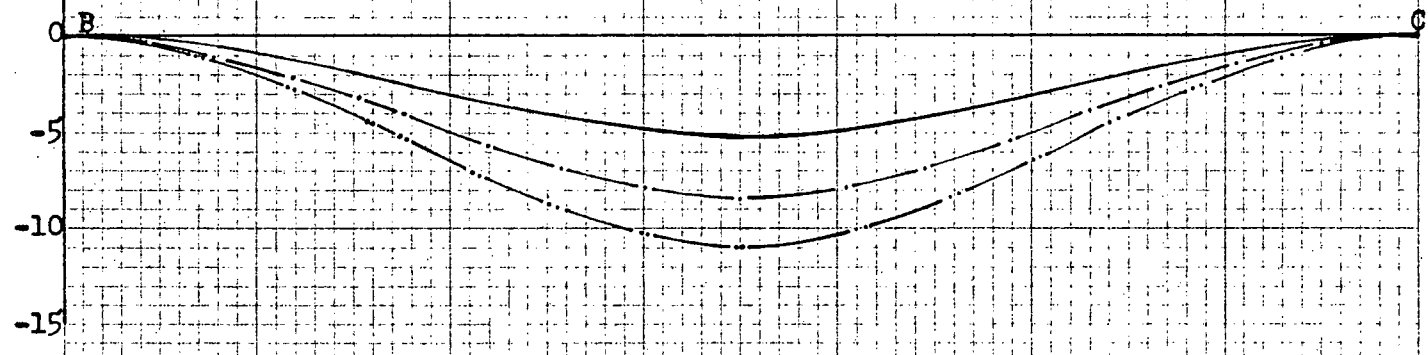
FOR  $H_p = 40$  ft.

FOR  $H_p = 60$  ft.

FOR  $H_p = 80$  ft.



CHANGES IN  $M_{KL}$  DUE TO TRANSLATION OF PIER TOPS



CHANGES IN  $M_{KL}$  DUE TO ROTATION OF PIER TOPS

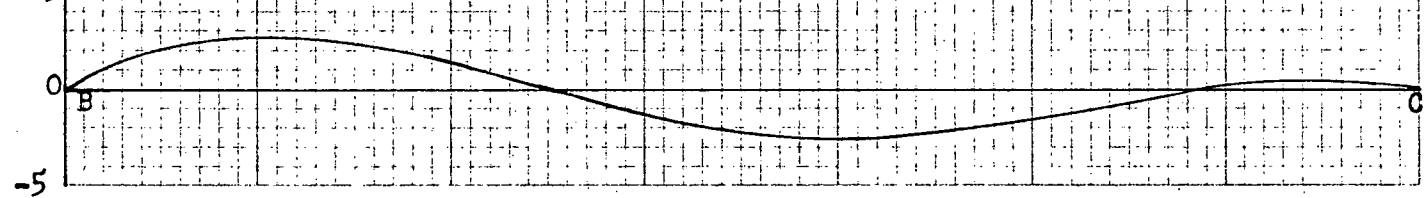


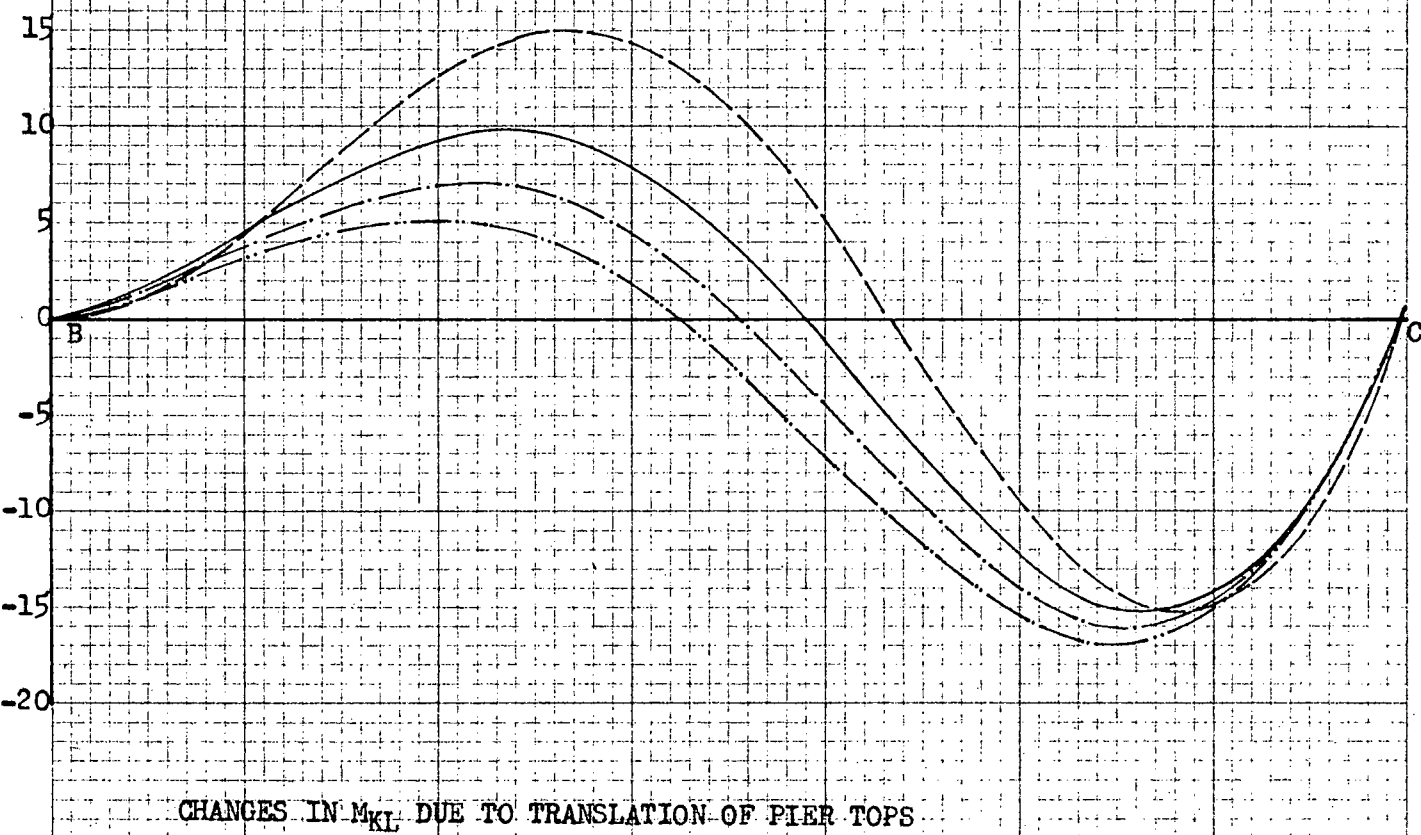
FIG. 28 INFLUENCE LINES (SPAN BC ONLY) FOR  $M_{KL}$  AT C OF ARCH BC, SYSTEM II

FOR FIXED ENDS

FOR  $H_p = 40$  ft.

FOR  $H_p = 60$  ft.

FOR  $H_p = 80$  ft.



CHANGES IN  $M_{KL}$  DUE TO TRANSLATION OF PIER TOPS

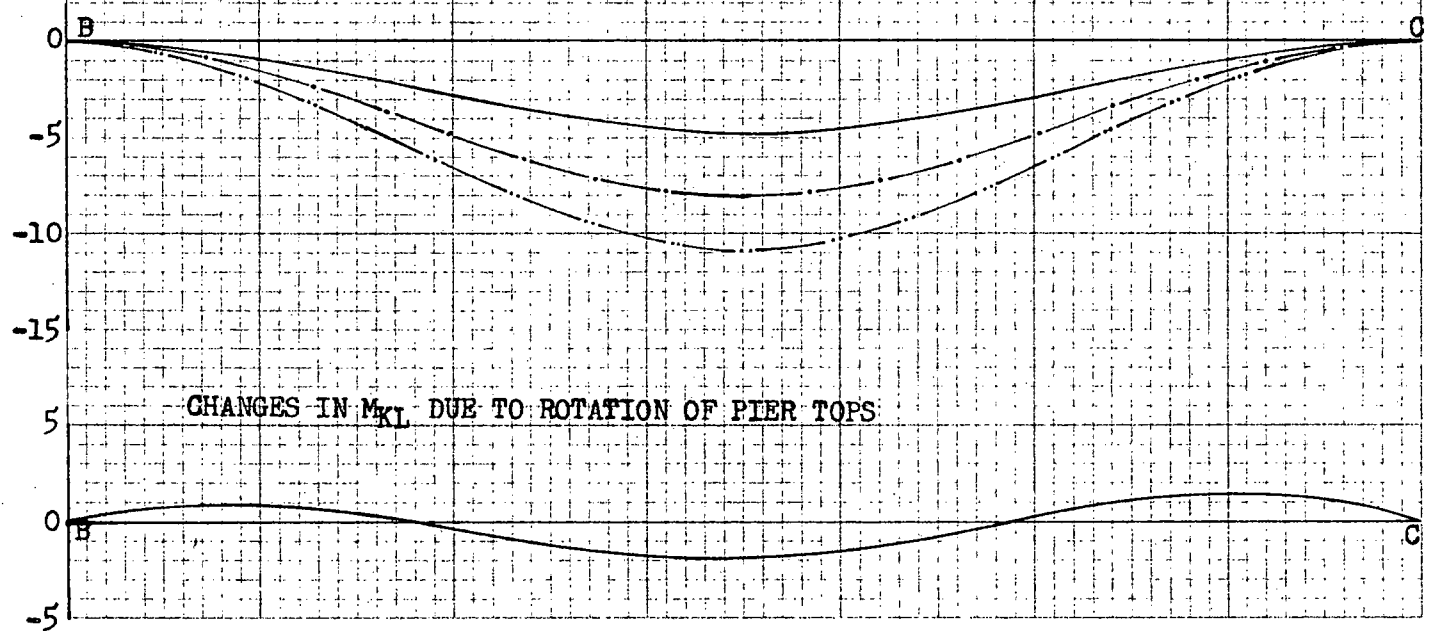


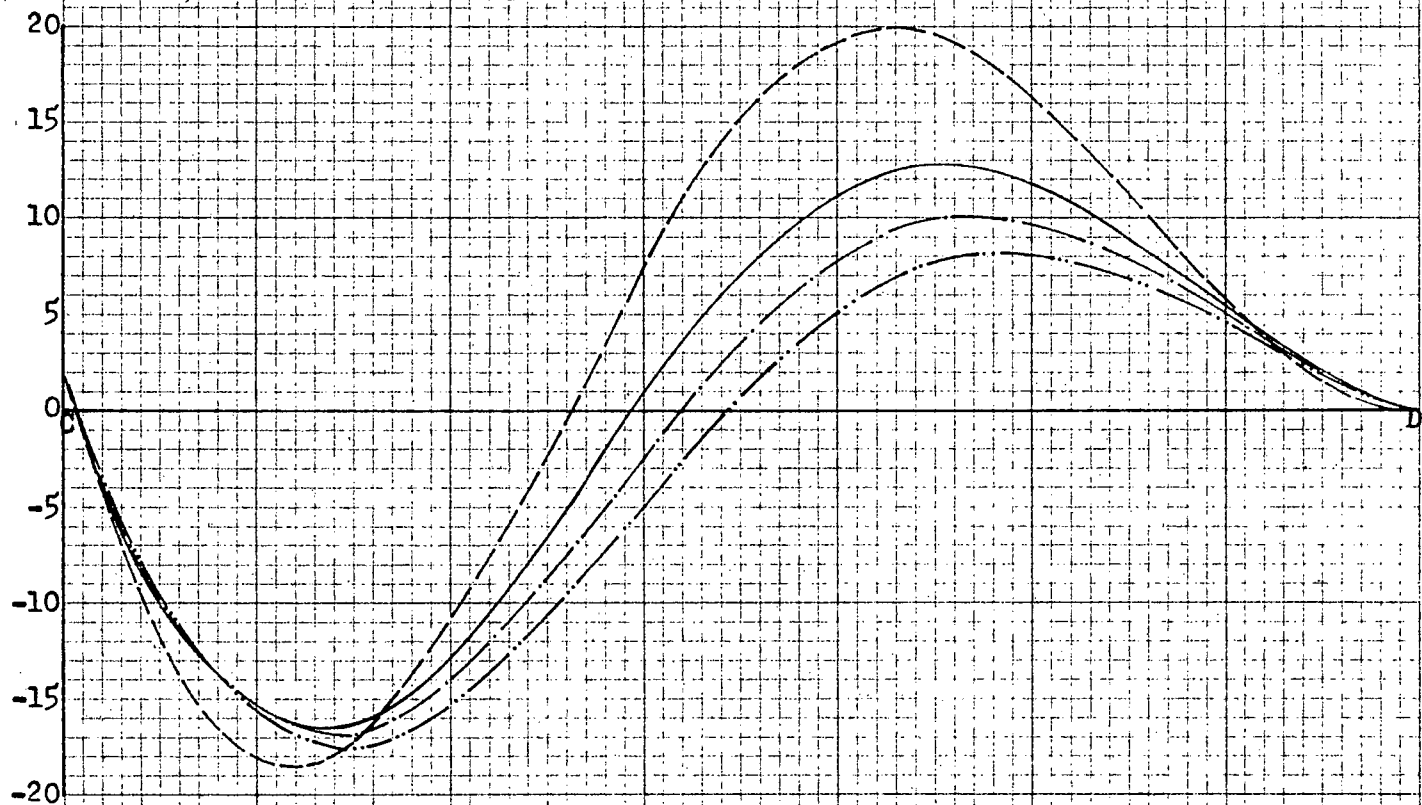
FIG. 29. INFLUENCE LINES (SPAN CD ONLY) FOR  $M_{KL}$  AT C OF ARCH CD, SYSTEM II

FOR FIXED ENDS

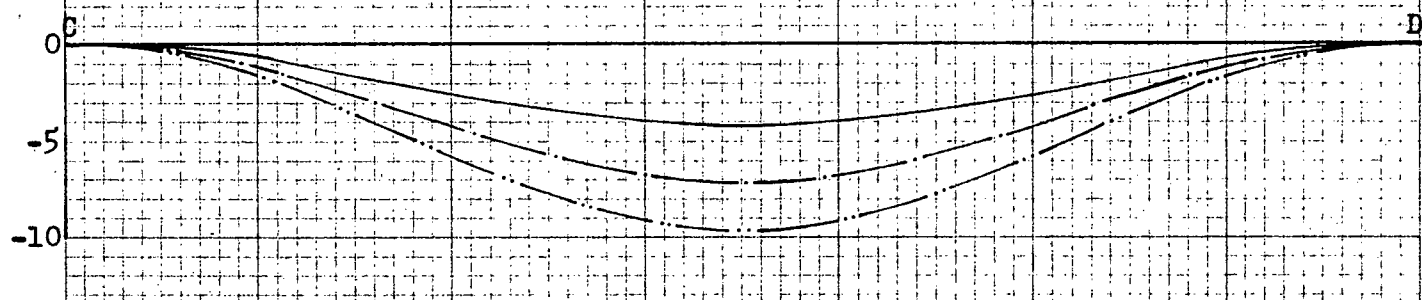
FOR  $H_p = 40$  ft.

FOR  $H_p = 60$  ft.

FOR  $H_p = 80$  ft.



CHANGES IN  $M_{KL}$  DUE TO TRANSLATION OF PIER TOPS



CHANGES IN  $M_{KL}$  DUE TO ROTATION OF PIER TOPS

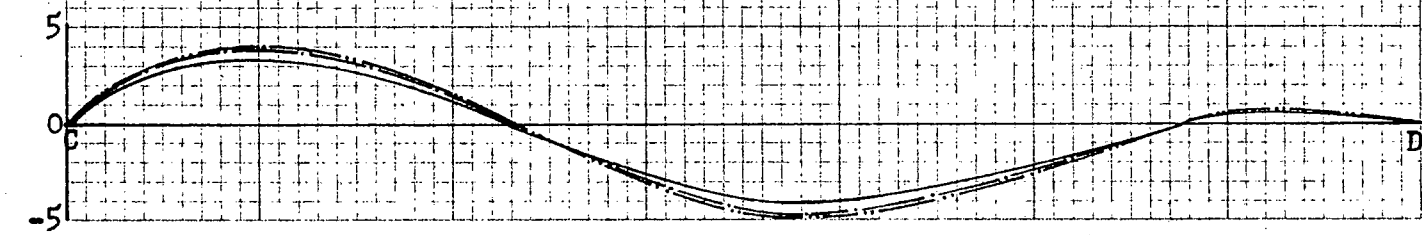
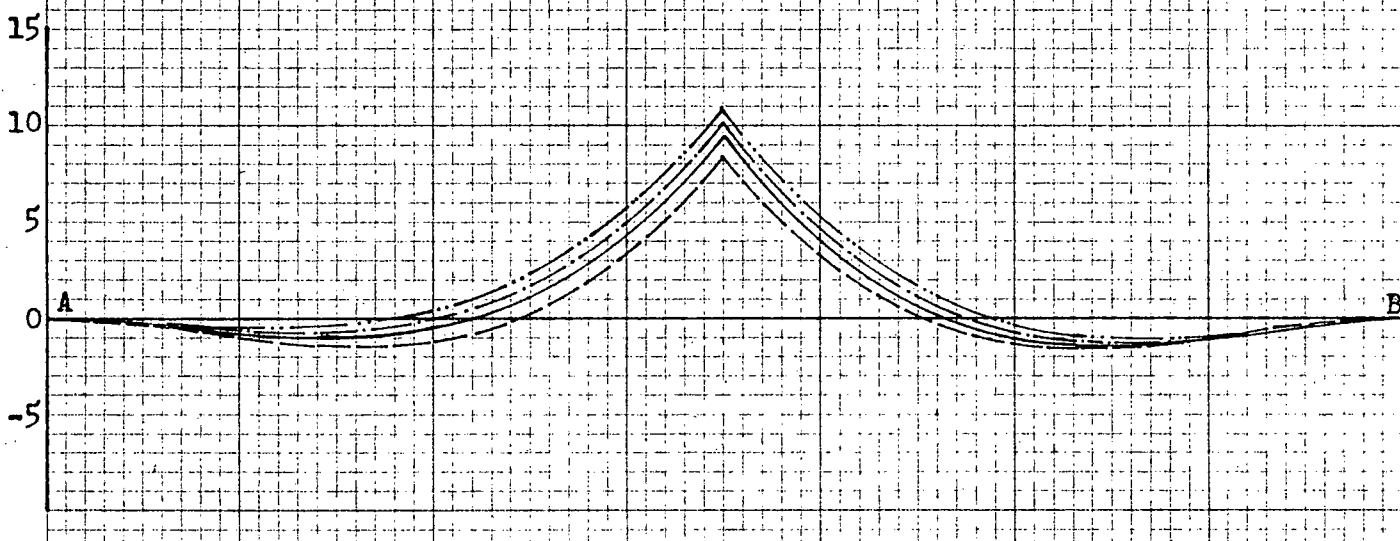
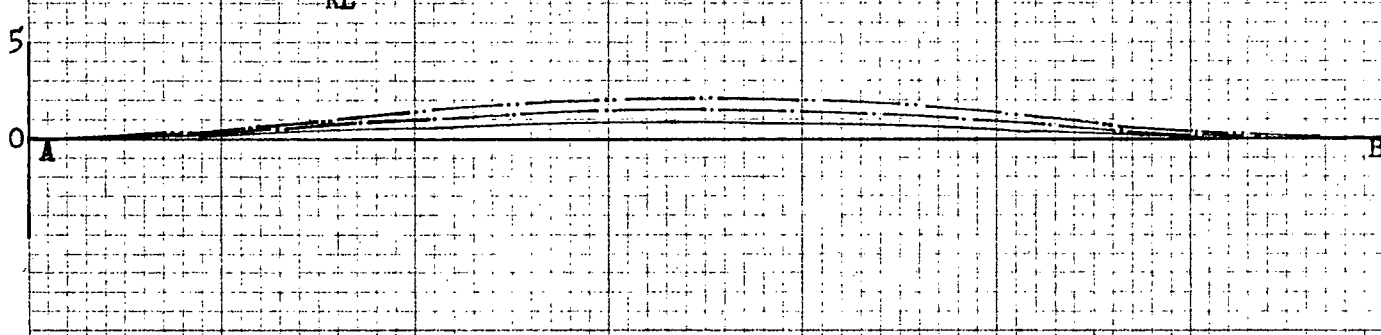


FIG. 30' INFLUENCE LINES (SPAN AB ONLY) FOR  $M_{KL}$  AT CROWN OF ARCH AB, SYSTEM II

- FOR FIXED ENDS
- - - FOR  $H_p = 40$  ft.
- - - FOR  $H_p = 60$  ft.
- - - FOR  $H_p = 80$  ft.



CHANGES IN  $M_{KL}$  DUE TO TRANSLATION OF PIER TOPS



CHANGES IN  $M_{KL}$  DUE TO ROTATION OF PIER TOPS

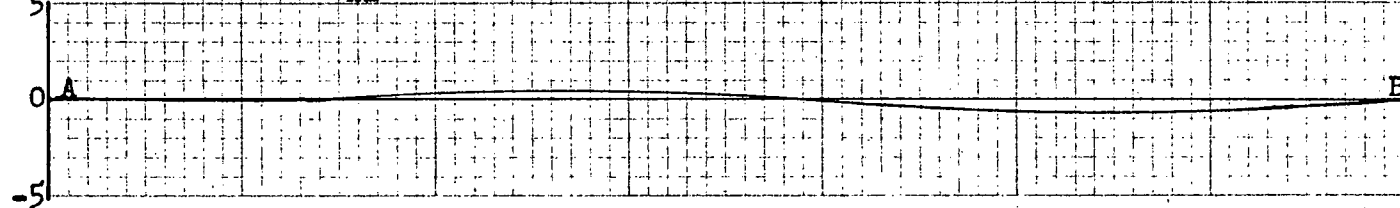


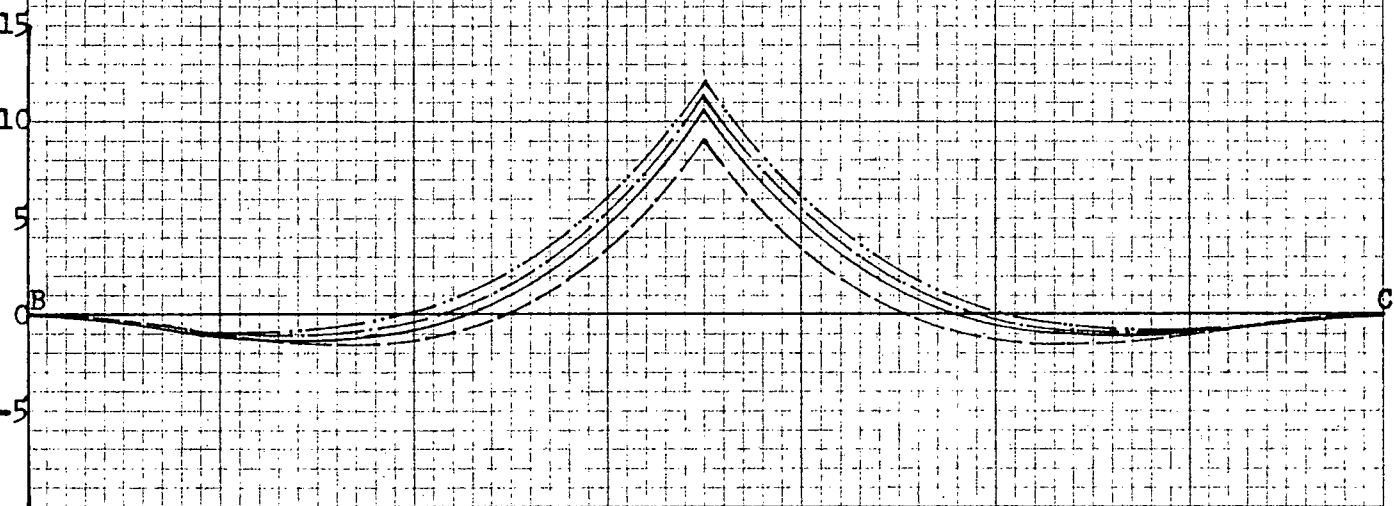
FIG. 31 INFLUENCE LINES (SPAN BC ONLY) FOR  $M_{KL}$  AT CROWN OF ARCH BC, SYSTEM II

FOR FIXED ENDS

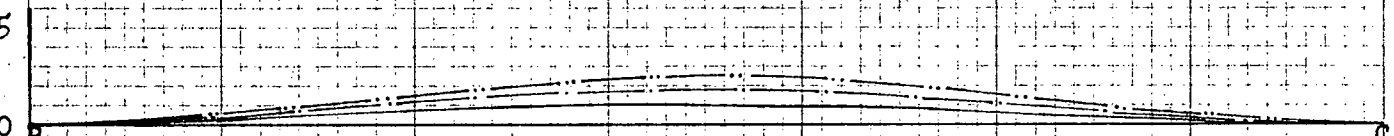
— FOR  $H_p = 40$  ft.

— FOR  $H_p = 60$  ft.

— FOR  $H_p = 80$  ft.



CHANGES IN  $M_{KL}$  DUE TO TRANSLATION OF PIER TOPS



CHANGES IN  $M_{KL}$  DUE TO ROTATION OF PIER TOPS

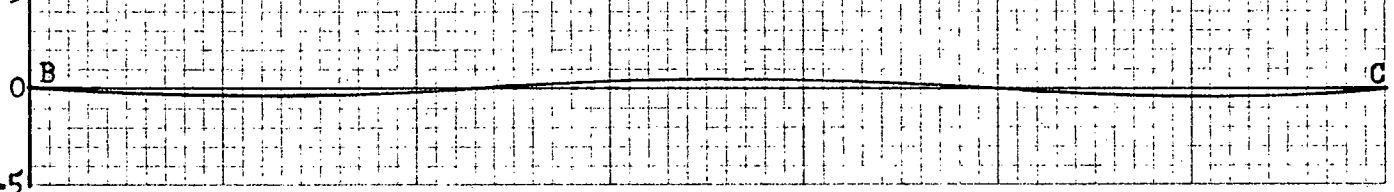
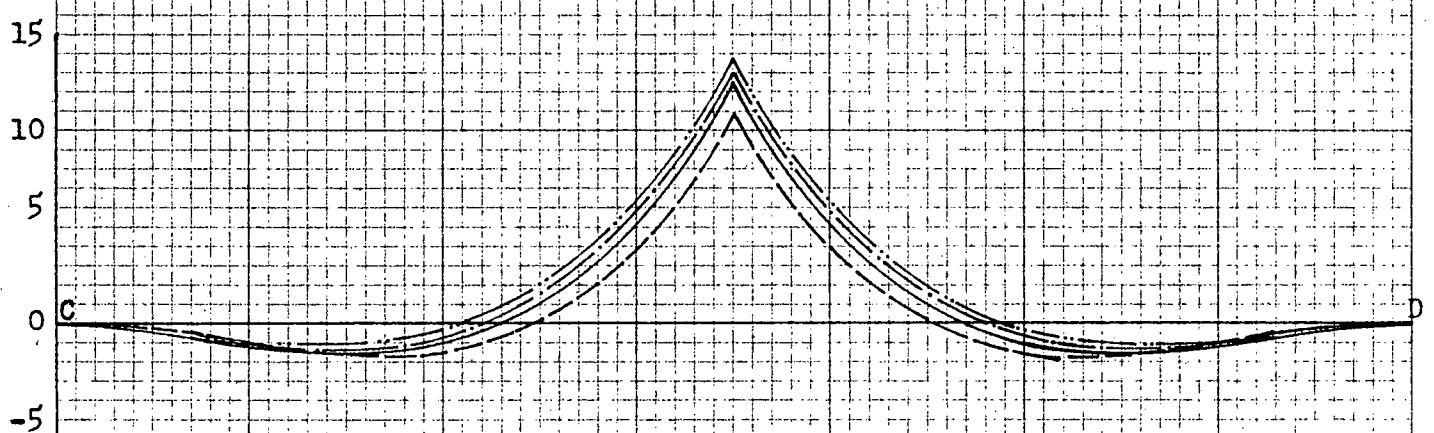
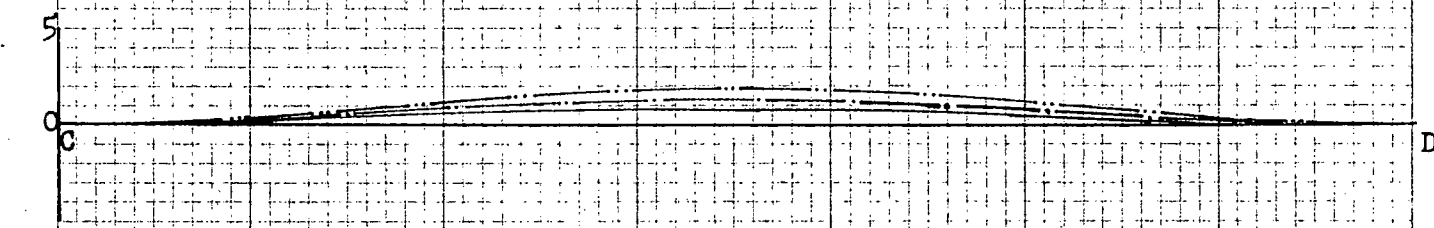


FIG. 32 INFLUENCE LINES (SPAN CD ONLY) FOR  $M_{KL}$  AT CROWN OF ARCH CD, SYSTEM II

- FOR FIXED ENBS
- FOR  $H_p = 40$  ft.
- FOR  $H_p = 60$  ft.
- FOR  $H_p = 80$  ft.



CHANGES IN MKL DUE TO TRANSLATION OF PIER TOPS



CHANGES IN MKL DUE TO ROTATION OF PIER TOPS

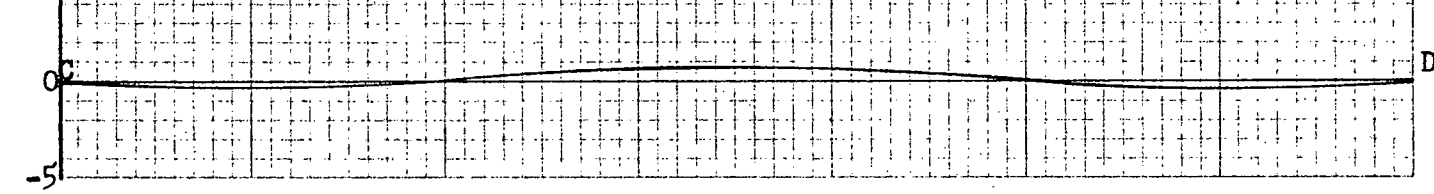


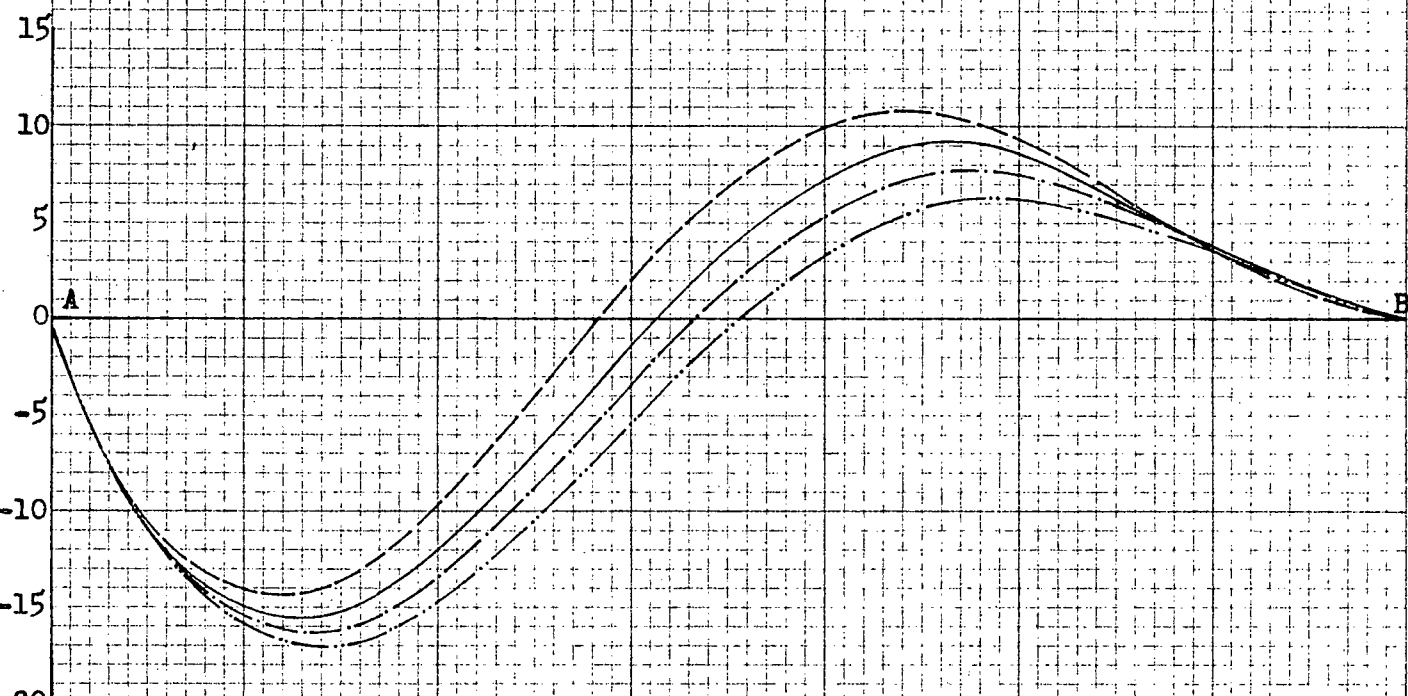
FIG. 33. INFLUENCE LINES (SPAN AB ONLY) FOR  $M_{KU}$  AT A, SYSTEM II

FOR FIXED ENDS

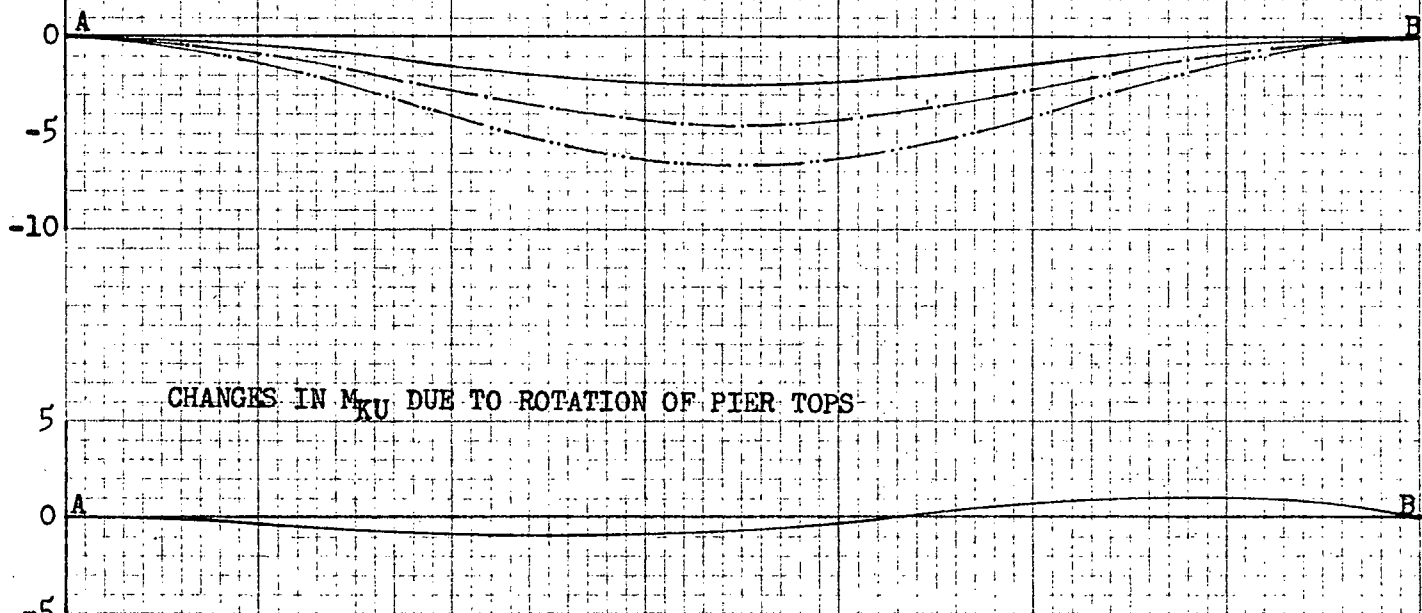
— FOR  $H_p = 40$  ft.

— FOR  $H_p = 60$  ft.

— FOR  $H_p = 80$  ft.



CHANGES IN  $M_{KU}$  DUE TO TRANSLATION OF PIER TOPS



CHANGES IN  $M_{KU}$  DUE TO ROTATION OF PIER TOPS

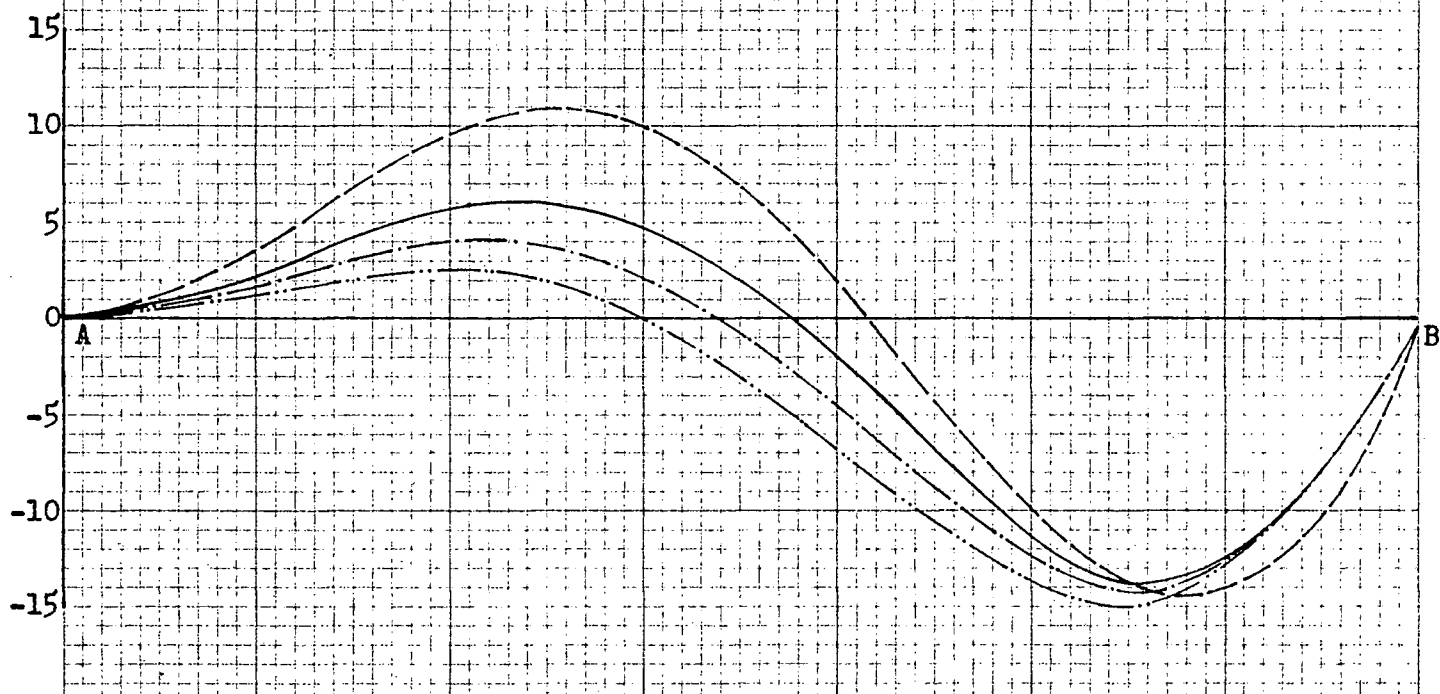
FIG. 34. INFLUENCE LINES (SPAN AB ONLY) FOR  $M_{KU}$  AT B OF ARCH AB, SYSTEM II

FOR FIXED ENDS

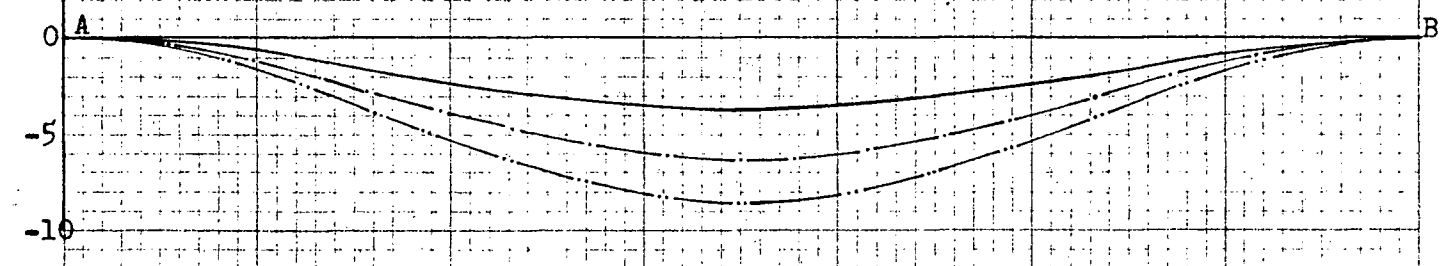
FOR  $H_p = 40$  ft.

FOR  $H_p = 60$  ft.

FOR  $H_p = 80$  ft.



CHANGES IN  $M_{KU}$  DUE TO TRANSLATION OF PIER TOPS



CHANGES IN  $M_{KU}$  DUE TO ROTATION OF PIER TOPS

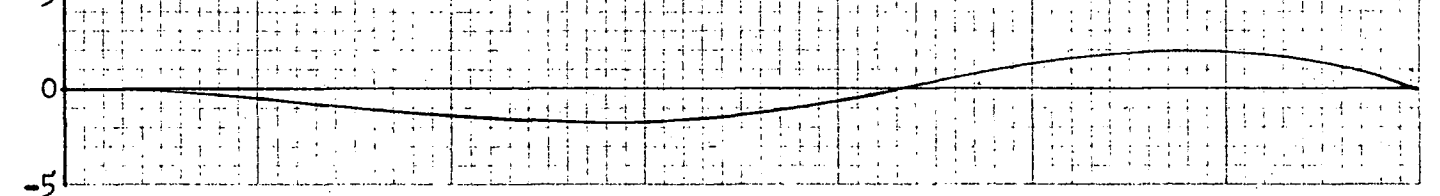


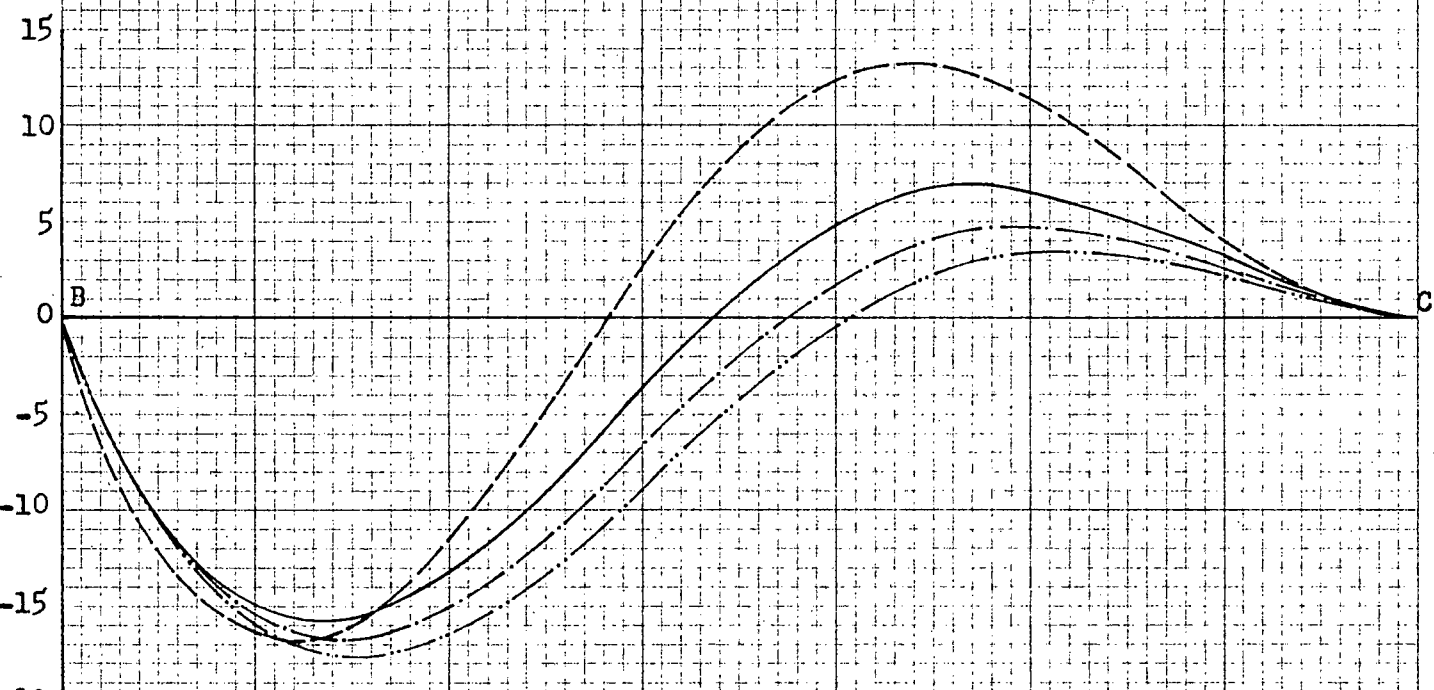
FIG. 35 INFLUENCE LINES (SPAN BC ONLY) FOR  $M_{KU}$  AT B OF ARCH BC, SYSTEM II

FOR FIXED ENDS

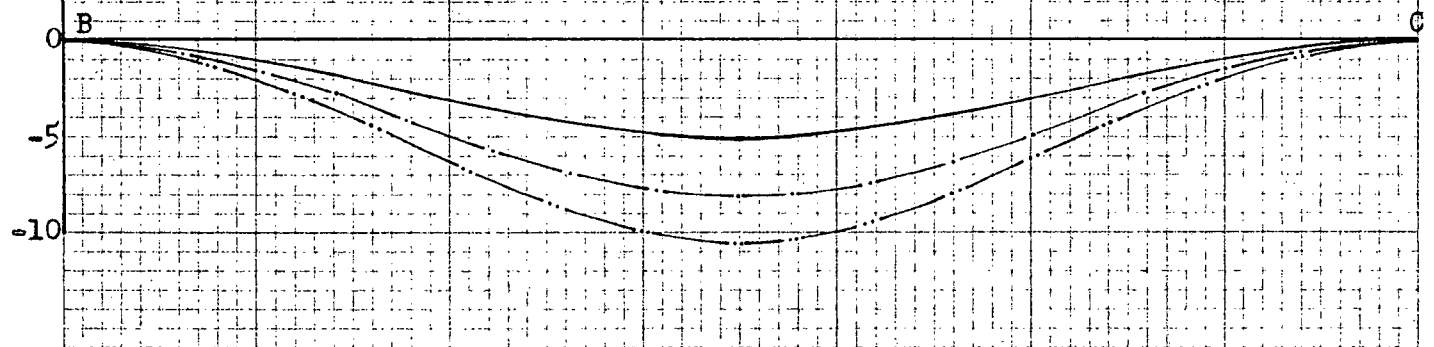
FOR  $H_p=40$  ft.

FOR  $H_p=60$  ft.

FOR  $H_p=80$  ft.



CHANGES IN  $M_{KU}$  DUE TO TRANSLATION OF PIER TOPS



CHANGES IN  $M_{KU}$  DUE TO ROTATION OF PIER TOPS

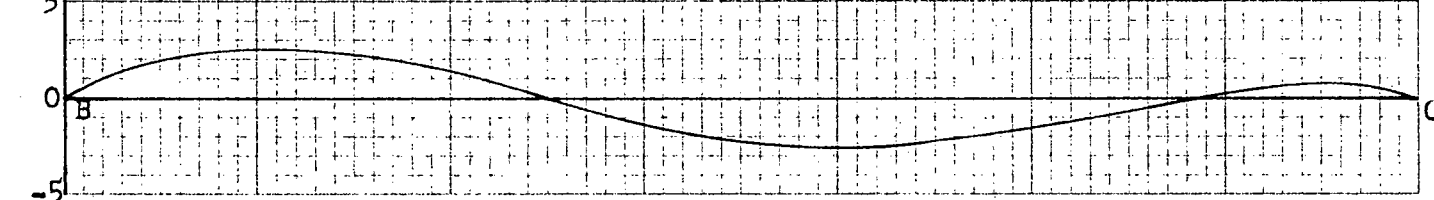


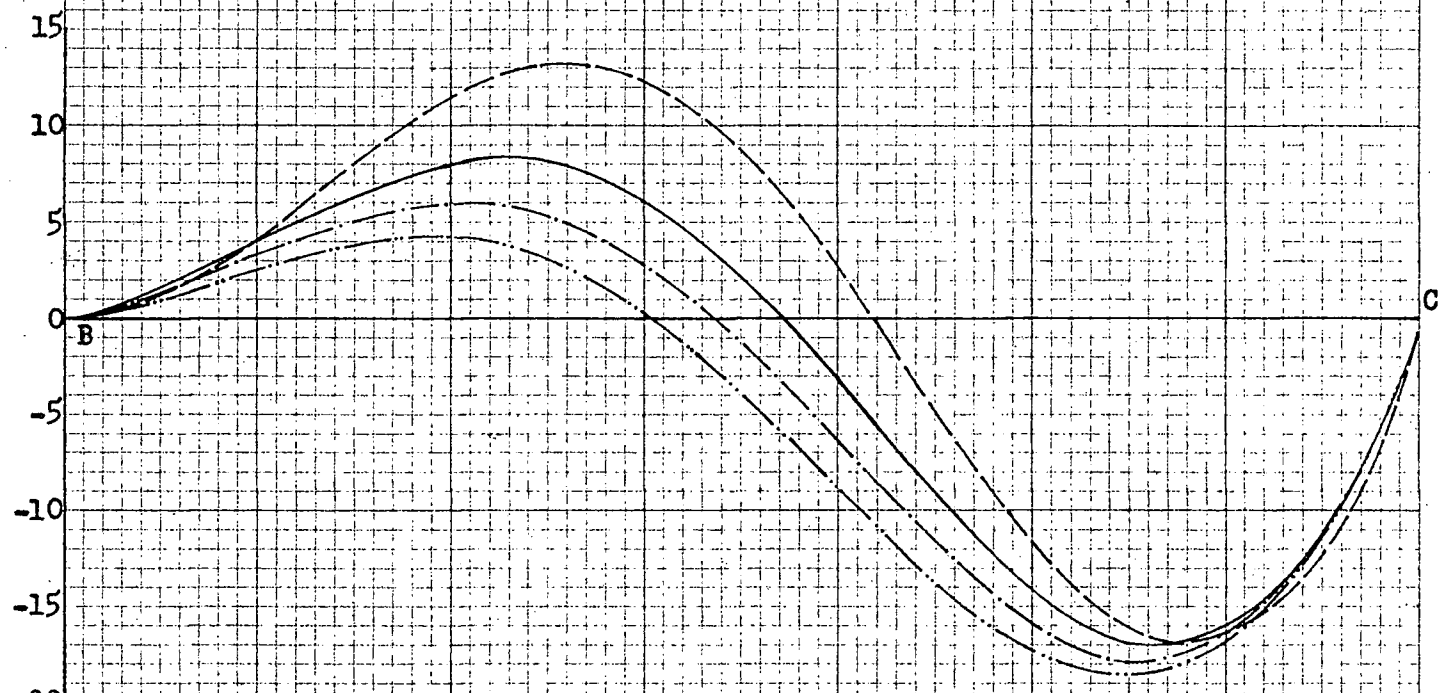
FIG. 36 INFLUENCE LINES (SPAN BC ONLY) FOR MKU AT C OF ARCH BC, SYSTEM II

FOR FIXED ENDS

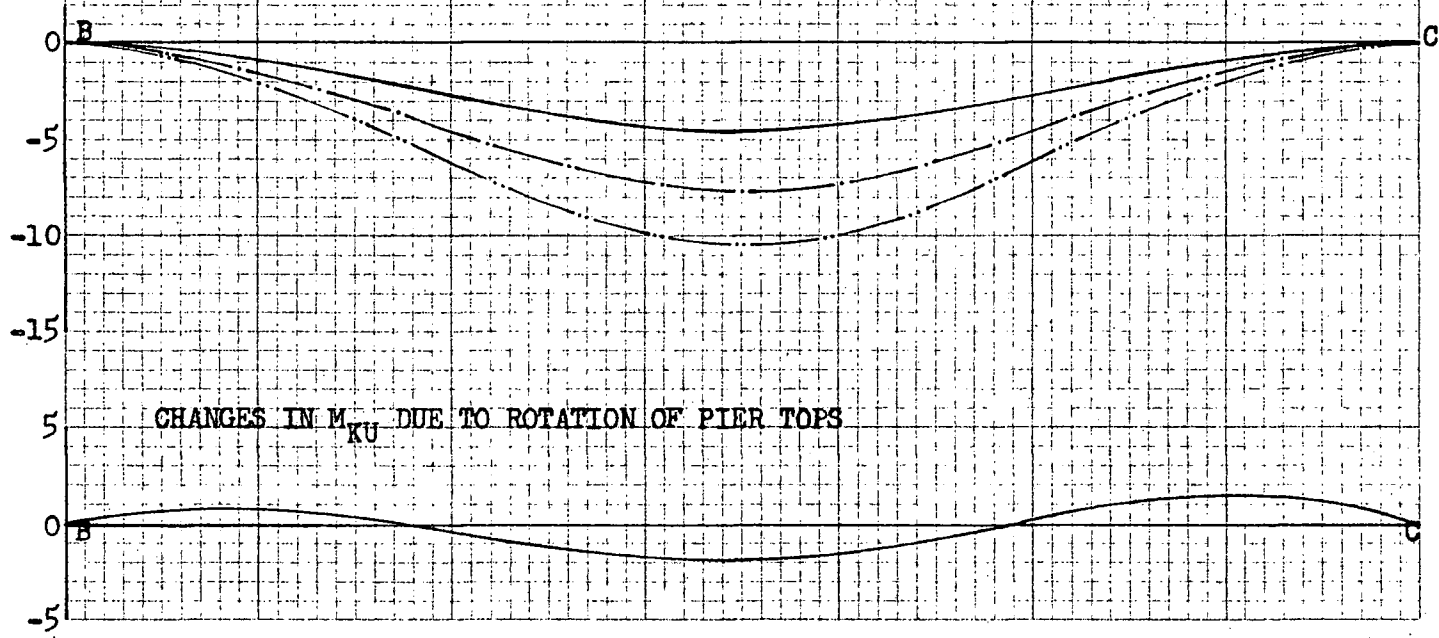
FOR  $H_p = 40$  ft.

FOR  $H_p = 60$  ft.

FOR  $H_p = 80$  ft.



CHANGES IN MKU DUE TO TRANSLATION OF PIER TOPS



CHANGES IN MKU DUE TO ROTATION OF PIER TOPS

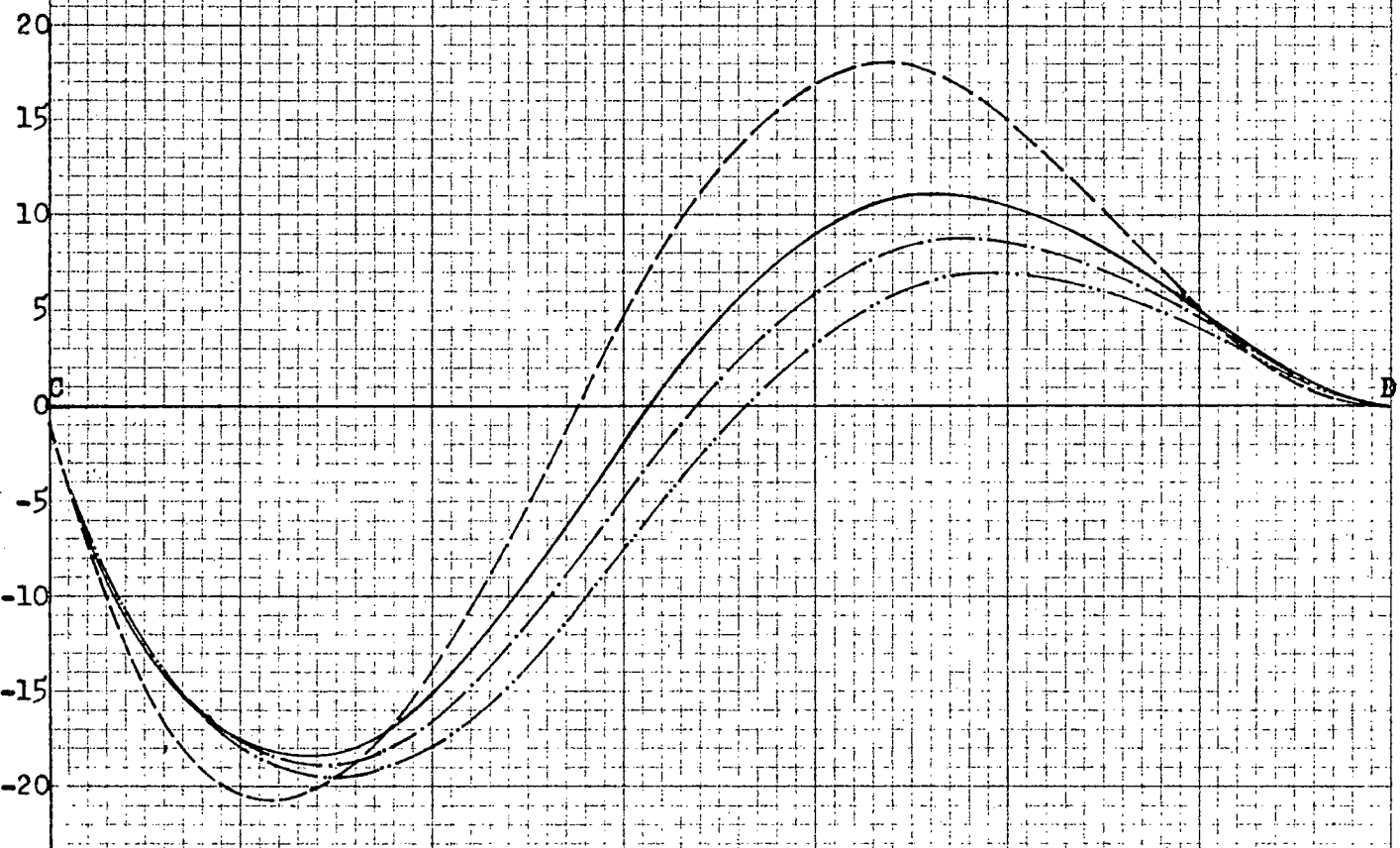
FIG. 37 INFLUENCE LINES (SPAN CD ONLY) FOR  $M_{KU}$  AT C OF ARCH CD, SYSTEM II

FOR FIXED ENDS

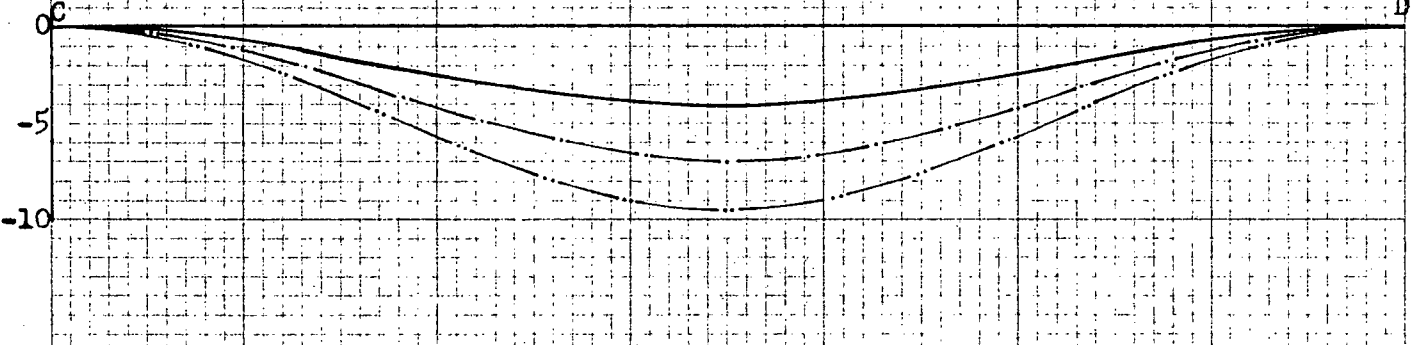
FOR  $H_p = 40$  ft.

FOR  $H_p = 60$  ft.

FOR  $H_p = 80$  ft.



CHANGES IN  $M_{KU}$  DUE TO TRANSLATION OF PIER TOPS



CHANGES IN  $M_{KU}$  DUE TO ROTATION OF PIER TOPS

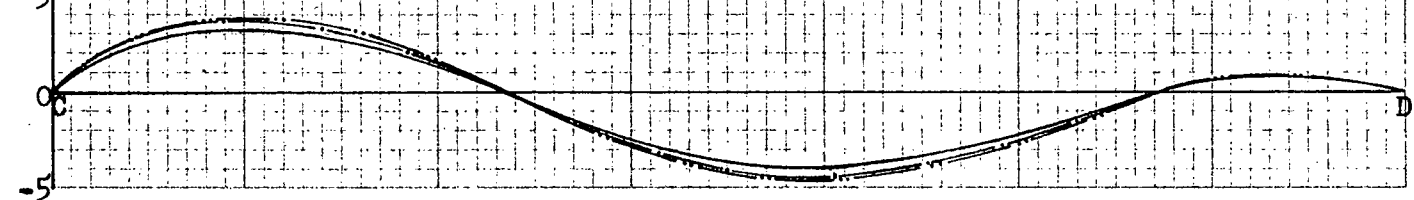


FIG. 38 INFLUENCE LINES (SPAN AB ONLY) FOR  $M_{KU}$  AT CROWN OF ARCH AB, SYSTEM II

— FOR FIXED ENDS

— FOR  $H_p = 10$  ft.

— FOR  $H_p = 60$  ft.

— FOR  $H_p = 80$  ft.

15

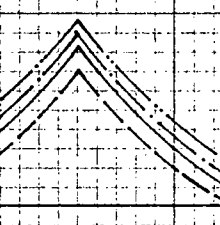
10

5

0

-5

B



CHANGES IN  $M_{KU}$  DUE TO TRANSLATION OF PIER TOPS

5

0

B

A

B

CHANGES IN  $M_{KU}$  DUE TO ROTATION OF PIER TOPS

5

0

B

A

B

-5

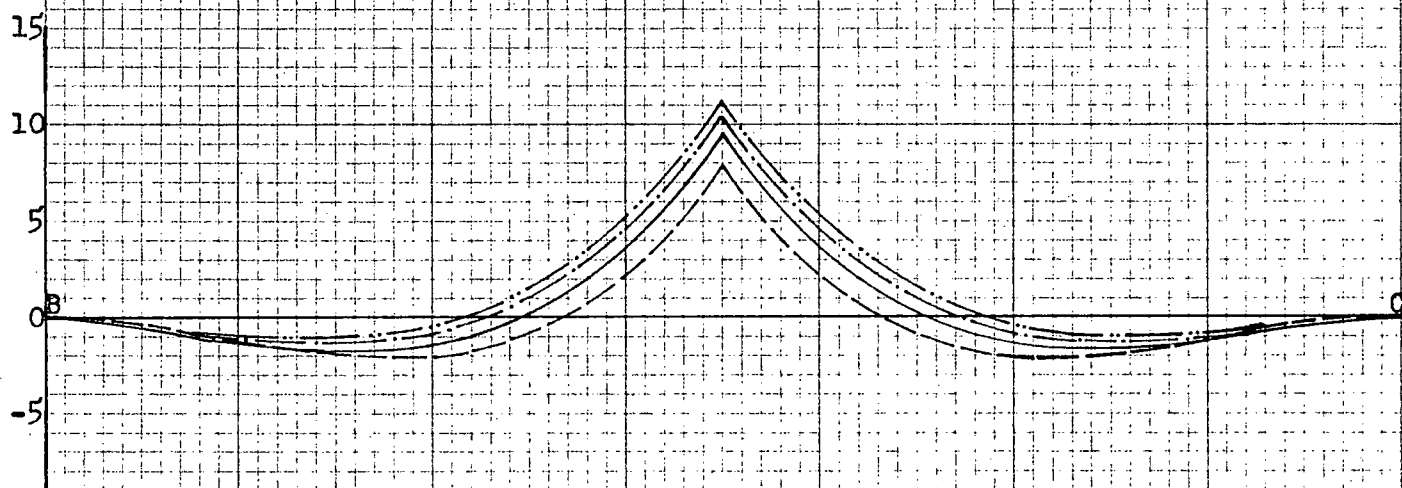
FIG. 39 INFLUENCE LINES (SPAN BC ONLY) FOR  $M_{KU}$  AT CROWN OF ARCH BC, SYSTEM II

## **FOR FIXED ENDS**

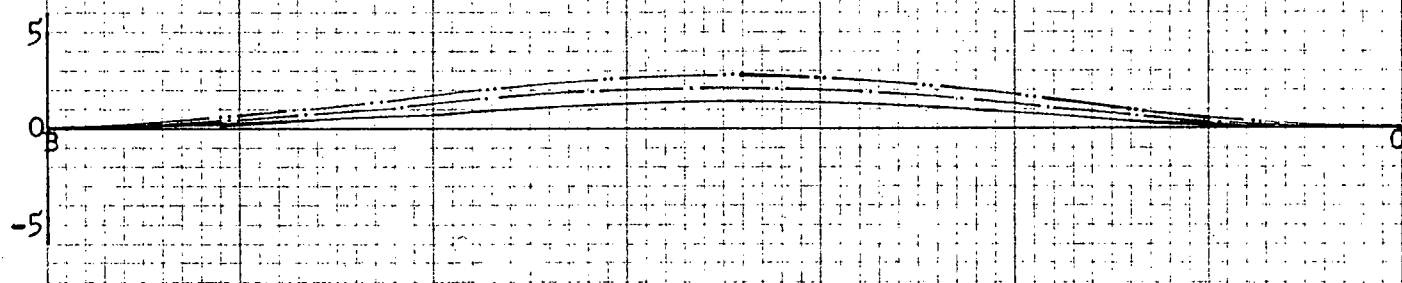
FOR HP=40 ft.

FOR  $H_p = 60$  ft.

FOR HP=80 ft.



## CHANGES IN MKII DUE TO TRANSLATION OF PIER TOPS



## CHANGES IN MKII DUE TO ROTATION OF PIER TOPS

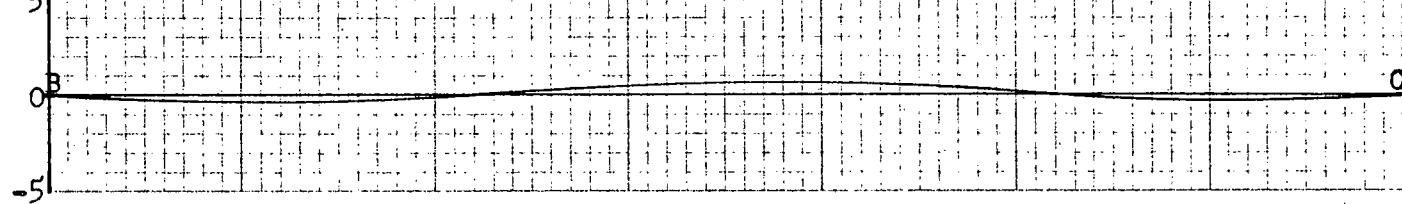
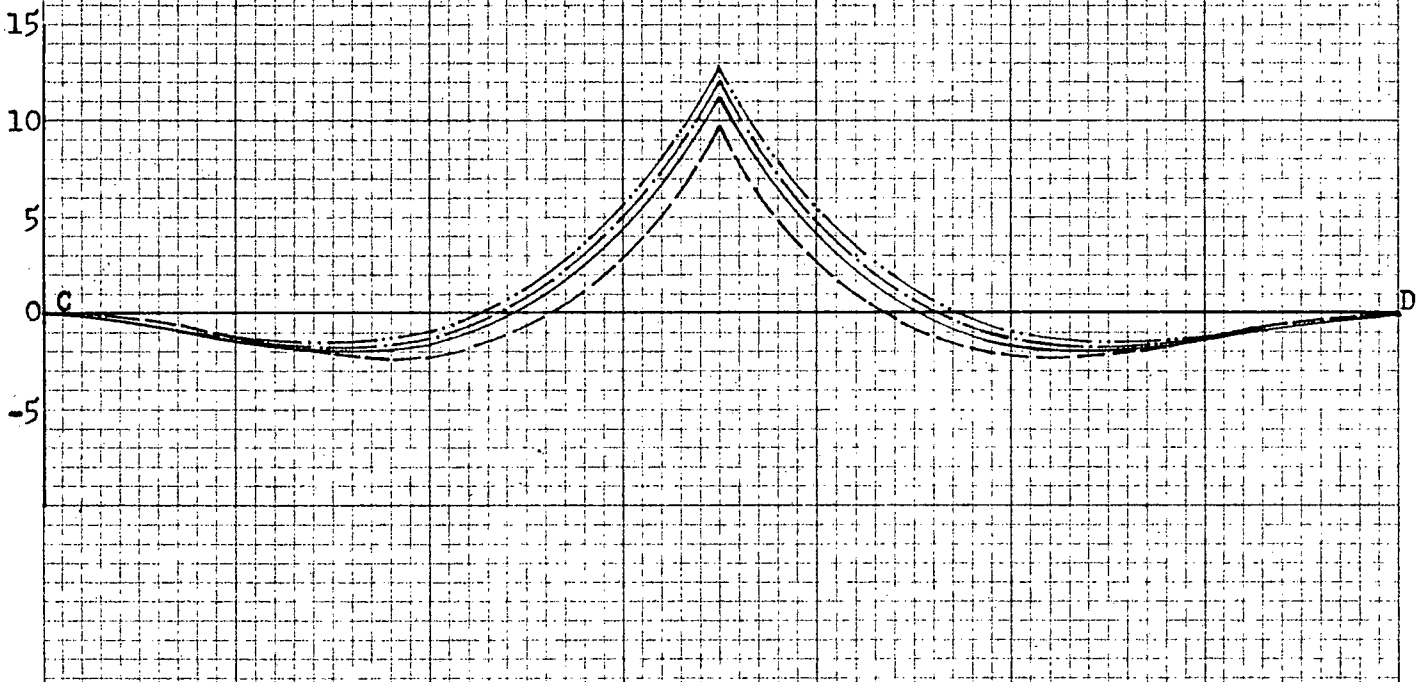
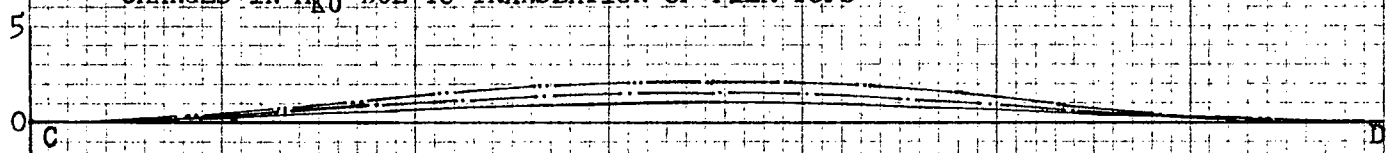


FIG. 4-0 INFLUENCE LINES (SPAN CD ONLY) FOR  $M_{KU}$  AT CROWN OF ARCH CD, SYSTEM II

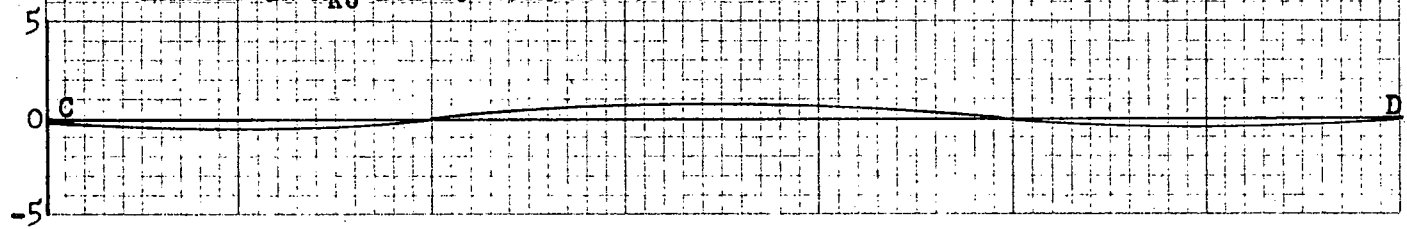
FOR FIXED ENDS  
 FOR  $H_P = 40$  ft.  
 FOR  $H_P = 60$  ft.  
 FOR  $H_P = 80$  ft.

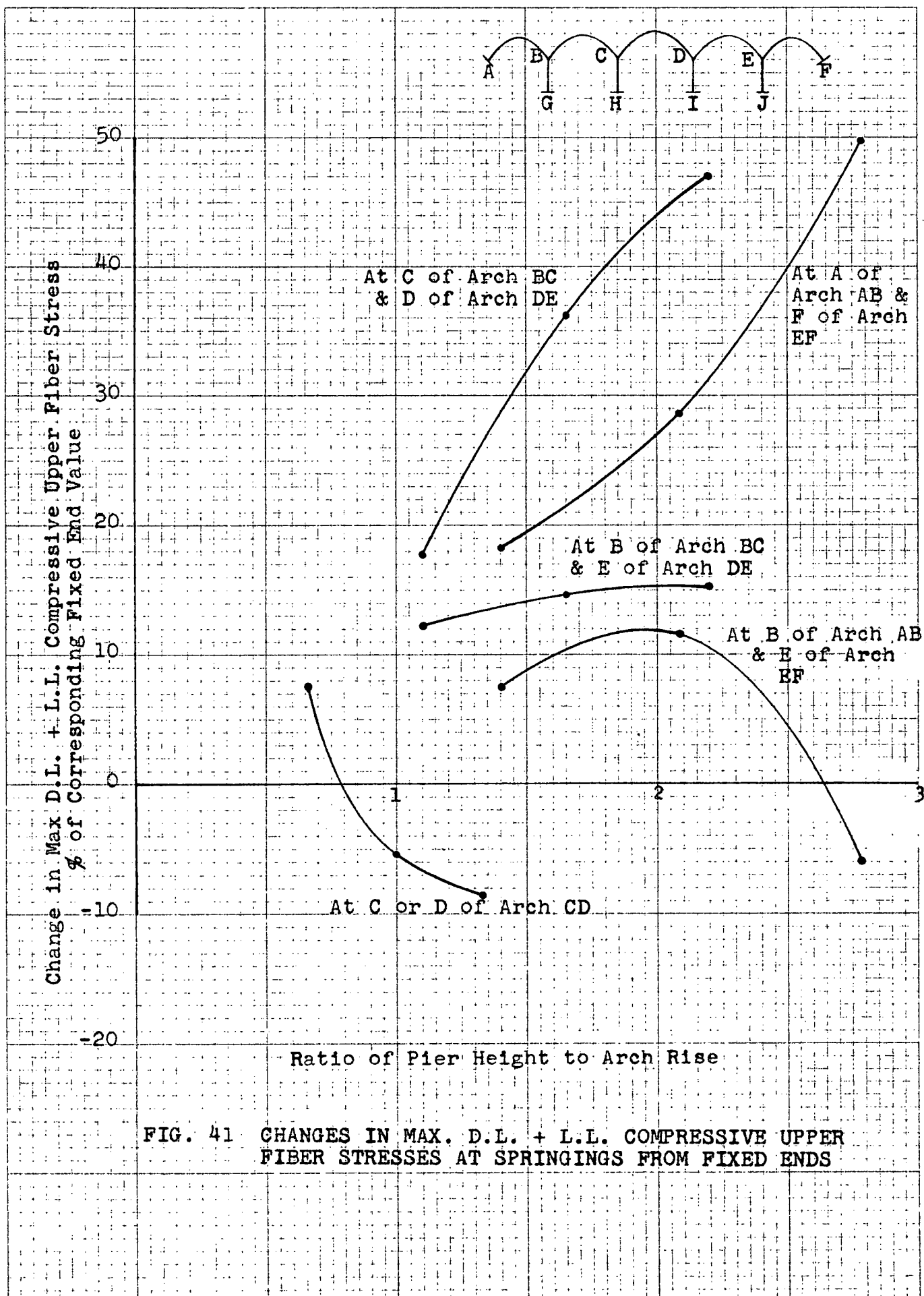


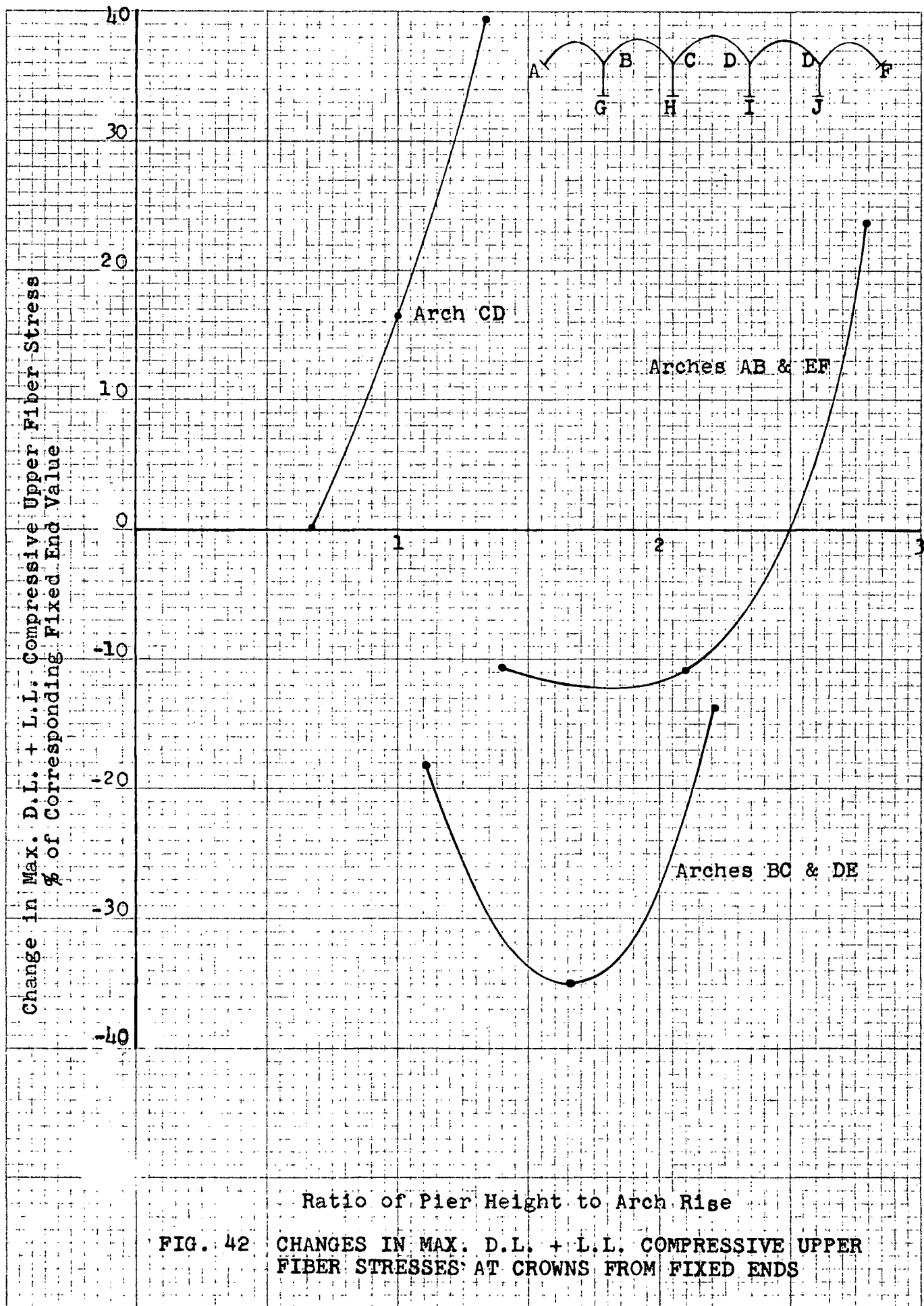
CHANGES IN  $M_{KU}$  DUE TO TRANSLATION OF PIER TOPS



CHANGES IN  $M_{KU}$  DUE TO ROTATION OF PIER TOPS







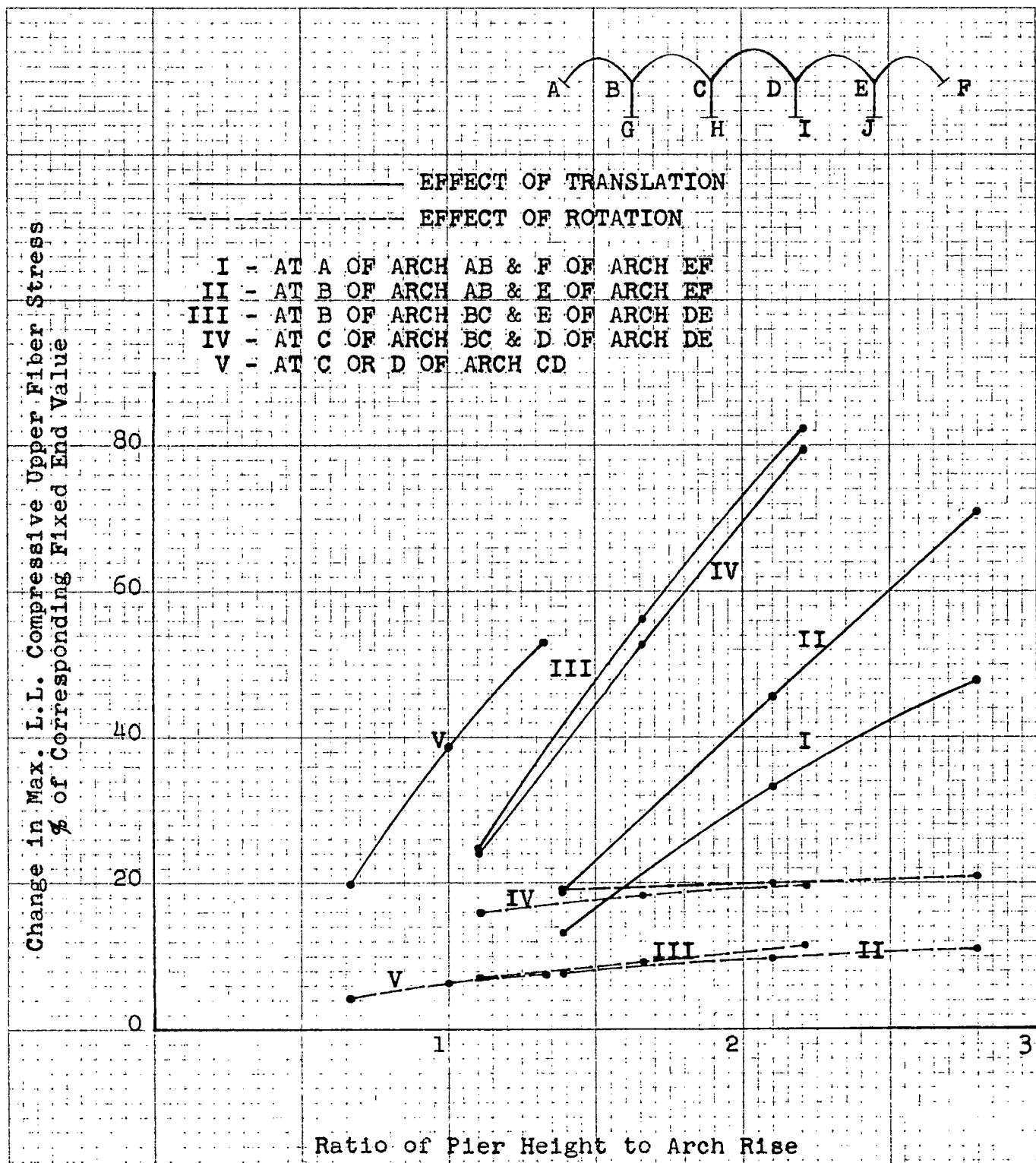


FIG. 43 CHANGES IN MAX. L.L. COMPRESSIVE UPPER FIBER STRESSES AT SPRINGINGS FROM FIXED ENDS DUE TO TRANSLATION AND ROTATION

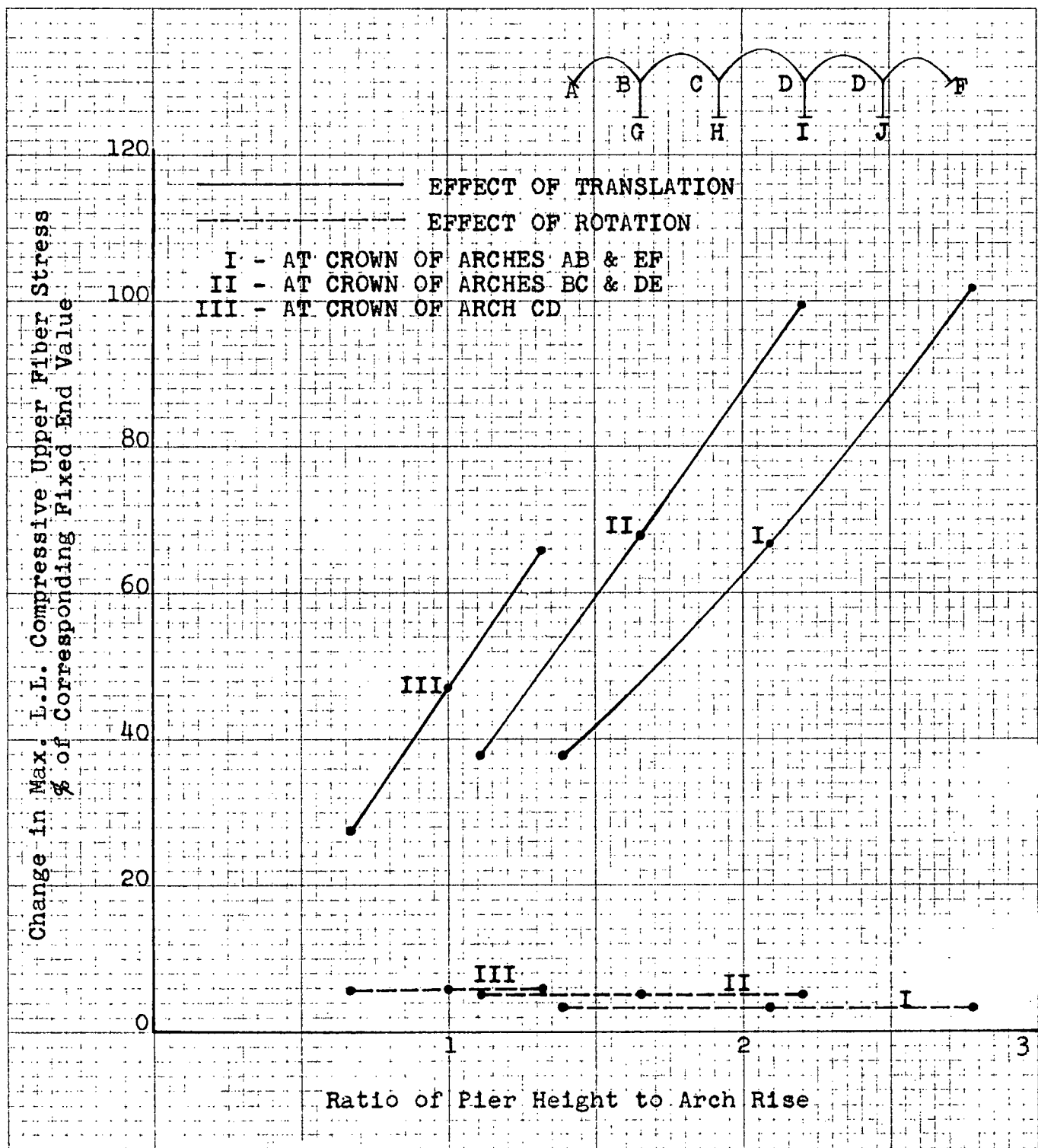


FIG. 44 CHANGES IN MAX. L.L. COMPRESSIVE UPPER FIBER STRESSES AT CROWNS FROM FIXED ENDS DUE TO TRANSLATION AND ROTATION

## CHAPTER III

### Conclusions

By inspecting the areas of the influence lines, the lower kern moments in arches, and the right kern moments in piers will govern the design in the arch systems analyzed, and that is probably true in general.

System I has been almost completely analyzed for dead load and live load by means of quantitative influence lines. In System II quantitative influence lines were constructed for the same stress functions but ordinates computed for but the span involved. These showed (vide Figs. 5 to 20 and Figs. 25 to 40) such similarity in shape as to justify in the author's opinion the deductions previously referred to although quantitative values for dead load and live load kern moments at springing and crown of the arches in System II were not computed.

Tables 8 to 10, inclusive, indicate that for Max. D.L. + L.L. stresses, (save for very flexible piers) studies may be confined to three spans for arches and two spans for piers. Errors involved are not significant in comparison with the variations of the elastic characteristics of the structures. (12,13)

Tables 8 and 9 also indicate the effect of pier dimensions on changes from fixed end conditions. All

maximum positive L.L. lower kern moments and maximum negative L.L. lower kern moments at the springings and crowns are greater than those for fixed ends, and the difference increases as the height of piers increases from 40' to 80', but the maximum lower kern moments due to the combination of dead load and live load do not of course exhibit this characteristic as is shown in Tables 11 and 12, and Figs. 41 and 42 where kern moments are replaced by fiber stresses.

Figs. 43 and 44 indicate the relative effect of rotation and translation of the pier tops on extreme fiber stresses at springings and crowns. The effect of rotation on crowns is quite small and almost independent of pier height, and that on springings is somewhat greater and increases slowly as the height of piers increases. The effect of translation on springings and crowns is usually the greatest and increases rapidly as the height of piers increases.

Tables 13 and 14 indicate the D.L. + Max. L.L. fiber stresses in arches and in piers. The moment of inertia used in the computations is based on the gross area of concrete section only. The data chosen for the numerical examples should be satisfactory as the usual amount of steel used in arches is small.

The results presented herein are only true for this particular type of continuous arch system.

Actually the problem is very complicated and the large number of variables involved in the design of continuous

arch systems makes it inadvisable to draw too definite conclusions, save that the effects of translation overshadow those of rotation in almost all cases. In this respect at least the author is in agreement with some previous workers in this little explored field.

## Appendix I

### Dead Load Horizontal Thrusts on Arches for Numerical Examples

Type of Structure - Open spandrel

Data - See Figs. 1, 2, and 3 and Table 1.

Slope of roadway surface:  $\frac{1}{100}$

Deck Load per Linear foot per Rib. - Assuming that the panel loads are uniformly distributed over the spacing of the floor beam, 20'-0" C/C.

Weight of handrail (50% of area removed by

openings) = 125 lbs

4" sidewalk slab = 305 lbs

Curb beam = 85 lbs

Floor slab = 1640 lbs

6" curtain wall = 187 lbs

Stringers (9"x14" @ 7'-0" C/C) = 460 lbs

18"x36" floor beam and bracket = 935 lbs

Total Deck Load = 3737 lbs/  
lin.ft./rib

Weight of hanger (or column) 18"x18" @ 20'-0" C/C = 338 lbs/  
foot of height

## System I

Span A B:

$$L = 180'$$

$$r = 28.6'$$

$$d_c = 3'$$

$$d_s = 4.65'$$

$$g = 1.455 \text{ (assumed)}$$

$$\tan \phi_s = \frac{2rk\sqrt{g^2 - 1}}{L(g - 1)} = 0.675$$

$$\phi_s = 34^\circ 2'$$

$$m = \frac{d_c^3}{d_s^3 \cos \phi_s} = 0.325$$

$$w_c = 3,737 + \frac{5.8(338)}{20} + 3(4)150 = 5,635 \text{ lbs}$$

$$w_s = 3,737 + \frac{32.5(338)2}{20} + 4.65(4)150(1.207) = 8,202 \text{ lbs}$$

$$\text{check } g = \frac{w_s}{w_c} = \frac{8,202}{5,635} = 1.445 \text{ o.k.}$$

The dead load horizontal thrust is:

$$H_d = w_c \left(\frac{L}{2}\right)^2 \frac{(g-1)}{r k^2} = 5,635(90)^2 \frac{(1.455 - 1)}{28.6(0.921)^2} = 855,000 \text{ lbs}$$

Span B C:

$$L = 200'$$

$$r = 36.175'$$

$$d_c = 3.25'$$

$$d_s = 5.24'$$

$$g = 1.543 \text{ (assumed)}$$

$$\tan \phi_s = \frac{r}{L} (4.328) = 0.761$$

$$\phi_s = 37^\circ 17'$$

$$m = 0.30$$

$$w_c = 3,737 + 3.25 (4) 150 = 5,687 \text{ lbs}$$

$$w_s = 3,737 + \frac{33(338)2}{20} + 5.24 (4) 150 (1.257) = 8,802 \text{ lbs}$$

$$\text{check } g = \frac{w_s}{w_c} = 1.545 \text{ o.k.}$$

The dead load horizontal thrust is:

$$H_d = 0.1358 \frac{w_c L^2}{r} = 855,000 \text{ lbs}$$

Span C D:

$$L = 240'$$

$$r = 60'$$

$$d_c = 4'$$

$$d_s = 7.03'$$

$$g = 1.756 \text{ (assumed)}$$

$$\tan \phi_s = 1.105$$

$$\phi_s = 47^\circ 52'$$

$$m = 0.275$$

$$w_c = 3,737 + \frac{13.75(338)}{20} + 4(4)150 = 6,370 \text{ lbs.}$$

$$w_s = 3,737 + \frac{33.5(338)2}{20} + 7.03(4)150(1.491) = 11,169 \text{ lbs}$$

$$\text{check } g = \frac{w_s}{w_c} = 1.745 \text{ o.k.}$$

The dead load horizontal thrust is:

$$H_d = 0.1397 \frac{w_c L^2}{r} = 855,000 \text{ lbs}$$

### System II

Span A B:

$$L = 180'$$

$$r = 35.8'$$

$$d_c = 3.25'$$

$$d_s = 4.95'$$

$$g = 1.543 \text{ (assumed)}$$

$$\tan \phi_s = 0.861$$

$$\phi_s = 40^\circ 44'$$

$$m = 0.375$$

$$w_c = 3,737 + \frac{7.975(338)}{20} + 3.25(4)150 = 5,822 \text{ lbs}$$

$$w_s = 3,737 + \frac{39.5(338)2}{20} + 4.95(4)150(1.3197) = 8,990 \text{ lbs}$$

$$\text{check } g = \frac{w_s}{w_c} = 1.543 \text{ o.k.}$$

The dead load horizontal thrust is:

$$H_d = 0.138 \frac{w_c L^2}{r} = 715,000 \text{ lbs}$$

## Span B C:

$$L = 200'$$

$$r = 45.55'$$

$$d_c = 3.5'$$

$$d_s = 6.05'$$

$$g = 1.756 \text{ (assumed)}$$

$$\tan \phi_s = 1.012$$

$$\phi_s = 45^{\circ}20'$$

$$m = 0.275$$

$$w_c = 3,737 + 3.5(4)150 = 5,837 \text{ lbs}$$

$$w_s = 3,737 + \frac{39.5(338)2}{20} + 6.05(4)150(1.4217) = 10,240 \text{ lbs}$$

$$\text{check } g = \frac{w_s}{w_c} = 1.756 \text{ o.k.}$$

The dead load horizontal thrust is:

$$H_d = 0.1397 \frac{w_c L^2}{r} = 715,000 \text{ lbs}$$

## Span C D:

$$L = 240'$$

$$r = 80'$$

$$d_c = 4.25'$$

$$d_s = 8.93'$$

$$g = 2.24 \text{ (assumed)}$$

$$\tan \phi_s = 1.56$$

$$\phi_s = 57^{\circ}20'$$

$$m = 0.20$$

$$w_c = 3,737 + \frac{24.125(338)}{20} + 4.25 \times 4 \times 150 = 6,694 \text{ lbs}$$

$$w_s = 3,737 + \frac{39.5(338)2}{20} + 8.93(4)150(1.853) = 15,013 \text{ lbs}$$

check  $g = \frac{w_s}{w_c} = 2.24$  o.k.

The dead load horizontal thrust is:

$$H_d = 0.1483 \frac{w_c L^2}{r} = 715,000 \text{ lbs}$$

## Appendix II

### Formulae for Analysis

The derivation of formulae is not a special feature of this thesis and will not be included in detail.

**Rotation and Translation Factors of a Symmetrical Arch rib.** - A single symmetrical span of a continuous arch is taken into consideration, one end is kept fixed rigidly and the other end is free to move.

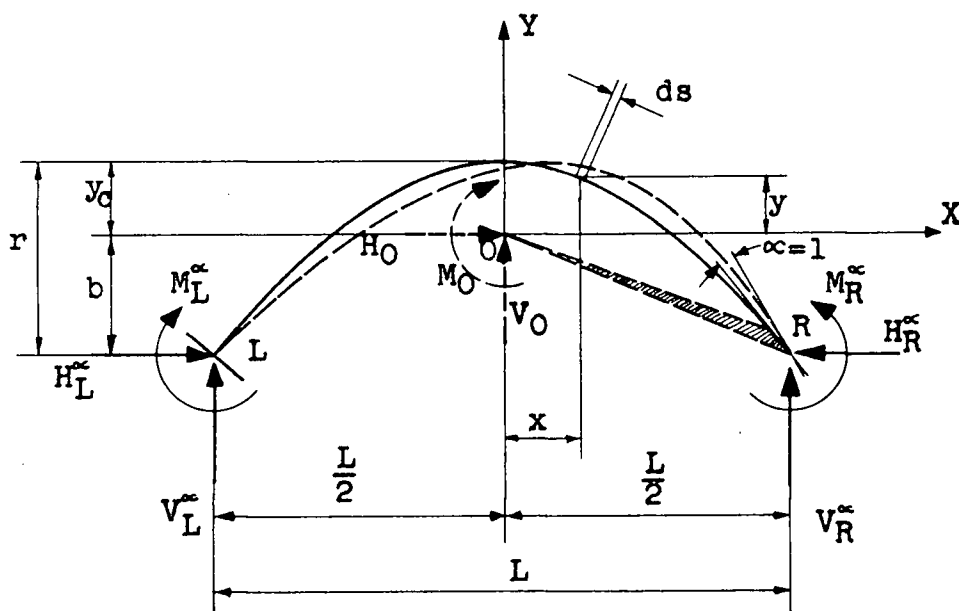


Figure 45

In Fig. 45 the left end of arch, L R, is kept fixed and the right end is given a unit clockwise rotation without any translation. From the neutral point method the resultant expressions for the rotation factors are found:

$$H_L^\alpha = H_R^\alpha = - \frac{b}{\int y^2 \frac{ds}{EI}} \dots \dots \dots \quad (1)$$

$$V_L^\infty = -V_R^\infty = -\frac{\frac{L}{2}}{\int x^2 \frac{ds}{EI}} \dots \dots \dots \quad (2)$$

$$M_L^\alpha = - \frac{1}{\int \frac{ds}{EI}} - \frac{b^2}{\int y^2 \frac{ds}{EI}} + \frac{\frac{L^2}{4}}{\int x^2 \frac{ds}{EI}} \dots \dots \dots (3)$$

$$\text{and, } M_R^{\infty} = - \frac{1}{\int \frac{ds}{EI}} - \frac{b^2}{\int y^2 \frac{ds}{EI}} - \frac{\frac{L^2}{4}}{\int x^2 \frac{ds}{EI}} \dots\dots\dots (4)$$

In Fig. 46 the left end of arch, L R, still remains fixed and the right end is given a unit length of horizontal

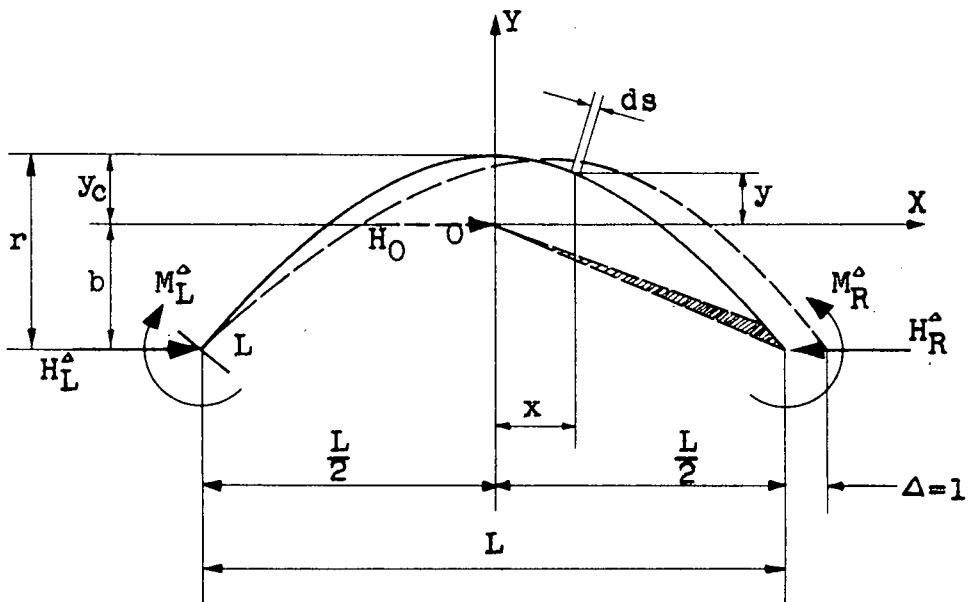


Figure 46

displacement to the right without any rotation. The resultant expressions for the translation factors are:

$$H_L^A = H_R^A = - \frac{1}{\int y^2 \frac{ds}{EI}} \dots\dots\dots (5)$$

and,

$$M_L^A = M_R^A = - \frac{b}{\int y^2 \frac{ds}{EI}} \dots\dots\dots (6)$$

The rotation and translation factors in Eqns. 1 to 6, inclusive, are in the same form and with the opposite sign for the left end of the arch moves and the right end is kept fixed.

The axes of the co-ordinates, X and Y, to which values of x and y are referred in the foregoing expressions, pass through the neutral point, o, and are directed horizontally and vertically.

According to Whitney's paper,<sup>(2)</sup> the equation of arch axis is,

$$y = y_c - \frac{r}{g-1} (\cosh zk - 1)$$

and the distance determining the location of the neutral point is,

$$y_c = \frac{2r}{(g-1)(1+m)} \left[ \frac{\sqrt{g^2-1}}{k} - 1 - (1-m) \left( \frac{\sqrt{g^2-1}}{k^2} - \frac{1}{2} - \frac{g-1}{k^2} \right) \right]$$

where,

$$g = \frac{w_s}{w_c}$$

$$m = \frac{I_c}{I_s \cos \theta_s}$$

$$z = \frac{2x}{L}$$

$$\text{and, } k = \operatorname{Cosh}^{-1} g$$

Rotation and Translation Factors for a Pier with Fixed Base. - Fig. 47 represents an elastic pier, fixed at the base. When the top is given a unit clockwise rotation without any translation the resultant expressions for the rotation factors

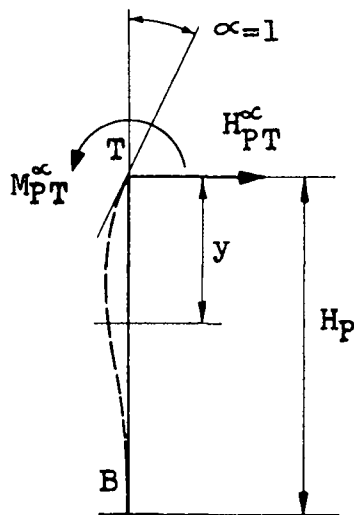


Figure 47

are:

$$H_{PT}^{\alpha} = \frac{\int y \frac{dy}{EIy}}{\left( \int y \frac{dy}{EIy} \right)^2 - \int y^2 \frac{dy}{EIy} \int \frac{dy}{EIy}} \quad \dots \dots \dots \quad (7)$$

and,

$$M_{PT}^{\alpha} = \frac{\int y^2 \frac{dy}{EIy}}{\left( \int y \frac{dy}{EIy} \right)^2 - \int y^2 \frac{dy}{EIy} \int \frac{dy}{EIy}} \quad \dots \dots \dots \quad (8)$$

In Fig. 48 when the pier top is given a unit length of horizontal displacement to the right without any

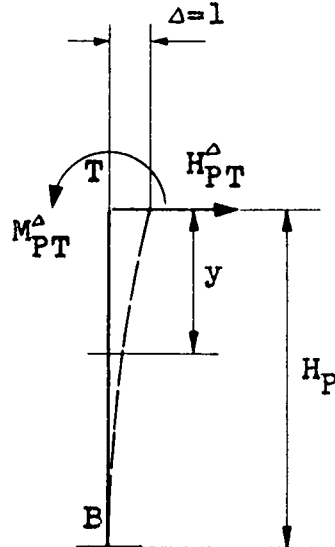


Figure 48

rotation the resultant expressions for the translation factors are:

$$H_{PT}^{\Delta} = \frac{\int \frac{dy}{EI_y}}{\int y^2 \frac{dy}{EI_y} \int \frac{dy}{EI_y} - \left( \int y \frac{dy}{EI_y} \right)^2} \quad \dots \dots \dots (9)$$

and,

$$M_{PT}^{\Delta} = \frac{\int y \frac{dy}{EI_y}}{\int y^2 \frac{dy}{EI_y} \int \frac{dy}{EI_y} - \left( \int y \frac{dy}{EI_y} \right)^2} \quad \dots \dots \dots (10)$$

The \$y\$ co-ordinates of the pier axis are measured from the pier top.

In order to evaluate the foregoing expressions the values of integrals have been determined. They are as follows:

For Arch Rib. -

$$\int \frac{ds}{EI} = \frac{L}{EI_c} \frac{1+m}{2}$$

$$\begin{aligned} \int y^2 \frac{ds}{EI} &= \frac{Lr^2}{EI_c} \left\{ \left[ \frac{g-2}{2(g-1)} - \frac{y_c}{r} \right] \sqrt{\frac{g^2-1}{k(g-1)}} + \frac{1}{2(g-1)^2} + \right. \\ &\quad \left. -(1-m) \left[ \left( \frac{g-2}{2(g-1)} - \frac{y_c}{r} \right) \sqrt{\frac{g^2-1}{k(g-1)}} + \frac{1}{4(g-1)^2} - \frac{1}{k^2} \left( \frac{g-3}{4(g-1)} - \frac{y_c}{r} \right) \right] \right\} \end{aligned}$$

$$\int x^2 \frac{ds}{EI} = \frac{L^3}{48EI_c} [1 + 3m]$$

For Pier. -

$$\int \frac{dy}{EI_y} = \frac{H_A(1+q)}{2EI_T q^2}$$

$$\int y \frac{dy}{EI_y} = \frac{H_p^2}{2EI_T q^2}$$

$$\int y^2 \frac{dy}{EI_y} = \frac{H_p^3}{EI_T (q-1)^3} \left[ \ln q + \frac{2}{q} - \frac{1}{2q^2} - \frac{3}{2} \right]$$

Distribution and Carry-Over Factors for Continuous Arch System. - They may be found by considering a two span system. The outer ends of the three members (by member is meant each individual arch span or pier) are rigidly fixed and

the inner ends, or say joints, are allowed to displace.

For convenience of reference to the distribution procedure described by Prof. A.H. Finlay,<sup>(11)</sup> the forces shown in Figs. 49 and 50, inclusive, are those which the members exert on their terminal points. Positive directions are to right for thrust and clockwise for moment.

In Fig. 49 Joint B moves horizontally a unit length to the right without any rotation.

From Eqns. 5 and 6 the forces at the ends of the arches as shown in Fig. 49(b) for accompanying the movement are:

From Eqns. 9 and 10 the forces at the pier top as shown in Fig. 49(b) are:

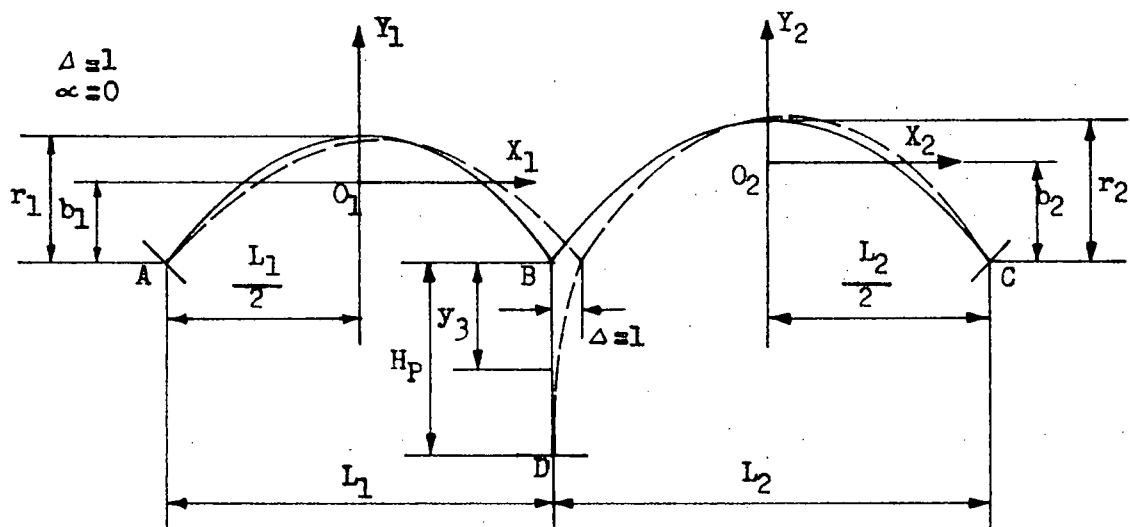


Figure 49(a)

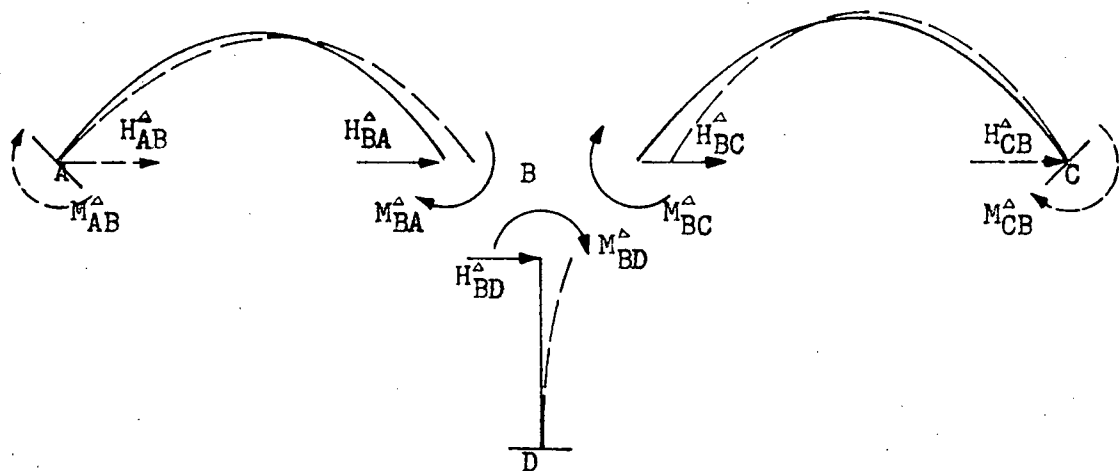


Figure 49(b)

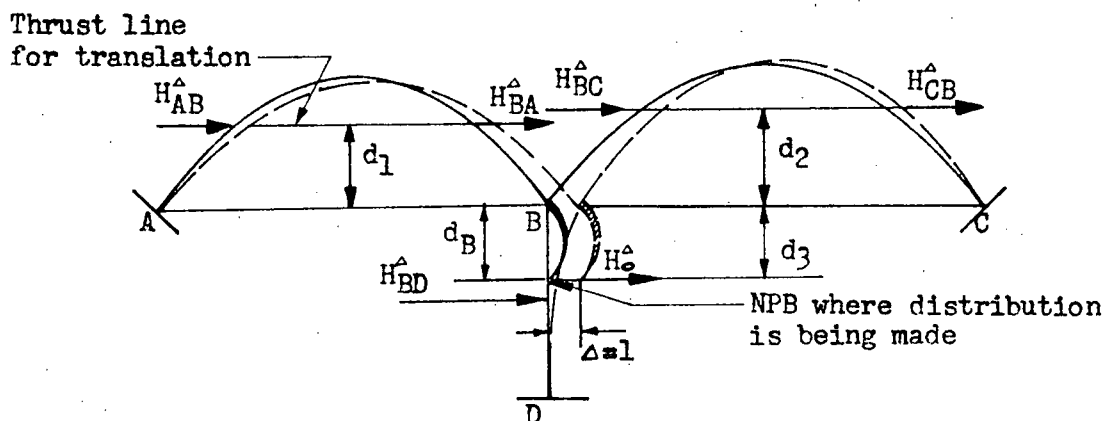


Figure 49(c)

The co-ordinates  $x_1$  and  $y_1$  are referred to the arch A B,  $x_2$  and  $y_2$  to the arch B C, and  $y_3$  to the pier B D, the origin of those axes is specified as before.

The force system shown in Fig. 49 (b) is equivalent to that shown in Fig. 49 (c) where the thrusts are acting along the thrust lines for translation. The distances from the thrust lines to the springing line are determined as below:

In Fig. 49 (c) the point, o, represents the neutral point of the joint, B, and the distance,  $d_B$ , determining its location, is found:

$$d_B = \frac{-M_{BD}^{\Delta} - M_{BA}^{\Delta} - M_{BC}^{\Delta}}{H_{BD}^{\Delta} + H_{BA}^{\Delta} + H_{BC}^{\Delta}}$$

The unbalanced thrust at the neutral point of the joint, B, is:

$\Delta = 0$   
 $\alpha = 1$

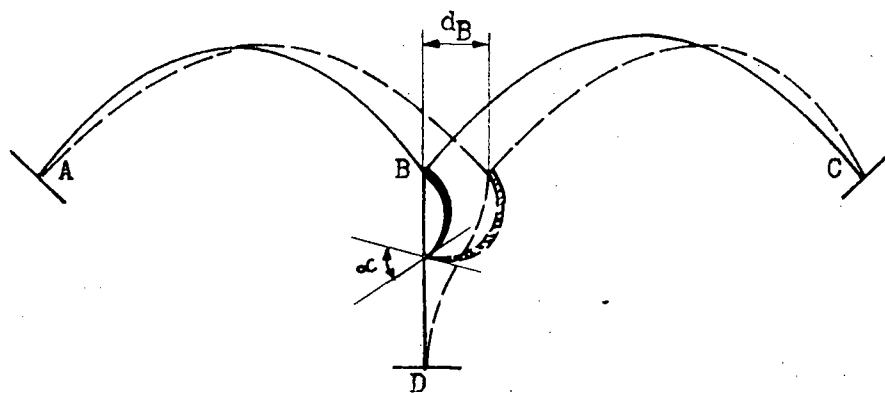


Figure 50(a)

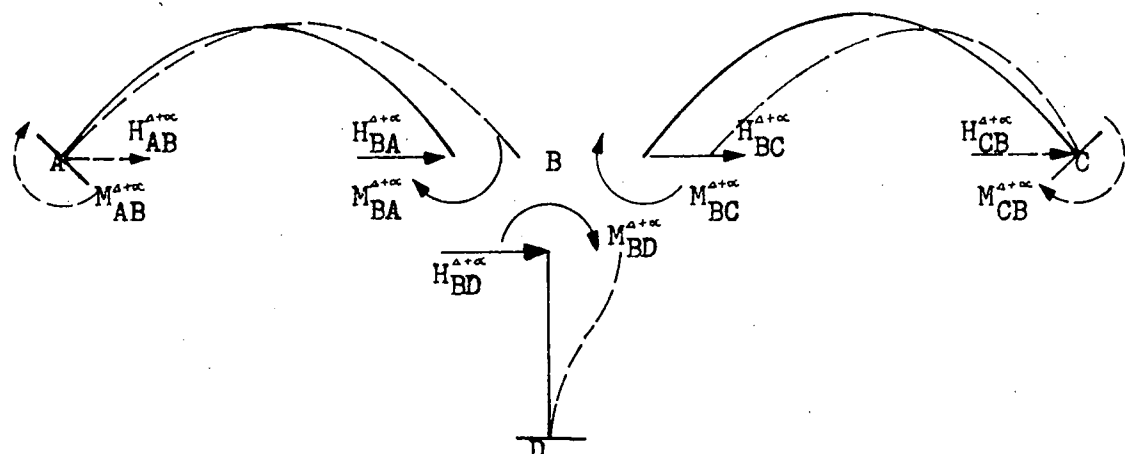


Figure 50(b) #1

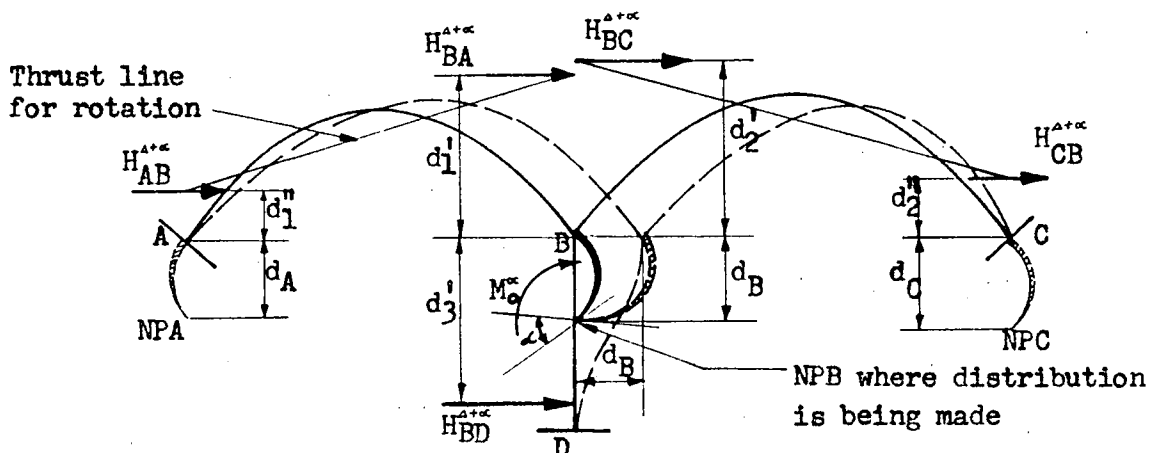


Figure 50(c) #2

#1 The vertical thrusts on arches and pier are not shown

#2 Only the horizontal components of the thrusts on arches are shown, and the vertical components may be obtained by proportion.

In Fig. 50 while the neutral point of joint, B, has rotated through a unit angle in the clockwise direction, the joint, B, moves a horizontal distance,  $d_B$ , to the right and rotates the same angle with the neutral point, the forces set up in the arches and pier as shown in Fig. 50 (b) are:

$$M_{AB}^{A+\alpha} = - \frac{b_1(d_B + b_1)}{\int y_1^2 \frac{ds}{EI}} - \frac{1}{\int \frac{ds}{EI}} + \frac{\frac{L_1^2}{4}}{\int x_1^2 \frac{ds}{EI}} \dots\dots\dots (22)$$

$$M_{BA}^{A+\alpha} = \frac{b_1(d_B + b_1)}{\int y_1^2 \frac{ds}{EI}} + \frac{1}{\int \frac{ds}{EI}} + \frac{\frac{L_1^2}{4}}{\int x_1^2 \frac{ds}{EI}} \dots\dots\dots(23)$$

$$M_{BC}^{a+\alpha} = \frac{b_2(d_B + b_2)}{\int y_2^2 \frac{ds}{EI}} + \int \frac{1}{\frac{ds_2}{EI}} + \frac{\frac{L_2^2}{4}}{\int x_2^2 \frac{ds}{EI}} \dots\dots\dots (25)$$

$$M_{CB}^{\alpha+\alpha} = \frac{b_2(d_B + b_2)}{\int y_2^2 \frac{ds}{EI}} + \frac{1}{\int \frac{ds}{EI}} - \frac{\frac{L}{2}}{\int x_2^2 \frac{ds}{EI}} \dots\dots\dots (26)$$

$$H_{BD}^{\alpha+\omega} = \frac{d_B \int \frac{dy}{EI} - \int y_3 \frac{dy}{EI}}{\int y_3^2 \frac{dy}{EI} \int \frac{dy}{EI} - \left( \int y_3 \frac{dy}{EI} \right)^2} \dots \dots \dots \quad (27)$$

In replacing the force system shown in Fig. 50(b) the thrusts are acting along the thrust lines for rotation as shown in Fig. 50(c). The distances determining the location of the thrust lines are:

The unbalanced moment at the neutral point of the joint B. is:

From Fig. 49(c) the distribution factors,  $h_{BA}$  and  $h_{BC}$ , and the carryover factors,  $h_{AB}$  and  $h_{CB}$ , at the neutral point of the joint, B, for thrust are:

$$h_{BA} = \frac{H_{BA}^{\Delta}}{H_O^{\Delta}} \dots \dots \dots \dots \dots \dots \dots \quad (35)$$

$$h_{BC} = \frac{H_{BC}^{\Delta}}{H_O^{\Delta}} \dots \dots \dots \dots \dots \dots \dots \quad (36)$$

$$\text{and, } h_{CB} = \frac{H_{CB}^A}{H_O^A} \dots \dots \dots \dots \dots \dots \dots \quad (38)$$

From Fig. 50(c) the distribution factors,  $m_{BA}$  and  $m_{BC}$ , and the carryover factors,  $m_{AB}$  and  $m_{CB}$ , for moment are:

$$m_{BA} = \frac{H_{BA}^{\alpha+\infty}}{M_\infty} (d_1' + d_B) \dots \dots \dots \quad (39)$$

$$m_{BC} = \frac{H_{BC}^{\alpha+\infty}}{M_C^\alpha} (d_2' + d_B) \dots \dots \dots \quad (40)$$

$$m_{AB} = \frac{H_{AB}^{\alpha+\alpha}}{M_O^\alpha} (d_1'' + d_A) \dots \dots \dots \quad (41)$$

$$\text{and, } M_{CB} = \frac{H^{4+\alpha}}{M^{\alpha}} (d_2'' + d_C) \dots \dots \dots \quad (42)$$

The distribution and carryover factors for the pier are unnecessary, but they may be found by statics.

**Extreme Fiber Stress.** - Let  $mn$  in Fig. 51 represent any section of the member.  $R$  is the total resultant force at the section and may be resolved as shown into the shear  $V$

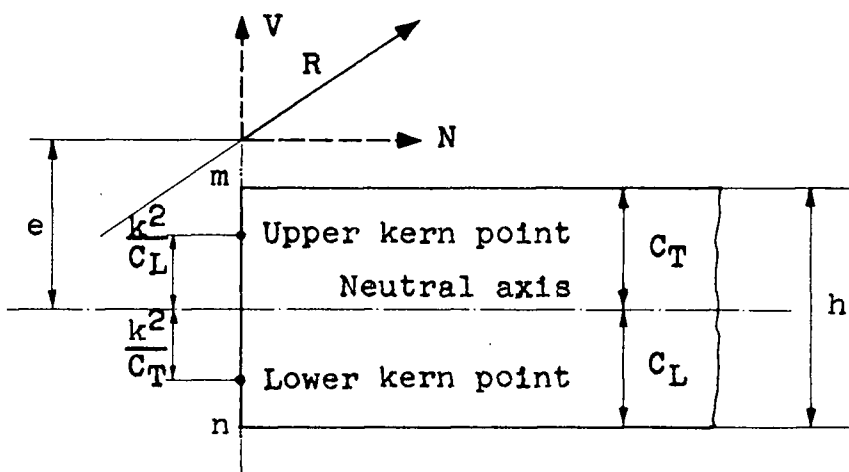


Figure 51

and normal thrust  $N$ . Then the compressive upper extreme fiber stress is:

$$f_{CU} = \frac{N}{A} + \frac{MC_T}{I} = N \left( \frac{k^2 + e C_T}{I} \right) = N \left( e + \frac{k^2}{C_T} \right) \frac{C_T}{I} = M_{KL} \frac{C_T}{I} \dots (43)$$

and the compressive lower extreme fiber stress is:

$$f_{CL} = \frac{N}{A} - \frac{M_C L}{I} = N \left( \frac{k^2 - e C_L}{I} \right) = -N \left( e - \frac{k^2 C_L}{C_L I} \right) = M_{KU} \frac{C_L}{I} \quad \dots (44)$$

For a rectangular section the distance from the kern point to the neutral axis is:

where,  $k^2 = \frac{I}{A}$

Kern Moment in Arch. - Let AC in Fig. 52 represent a half span of the arch rib. The kern moments in the arch

are:

At the crown,

$$M_{KL} = M_C + \frac{d_C}{6} H \quad \dots \dots \dots \dots \dots \dots \quad (46)$$

and,  $M_{KU} = M_C - \frac{d_C}{6} H \quad \dots \dots \dots \dots \dots \dots \quad (47)$

At the springing line,

$$M_{KL} = M_S + \frac{d_S}{6} (H \cos \phi_s + V \sin \phi_s) \quad \dots \dots \dots \dots \dots \quad (48)$$

and,  $M_{KU} = M_S - \frac{d_S}{6} (H \cos \phi_s + V \sin \phi_s) \quad \dots \dots \dots \dots \dots \quad (49)$

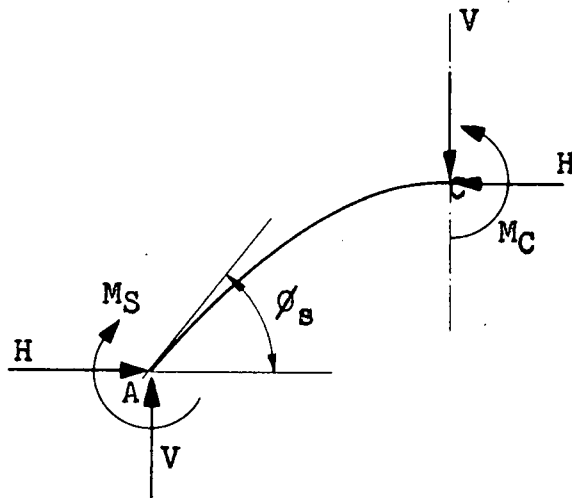


Figure 52

Kern Moment at Pier Top. - Let BD in Fig. 53 represent an elastic pier, supporting the arches A B and B C. The right kern moment at the pier top is:

$$M_{KRPT} = M + \left( \frac{d_{PT}}{6} \right) V \quad \dots \dots \dots \dots \dots \dots \quad (50)$$

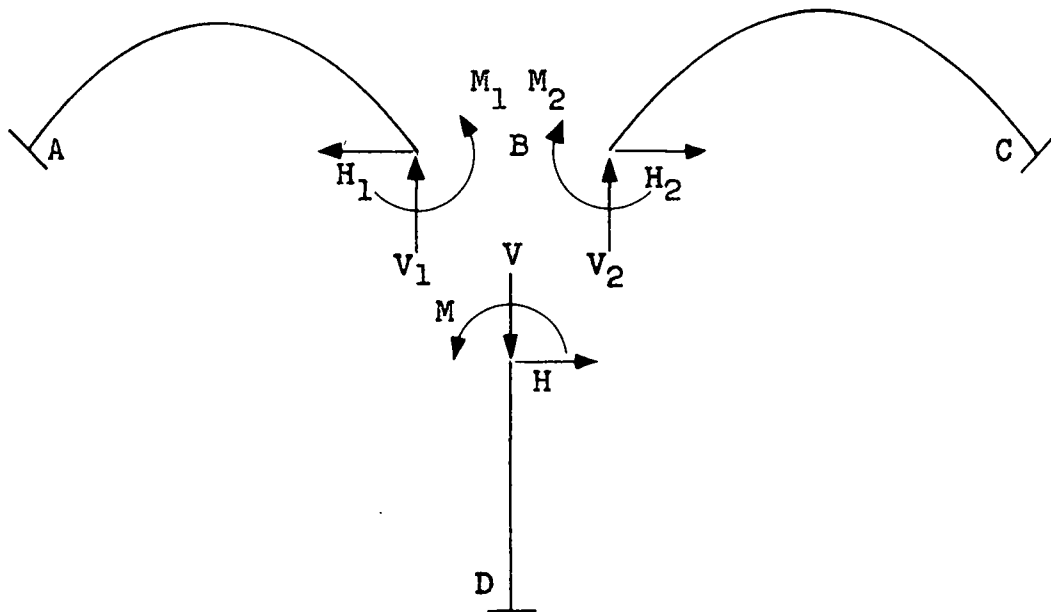


Figure 53

and the left kern moment is:

$$\text{where, } V = V_1 + V_2$$

$$\text{and, } M = M_2 - M_1$$

## Bibliography

1. Cross, H. "Analysis of Continuous Frames by Distributing Fixed-End Moments," Transactions, ASCE, Vol. 96, 1932, p. 1.
2. Whitney, C.S., "Design of Symmetrical Concrete Arches," Transactions, ASCE, Vol. 88, 1925, p. 931.
3. Whitney, C.S., "Analysis of Continuous Concrete Arch System," Transactions, ASCE, Vol. 90, 1927, p. 1094.
4. Cross, H., and Morgan, N.D., "Continuous Frames of Reinforced Concrete," John Wiley & Sons, Inc., New York, 1932, p. 316.
5. Hjort, A.P., "Design of Continuous Arches on Elastic Piers," Proceedings, ACI, Vol. 29, 1932/33, p. 143.
6. Hrennikoff, A., "Analysis of Multiple Arches," Transactions, ASCE, Vol. 101, 1936, p. 388.
7. Maught, L.C., "Statically Indeterminate Structures," John Wiley & Sons, Inc., New York, 1946, p. 230.
8. Morgan, V.A., "An Exact Method of Analysis of Continuing Parabolic Arches," Concrete and Constructional Engineering, London, Vol. 47, No. 11, Nov. 1952, p. 343.
9. Michalos, J., and Girton, D.D., "Continuous Arches on Elastic Piers," Proceedings, ASCE, Vol. 81, Nov. 1955, Paper No. 827, p. 827-1.
10. Riley, W.E., "Analysis of Continuous Arches on Flexible Piers," Proceedings, ACI, Vol. 28, 1956/57, p. 999
11. Finlay, A.H., Discussion on "Analysis of Multiple Arches," Transactions, ASCE, Vol. 101, 1936, p. 410, and lectures given to his graduate class in the University of British Columbia, Canada, 1958.
12. Cross, H., "Dependability of the Theory of Concrete Arches," Bulletin No. 203, Univ. of Illinois Eng. Experiment Station, 1930.
13. Wilson, W.M., Kluge, R.W., and Coombe, J.V., "An Investigation of Rigid Frame Bridges," Bulletin No. 308, Univ. of Illinois Eng. Experiment Station, 1938, Pt. 2.

### Notations

$L$  = theoretical span of neutral axis of rib.

$r$  = rise of neutral axis of rib.

$w$  = width of rib

$d_s$  = depth of rib at springing line.

$d_c$  = depth of rib at crown.

$y_c$  = the distance from the rib axis at the crown to the neutral point of the rib.

$b$  = the vertical distance from the springing line to the neutral point of the rib.

$\theta_s$  = the angle between the horizontal and the tangent to the neutral axis at the springing line.

$I$  = the moment of inertia of the rib at any section.

$I_s$  = the moment of inertia of the rib at the springing line.

$I_c$  = the moment of inertia of the rib at the crown.

$$m = \frac{I_c}{I_s \cos \theta_s}$$

$E$  = modulus of elasticity.

$P$  = uniform live load per linear foot of span.

$w_s$  = dead load per linear foot at springing line.

$w_c$  = dead load per linear foot at crown.

$$g = \frac{w_s}{w_c}$$

$H_p$  = height of pier.

$w_p$  = width of pier.

$d_T$  = depth of pier at the top.

$d_{T1}$  = the depth of the exterior piers at the top

$d_{T2}$  = the depth of the interior piers at the top

$d_B$  = depth of pier at the bottom

$$q = \frac{d_B}{dT}$$

$I_y$  = the moment of inertia of the pier at any section.

$I_T$  = the moment of inertia of the pier at the top.

$A$  = the area of the cross-section of the rib or pier.

$M_{KL}$  = the lower kern moment for the continuous arch on  
elastic piers.

$M_{KU}$  = the upper kern moment for the continuous arch on elastic piers.

$M_{KRPT}$  = the right kern moment at the pier top.

$M_{KLPT}$  = the left kern moment at the pier top.